medRxiv preprint doi: https://doi.org/10.1101/2023.05.10.23289779; this version posted November 4, 2024. The copyright holder for this preprint (which was not certified by peer review) is the author/funder, who has granted medRxiv a license to display the preprint in perpetuity. All rights reserved. No reuse allowed without permission.

TITLE

Glucocorticoid-driven gene expression in circulating monocytes and neutrophils in health and severe inflammation

AUTHORS

Arthur Molendijk, PhD

Affiliation :

Center for Translational Immunology,

University Medical Center Utrecht,

Netherlands

Email : molendijkarthur@gmail.com

Leo Koenderman, PhD

Department of Respiratory Medicine,

Center for Translational Immunology,

University Medical Center, Utrecht,

Netherlands

Email : l.koenderman@umcutrecht.nl

NOTE: This preprint reports new research that has not been certified by peer review and should not be used to guide clinical practice.

medRxiv preprint doi: https://doi.org/10.1101/2023.05.10.23289779; this version posted November 4, 2024. The copyright holder for this preprint (which was not certified by peer review) is the author/funder, who has granted medRxiv a license to display the preprint in perpetuity. All rights reserved. No reuse allowed without permission.

SUMMARY

Glucocorticoids (GCs) are used as anti-inflammatory and immunosuppressive drugs in many immune mediated diseases, but their use in sepsis and shock is controversial. This is caused in part by a lack of information regarding the responding cell types and GC-regulated genes *in vivo*. We used public blood transcriptomic datasets and GC-induced query genes to obtain 2 robust gene expression correlation signatures of GC induction, either in the absence or in the presence of severe inflammation. GC signature 1 originated from circadian cortisol with biases for gene expression in NK cells and neutrophils. GC signature 2 originated from GC in severe inflammation, mainly with biases for gene expression in monocytes and neutrophils. Many genes upregulated by GC treatment in septic shock and burn shock were also present as high-ranking genes in GC signatures, which pointed to their direct regulation by GC. Robust GC signatures were also obtained from dataset collections of monocytes and neutrophils, separately, and predicted cellular effects. Additionally, gene induction by GC was put into a wider framework of gene expression in circulating monocytes and neutrophils in health and systemic inflammation. We present and interpret a large number of GC-regulated genes in different blood cells and tissues, and select 2 whole blood transcriptomic biomarker gene sets, GC-1 and GC-2, for monitoring cortisol action in health, and in severe inflammation, respectively. GC signature 2 was found in sepsis and many other inflammatory diseases, both from treatment with GC, and from endogenous GC.

medRxiv preprint doi: https://doi.org/10.1101/2023.05.10.23289779; this version posted November 4, 2024. The copyright holder for this preprint (which was not certified by peer review) is the author/funder, who has granted medRxiv a license to display the preprint in perpetuity. All rights reserved. No reuse allowed without permission.

INTRODUCTION

Use of glucocorticoids in therapy

Endogenous cortisol links the endocrine and immune system, and has an important role in regulating inflammatory events. Synthetic glucocorticoids (GCs) are widely used in medicine because of their strong anti-inflammatory and immunosuppressive mode of action. Systemic corticosteroid therapy is routinely used in autoimmune diseases such as rheumatoid arthritis (RA) and systemic lupus erythematosus (SLE), during flares in MS, during severe exacerbation in pulmonary diseases such as COPD and asthma, and as cortisol replacement in Addison's disease (Chan et al., 2020; Johannsson et al., 2015; Reichardt et al., 2021; Strehl et al., 2019). GCs with reduced systemic bioavailability are also used in active inflammatory bowel disease (IBD) (Dubois-Camacho et al., 2017). A controversy is present concerning the use of GCs in the treatment of acute inflammation such as found during septic and burn shock as well as in ARDS and COVID-19 (Djillali Annane et al., 2017; Briegel et al., 2018; Carlet et al., 2020; Chan et al., 2020; Vandewalle & Libert, 2020; Venet et al., 2015). Clinical trials have shown a beneficial effect of GC treatment in shortening septic shock duration, but inconsistent results have been published regarding survival at 180 days (Annane et al., 2018; Venkatesh et al., 2018). The use of GC as additional therapy in septic shock is now recommended if vasopressor therapy is not effective enough in maintaining target blood pressure (Evans et al., 2021). Considering the physiological importance of endogenous GCs and the wide use of systemic GC therapy, biomarkers for monitoring GC activity at the cellular level are very useful (Alder et al., 2018; Chan et al., 2020; Russell, 2018). Blood transcriptomics is an important technology for obtaining such biomarkers, and has been used to develop an 8 gene biomarker of GC exposure especially in RA and SLE (Hu et al., 2018). Blood transcriptomics has also been used to classify heterogeneity in sepsis (Leligdowicz & Matthay, 2019; Tsakiroglou et al., 2023), but without using GC-induced genes, as biomarkers, to assist in classification. Furthermore, the use of GC-induced genes for monitoring the cellular effects of GC therapy in septic and burn shock has not been adequately applied.

Objective

Our objective here was to use large collections of blood transcriptomics datasets to obtain GC-driven gene signatures in the absence or presence of severe systemic inflammation, such as found in sepsis, ARDS, and trauma. Secondly, profiling signature gene expression based on

medRxiv preprint doi: https://doi.org/10.1101/2023.05.10.23289779; this version posted November 4, 2024. The copyright holder for this preprint (which was not certified by peer review) is the author/funder, who has granted medRxiv a license to display the preprint in perpetuity. All rights reserved. No reuse allowed without permission.

cell type and inflammatory state was performed to help select suitable biomarkers for monitoring cortisol activity in different illnesses.

Cortisol, GR, and cellular effects

Cortisol is a steroid hormone and the major end product of the HPA (Hypothalamic Pituitary Adrenal) axis, which plays an important role in the body's stress response. Different stresses, both physical or emotional, stimulate the HPA axis and thereby transiently increase systemic ACTH and cortisol concentrations (Herman et al., 2016; Oster et al., 2017). Moreover, circadian stimulation of the HPA axis results in increasing cortisol concentration during late sleep, before sunrise, peaking around the sleep wake transition at 6h-10h, and bottoming in the evening, early night between 22h-2h (Oster et al., 2017). Changes in cortisol concentration affect blood cell trafficking and mobilization, resulting in stress and circadian rhythm related shifts in different immune cell percentages (Ince et al., 2019; Olnes et al., 2016; Sautron et al., 2015; Shimba & Ikuta, 2020). In sepsis and critical illness more generally, the central HPA axis is first transiently activated, but then becomes suppressed as indicated by low plasma ACTH concentration. However, plasma cortisol levels remain elevated partially due to increased production and mainly due to decreased breakdown in liver and kidney (Boonen et al., 2013; Langouche et al., 2023; Van den Berghe et al., 2022). Cortisol availability is further increased by different peripheral adaptations such as decreased hepatic synhesis of GC carrier proteins resulting in more free cortisol. Intracellular cortisol availability in target tissues might also be increased by enhanced inactive cortisone to cortisol enzymatic conversion (Langouche et al., 2023; Van den Berghe et al., 2022). Early research indicated that high cortisol levels occurring in septic shock might still be inadequate in relation to the severity of the disease (Annane et al., 2000). This insufficiency was referred to as CIRCI (critical illness-related corticosteroid insufficiency), and was caused by adrenal insufficiency together with tissue corticosteroid resistance, and characterized by a strong proinflammatory response (Marik et al., 2008). Presently, CIRCI is hard to diagnose, but might still require treatment with GC (D. Annane et al., 2017; Djillali Annane et al., 2017). Recently, it has been argued that a form of CIRCI might only occur in prolonged critical illness (Téblick et al., 2022), and that CIRCI is a poor rationale for the use of GC in septic shock (Langouche et al., 2023; Téblick et al., 2022; Van den Berghe et al., 2022). In this view, high doses of GC in septic shock would not remedy insufficiency due to GC resistance in CIRCI, but improve blood pressure as a pharmalogical effect (Langouche et al., 2023; Van den Berghe et al., 2022).

medRxiv preprint doi: https://doi.org/10.1101/2023.05.10.23289779; this version posted November 4, 2024. The copyright holder for this preprint (which was not certified by peer review) is the author/funder, who has granted medRxiv a license to display the preprint in perpetuity. All rights reserved. No reuse allowed without permission.

Natural (cortisol in humans) and synthetic (e.g. dexamethasone) GCs are lipophilic molecules, that can traverse cell membranes. Cellular effects of GCs can be genomic (transcriptional) mediated by the glucocorticoid receptor (GR), or non-genomic (transcription independent), involving GR or other putative GC receptors (Escoter-Torres et al., 2019; Timmermans et al., 2019). In the absence of GC ligand, the glucocorticoid receptor (GR) is a part of a matured protein heterocomplex in the cytoplasm (Escoter-Torres et al., 2019; Petta et al., 2016; Timmermans et al., 2019). Upon ligand binding, GR translocates to the nucleus, and binds as a monomer, dimer or tetramer to half site or pseudo-palindromic GREs (glucocorticoid response elements) in DNA, which are situated in promoters and enhancers, to activate its target genes (Escoter-Torres et al., 2019; Gerber et al., 2021; Johnson et al., 2021; Petta et al., 2016; Strickland et al., 2022; Timmermans et al., 2019; Vettorazzi et al., 2021). Important GR gene targets for activation produce anti-inflammatory factors, such as DUSP1/MKP-1, NFKBIA/IkBalpha, TSC22D3/GILZ, and TNFAIP3/A20 (Oh et al., 2017). GR physically interacts with c-Jun of AP-1 (Diamond et al., 1990; Yang-Yen et al., 1990), and with the p65 subunit (RelA) of NF-kB (Caldenhoven et al., 1995; Ray & Prefontaine, 1994; Scheinman et al., 1995). These protein-protein interactions are important for mutual antagonism between anti-inflammatory GR and inflammatory NF-kB and AP-1 activity, as reviewed (Petta et al., 2016). GR also functions in repression of gene transcription, which requires direct DNA binding of the GR to GREs (Escoter-Torres et al., 2020). The exact mechanisms of gene repression, including a possible role of tethering of GR to DNA-bound AP-1 or NF-kB, are being investigated (Escoter-Torres et al., 2019; Fadel et al., 2023; Gerber et al., 2021; Strickland et al., 2022; Vettorazzi et al., 2021). Many effects of GCs on neutrophils, monocytes, and monocyte-derived macrophages, are thought to relate to the cell biology of different phases of the local inflammatory response to injury and infection, where a pro-inflammatory phase triggered by DAMPS and PAMPS, is followed by a resolution phase, and a tissue repair phase (Desgeorges et al., 2019; Ehrchen et al., 2019; Ronchetti et al., 2018). GCs affect monocytes, and monocyte-derived macrophages depending on their differentiation and activation status, suppressing the pro-inflammatory phenotype, and stimulating the anti-inflammatory phenotype by increasing their phagocytosis of apoptotic cells (Desgeorges et al., 2019; Ehrchen et al., 2019). Phenotypic effects of GCs on immune cells can be deduced, to some degree, from their transcriptomes and epigenomes. Transcriptomes of different isolated blood cells and primary cell types, treated *in vitro* with GC, are highly cell type-dependent, and predict testable phenotypic effects (Franco et al., 2019). Such transcriptomes are potentially valuable data for development of selective therapies (Buttgereit, 2021; Franco

medRxiv preprint doi: https://doi.org/10.1101/2023.05.10.23289779; this version posted November 4, 2024. The copyright holder for this preprint (which was not certified by peer review) is the author/funder, who has granted medRxiv a license to display the preprint in perpetuity. All rights reserved. No reuse allowed without permission.

et al., 2019), which would also be true for cell specific transcriptomes induced by GC *in vivo*, as accessible by a gene expression correlation approach.

Trauma and sepsis

Protective responses to mild or moderate trauma are thought to become exaggerated and destructive after massive trauma, of the type that was unsurvivable before the advent of medicine (Lord et al., 2014). Severe trauma leads to rapid systemic inflammation, which is excessive and commonly referred to as SIRS (systemic inflammatory response syndrome). Pro- and anti-inflammatory processes occur together, as studied at the level of blood plasma cytokines/chemokines and the leukocyte transcriptome (Xiao et al., 2011). Patients who survive SIRS and early MOF (multiple organ failure) are still at low risk of developing PICS (persistent inflammation, immunosuppression and catabolism syndrome) (Gentile et al., 2012; Hesselink et al., 2020). After severe injury, systemic exposure to DAMPS leads to activation of complement and coagulation pathways, and to activation of innate immune cells. Therefore, trauma can lead to remote organ injury and sepsis (Huber-Lang et al., 2018; Lord et al., 2014; Pottecher et al., 2019). Sepsis is defined as a life-threatening organ dysfunction caused by a dysregulated host response to infection (Singer et al., 2016). The degree of organ dysfunction is represented by a SOFA (sequential organ failure assessment) score (Singer et al., 2016). Patients who survive early multiple organ failure from SIRS in sepsis often develop chronic critical illness involving PICS (Darden et al., 2021). For therapy of sepsis, the immunology of the host response is very important besides the nature of the infection (Jarczak et al., 2021). Sepsis is heterogenous, for example in the relative presence of hyperinflammation and immune suppression which may also change over time, and a major effort is ongoing in patient stratification, including the use of blood leucocyte transcriptomics, to possibly improve effects of standard and future therapies (Leite et al., 2024; Leligdowicz & Matthay, 2019; Pelaia et al., 2023; Stanski & Wong, 2020; Tsakiroglou et al., 2023; van der Poll et al., 2021; Van Der Poll et al., 2017). Sepsis starts with detection of PAMPs from pathogens, and DAMPs from tissue damage, causing a systemic inflammatory response. Several pro-inflammatory mechanisms become deregulated including activation of complement and coagulation, immune cells, endothelial cells, and platelets. On the other hand, immunosuppressive responses are induced in parallel including lymphocyte apoptosis, reduced antigen presentation by APCs, and macrophages shifting to an alternative (M2) activation state (Hotchkiss et al., 2016; Jarczak et al., 2021; van der Poll et al., 2021; Van Der Poll et al., 2017; Wiersinga & van der Poll, 2022).

medRxiv preprint doi: https://doi.org/10.1101/2023.05.10.23289779; this version posted November 4, 2024. The copyright holder for this preprint (which was not certified by peer review) is the author/funder, who has granted medRxiv a license to display the preprint in perpetuity. All rights reserved. No reuse allowed without permission.

Monocytes and neutrophils in severe inflammation

Low surface expression of HLA-DR on blood monocytes is an important marker for immunosuppression in sepsis, in surgery, and in cancer (Hibbert et al., 2018; Venet & Monneret, 2018), and correlates negatively with serum cortisol concentrations (Kim et al., 2010; Mengos et al., 2019; Tulzo et al., 2004). Monocytes found in sepsis are more phagocytic, and less responsive to endotoxin stimulation (endotoxin tolerant), but express higher levels of cytokines and interleukins compared to monocytes from healthy controls (Shalova et al., 2015). They display an activation pattern that is similar as found in macrophages as judged by gene expression analysis (Liepelt et al., 2020; Washburn et al., 2019). Recently, single cell sequencing has allowed a better description of monocyte heterogeneity in sepsis, ARDS, and COVID-19, and different monocyte cellular states have been identified, some of which are strongly expanded (Jiang et al., 2020; N. Liu et al., 2021; Reyes et al., 2020; Reyes et al., 2021; Schulte-Schrepping et al., 2020; Wang et al., 2021; Wen et al., 2020). In case of COVID-19, a gene expression signature of GC treatment has been identified for monocytes (Knoll et al., 2024), but not yet for 'sepsis monocytes'. Neutrophils in severe systemic inflammation, such as found after trauma and in sepsis, are dysfunctional which is associated with the susceptibility to infections, and cause of tissue damage. The functions of neutrophils in acute inflammation act as a double edged sword. At the one hand, neutrophils are essential in pathogen defense and tissue repair, but on the other hand deregulated neutrophils are involved in collateral damage to host healthy tissue (Hesselink et al., 2019; Kovtun et al., 2018; Leliefeld et al., 2016; Mortaz et al., 2018). Neutrophils isolated from the blood of sepsis or ARDS patients are functionally altered including reduced chemotaxis, and delayed apoptosis. Interestingly enough no change in phagocytic capacity was found for these cells (Demaret et al., 2015; Juss et al., 2016). Different neutrophil populations occur in severe systemic inflammation, based on cell surface markers, nuclear shape, cellular density, and functional characteristics (Hellebrekers et al., 2018; Hesselink et al., 2019; Leliefeld et al., 2016; Mortaz et al., 2018; Pillay et al., 2012; Shen et al., 2017). Severe systemic inflammation results in the appearance of low density neutrophils (LDNs), with different origins, including degranulated neutrophils, immature neutrophils, granulocytic MDSCs, and pro-inflammatory/primed LDNs (Hesselink et al., 2019). Transcriptomic studies, on bulk neutrophils or single cells in systemic severe inflammation including severe COVID-19 (Aschenbrenner et al., 2021; de Kleijn et al., 2012; Demaret et al., 2015; Juss et al., 2016; Kwok et al., 2023; Kwok et al., 2020; Reusch et al.,

medRxiv preprint doi: https://doi.org/10.1101/2023.05.10.23289779; this version posted November 4, 2024. The copyright holder for this preprint (which was not certified by peer review) is the author/funder, who has granted medRxiv a license to display the preprint in perpetuity. All rights reserved. No reuse allowed without permission.

2021; Schulte-Schrepping et al., 2020; Sinha et al., 2022; Vieira Da Silva Pellegrina et al., 2015) have not evaluated the identification of co-expressed GC-induced genes.

Result, importance

Here we used a meta-analysis to overcome some of the limitations of identifying glucocorticoid-induced genes in single blood transcriptomics datasets. Different GC inducible query genes were used on defined dataset collections, applying an expression correlation search to obtain large, robust signatures of glucocorticoid-driven gene expression. Signature genes were profiled for cell type-dependent expression, induction by GC *in vitro*, as well as for circadian expression, and upregulation during mild and severe inflammation. Signature 1 of glucocorticoid-driven gene expression in blood in the absence of severe inflammation, was largely derived from responses to circadian cortisol in NK cells and neutrophils. A set of genes (GC-1) selected from this signature was suitable for use as a blood transcriptional biomarker for the involvement of cortisol in the absence of severe inflammation. Signature 2 of glucocorticoid-driven gene expression in blood in severe inflammation, mainly originated from “severe inflammatory” neutrophils, among others characterized by upregulation of ARG1 encoding arginase 1, and from monocytes including M2 alternatively activated macrophage-like monocytes. Many GC signature genes were specifically upregulated upon GC treatment in septic and burn shock. A selection of genes (set GC-2) was used to demonstrate the presence of GC signature 2 in a wide range of inflammatory illnesses, originating both from exogenous and endogenous GC, which indicated a general importance of GCs in immunosuppression. This analysis extends the description of GC action on different immune cells and tissues *in vivo*, and gene set GC-2, derived from GC signature 2, will potentially be a useful biomarker for stratification of sepsis and other inflammatory diseases, and for monitoring of cellular responses to GC in severe inflammation.

METHODS

Datasets

This study made use of data in the public domain. Microarray gene expression data were downloaded from the NCBI GEO database (Barrett et al., 2013) and loaded into R, using Biobase and GEOquery packages from the Bioconductor software repository (Huber et al., 2015; Sean & Meltzer, 2007). Expression matrices from GSE expression sets were put into

medRxiv preprint doi: https://doi.org/10.1101/2023.05.10.23289779; this version posted November 4, 2024. The copyright holder for this preprint (which was not certified by peer review) is the author/funder, who has granted medRxiv a license to display the preprint in perpetuity. All rights reserved. No reuse allowed without permission.

GEO DataSet (GDS) format-like expression tables (i.e. dataframes with ID_REF and IDENTIFIER columns for platform probe ID and gene symbol, respectively, and followed by sample value columns). If gene symbols were not directly provided with the platform, other platform probe identifiers were used to obtain matching gene symbols, via HGCN custom downloads, using the approved gene symbols from HGNC (Seal et al., 2023). RNA-sequencing phenotypic data were downloaded from NCBI GEO using GEOquery. The corresponding expression data were downloaded from the GEO website, and put into a GDS expression table-like format. Processed microarray and RNA-seq expression data were also downloaded from the ArrayExpress website (Athar et al., 2019), and read into R, along with the corresponding sample and data relationship (sdr) files, and array design files. Microarray and RNA sequencing data from ArrayExpress were also put into a GDS expression table-like format, using HGCN custom downloads in case of missing gene symbol columns in expression tables or platform.

Dataset collections

Collections of datasets were assembled based on experimental description as provided in the accompanying metadata. Dataset collections varied in size, from whole blood in the absence of severe inflammation (40 and a subset thereof, 15), whole blood in the presence of severe inflammation (38 and a subset thereof, 15) (Table S1, sheet 15) to smaller sizes in case of separated monocytes and neutrophils (6-11), PBMCs (7), and tissues muscle, skin, and fat (5-11). (Table S3, sheet 13). Gene expression tables, or subsets thereof, were left unchanged, without transformation of the original values except in a few cases where mentioned in results and supporting information for different collections. The original values mostly came in either base 2 logarithmic or linear scales. Single microarray platform IDs correspond with probe in Illumina or probeset in Affymetrix datasets, and are hereafter named probe for simplicity. The number of probes present in the ID-REF column corresponding to a single gene varies depending on microarray platform, whereas in case of the RNA-seq expression tables, each gene was uniquely represented by a single observation (row).

Single gene expression correlation profiles from single datasets in a collection

Pearson correlation coefficients between the different probe expression values corresponding with a single query gene and all other gene probes in an expression table were calculated. A

medRxiv preprint doi: https://doi.org/10.1101/2023.05.10.23289779; this version posted November 4, 2024. The copyright holder for this preprint (which was not certified by peer review) is the author/funder, who has granted medRxiv a license to display the preprint in perpetuity. All rights reserved. No reuse allowed without permission.

given query gene was used to obtain ranked expression correlation profiles for different datasets in a collection using the corresponding gene query probes present in each gene expression table from a collection. The number of profiles acquired per query gene depended on the presence of genes and corresponding probe numbers on dataset platforms.

Averaging correlation coefficients in meta-analysis

Pooling correlation coefficients in meta-analysis, as used here of Pearson correlation coefficients of expression values for a pair of genes in different transcriptomic datasets, can be performed differently; either after Z transform, weighting, taking mean, and transformation of weighted mean value back to average correlation coefficient according to Fisher, or by taking mean of weighted correlations coefficients directly (Alexander, 1990; Field, 2005). Weighing of different studies is applied according to within and between study variances, or according to study sample size, depending on method. Both methods are sufficiently accurate in obtaining an estimate, when population correlations vary (Field, 2005). Here, average correlation coefficients were directly taken as mean, without weighing by sample size, not to give too much weight to a few large datasets, and to have equal contributions of all datasets, which are potentially unique with respect to biased sampling of illnesses and other conditions. Average correlations obtained from meta-analysis were primarily used for ranking, and less as estimates of "true" correlations.

Average gene expression correlation profile in a dataset collection

An average gene expression correlation profile per query gene in a dataset collection was derived by first selecting different profiles for consistent results between probes, and between datasets, and using maximally one probe per dataset. Since probes for a single gene on a microarray platform can perform differently, also with some probes being inadequate, it was important to select for each microarray dataset the query probe giving the largest average overlap with the correlation results of all other datasets. Profiles were pre-filtered by setting a low threshold (5) for average overlap of the 200 highest ranking genes with all other profiles. Not all datasets gave correlation hits, and this may depend on the quality of specific probes on different platforms, number of samples in a dataset, or type of experiment. In case of smaller dataset collections of separated monocytes, neutrophils, PBMCs and tissues, all available profiles were used to select a single profile for each dataset using largest average overlap with

medRxiv preprint doi: https://doi.org/10.1101/2023.05.10.23289779; this version posted November 4, 2024. The copyright holder for this preprint (which was not certified by peer review) is the author/funder, who has granted medRxiv a license to display the preprint in perpetuity. All rights reserved. No reuse allowed without permission.

all other profiles, without the pre-filter, to use all datasets in the collection. Next, average correlation profiles were obtained by aggregation of probes per gene in each selected profile using the maximal correlation value with the query gene, and then taking the mean correlation value for all genes in the contributing profiles for ranking, without applying Fisher Z transform, or weighing by dataset sample sizes. Genes present below a threshold number of supporting datasets (6 in case of collections of size 15) were discarded from the combined profile. Since inadequate gene probes, if present, will have higher correlation values with the query (closer to 0), than corresponding adequate gene probes, in case of actual negative correlation, this averaging method is best suited for the positive correlation part of the profiles. To reliably determine the negative correlation end of ranked average gene expression correlation profiles, probes can also be aggregated per gene taking the minimal correlation value. An annotated R script which can be used for multiple gene queries (selectcollections.R), and 2 dataset collections, whole blood in the absence of severe inflammation (n= 15), and whole blood in the presence of severe inflammation (n= 15) are provided to reproduce results of average correlation profiles for single genes using these same collections (Table S1, sheets 1 and 5). This also replicates the results seen using the larger collections (n= 40, and n = 38) (Table S1, sheets 8 and 12).

Multi-gene signatures

Multiple average gene expression correlation profiles obtained on a given dataset collection, for different co-expressed query genes, can be combined again to give a single robust result for a chosen gene set. In case of using GC-induced gene queries this resulted in multi-gene signatures of GC-driven gene expression. Suitable GC-induced query gene combinations were chosen based on highly similar correlation profiles, which introduced cell type biases in case of blood, or were more balanced for correlation profiles. Ranked gene expression correlation profiles for whole blood GC signatures 1 and 2 with different cell type biases (Table S1) can be reproduced using precalculated results obtained with R script (selectcollections.R) on dataset collections of whole blood in the absence of severe inflammation (n= 15), and whole blood in the presence of severe inflammation (n= 15), using the provided R script (signaturescollections.R). Both R scripts are in folder “code” in GitHub repository (https://github.com/ArthurJohannes/GCblood_repo).

medRxiv preprint doi: https://doi.org/10.1101/2023.05.10.23289779; this version posted November 4, 2024. The copyright holder for this preprint (which was not certified by peer review) is the author/funder, who has granted medRxiv a license to display the preprint in perpetuity. All rights reserved. No reuse allowed without permission.

Relating gene expression correlation profiles

Average gene expression correlation profiles were compared for reciprocal ranking of genes in related profiles to determine the existence of clusters of correlated gene expression by meta-analysis. Using the method described above, reciprocal average correlation values between gene pairs (a,b and b,a) were only identical if identical corresponding gene probes were used, which mostly applies to RNA sequencing data, and when using the same (all) datasets in the dataset collection for both genes. Ranking gene expression correlation values in profiles obtained either on a single dataset or from meta-analysis, results in different reciprocal rankings for gene pairs (rankings for a,b and b,a are different), and asymmetric matrices of gene rankings. An "inside" gene in a large tight co-expression cluster may have higher ranking (closer to 1) in a profile of an "outside" gene than the other way around. This allows easier grouping of the "outside" gene with the large cluster which can be useful, and indicate (marginal) gene induction in case of such clusters resulting from specific gene induction. Initial ordering of rows and columns was guided by hierarchical clustering using the corresponding matrix of reciprocal average correlation coefficients. The order of rows of gene profiles and genes in profiles (columns) was then modified and set to indicate relevant gene groups such as co-expression clusters, and also genes with shared inductions but found outside tight co-expression clusters for the induction, and possibly in other co-expression clusters. The latter groupings were aided by sorting genes present in marker gene profiles according to ranking, and reciprocally, sorting profiles for their ranking of marker genes. The final chosen setting kept order of genes in rows and columns identical. An annotated R script (reciprocalcollections.R), and precalculated results obtained for 19 genes including sets GC-1 and GC-2, using the R script described earlier (selectcollections.R) replicates similar matrices as shown for larger dataset collections on blood in the absence of severe inflammation (n= 40), and on blood in the presence of severe inflammation (n = 38) (Figure 3A, 3B). Both R scripts are in folder "code" in GitHub repository (https://github.com/ArthurJohannes/GCblood_repo).

Using gene sets and modules

Different methods exist to summarize expression values of co-expressed genes in a single composite score. Using arithmetic mean expression of all genes in a module is inadequate considering the large differences in relative expression levels between genes. Gene module

medRxiv preprint doi: https://doi.org/10.1101/2023.05.10.23289779; this version posted November 4, 2024. The copyright holder for this preprint (which was not certified by peer review) is the author/funder, who has granted medRxiv a license to display the preprint in perpetuity. All rights reserved. No reuse allowed without permission.

expression values can be determined for single samples, using the geometrical mean expression of genes in a module (Petri et al., 2019), using eigengenes (Langfelder & Horvath, 2008), single sample GSEA (Barbie et al., 2009), the percentage of upregulated or downregulated genes in a module, compared to a control group, and using normalized expression, such as averaging fold change for individual genes compared to median expression in a control group (Altman et al., 2021; Chaussabel & Baldwin, 2014; Chaussabel et al., 2008), and such as mean of Z-scores for each gene in a set (Petri et al., 2009). While mean of Z-scores, possibly followed by rescaling, might be optimal, to compare module expression between samples in a single experiment, it does not indicate fold change. For a balanced use of GC inducible genes in gene sets GC-1 (n= 7) and GC-2 (n= 9), it was important to account for differences in ratios of maximal and minimal expression for different genes in the set, and also for the presence of microarray platform background levels which varied with specific gene probes, and which also depended on the method used in data processing. Datasets were first converted to linear scale, if necessary. When using gene modules with microarray data, only adequate and identical gene probes were used in case of Affymetrix GPL570, or Illumina GPL10558 microarray platforms, or else gene probes with highest expression levels in the experiment. Gene expression values in a sample were divided by expression range (max-min) of the corresponding gene in the whole dataset, and then multiplied by a constant (sum of gene expression ranges in module divided by number of genes in module) to keep expression values closer to starting values. In case of microarray data, the resultant gene expression values were subtracted with their minimal value to avoid potentially large contribution of background for specific probes. The arithmetic mean was then taken for resultant values of all genes in the module per sample, as a measure of gene module expression. Module expression values were plotted as binned dot plots with boxplot overlay, excluding the boxplot outlier points, on the log2 scale, and using similar Y axis interval sizes to allow for a better comparison between datasets. Annotated R scripts and corresponding datasets are provided in a GitHub repository folder to reproduce results of gene module expression in burn shock (plotmodulesgse77791.R, GSE77791, microarray GPL570 (Plassais et al., 2017)) (Figure S14 C), severe malaria (plotmodulesgse34404.R, GSE34404, microarray GPL10558 (Idaghdour et al., 2012)) (Figure S15 F), and obtain results of single gene, and gene module expression in sepsis (plotgenesgse154918.R, plotmodulesgse154918.R, GSE154918, RNA-seq (Herwanto et al., 2021)) (https://github.com/ArthurJohannes/GCblood_repo/tree/main/plotting).

medRxiv preprint doi: https://doi.org/10.1101/2023.05.10.23289779; this version posted November 4, 2024. The copyright holder for this preprint (which was not certified by peer review) is the author/funder, who has granted medRxiv a license to display the preprint in perpetuity. All rights reserved. No reuse allowed without permission.

Using R and figures preparation

Data were analyzed using R programming language for statistical computing and graphics, in RStudio IDE desktop. The gGPLot2 R package (Wickham, 2016) was used for plotting. For aligning plots, use was made of the R packages grid (Murrell, 2002), gridExtra (Auguie et al., 2017), and package gtable contained in gGPLot2. Package pheatmap (Kolde, 2019) was used for hierarchical clustering of correlation matrices, using Euclidean distance (not directly using correlation dissimilarity as a distance), and clustering method complete, and for custom annotation. R packages xlsx (Dragulescu, 2012), and readxl (Wickham et al., 2019) were used for writing and reading Excel files, or WPS spreadsheet files. Tables were edited in WPS or Excel spreadsheets. Figure PDFs were arranged and edited in Inkscape (Inkscape project, 2020), or created with BioRender.com.

RESULTS

Obtaining 2 blood transcriptomic signatures of GC induction

Two different gene expression correlation clusters originating from induction by GC were observed in many blood transcriptomic datasets, one in health, and another in severe inflammation, for example, in health for datasets GSE11761, GSE14642, and GSE57065 (Cazalis et al., 2014; Radom-Aizik et al., 2009a, 2009b), and in critical illness and sepsis for datasets GSE9960 (Tang et al., 2009), and GSE57065 (Figure S1). Exploratory work using programmatically selected datasets from a large collection of 375+ blood transcriptomic datasets indicated that 2 corresponding gene expression correlation signatures could be obtained in meta-analysis: One in the relative absence of severe inflammation (signature 1), the other in the presence of severe inflammation (signature 2). A gene set (n = 227) of candidate GC-regulated genes was derived from high-ranking genes in these earlier signatures of GC-driven gene expression *in vivo* (Table S2). To obtain reproducible, corresponding gene expression correlation signatures, 2 whole blood dataset collections were assembled based on experimental description. The dataset collection in the absence of severe inflammation (n = 40) included health and vaccination, and also excluded diseases where GC usage in treatment is common, such as SLE, RA, and MS. The collection in the presence of severe inflammation (n = 38) mainly included datasets on sepsis (Table S1). Gene expression correlation rankings for all datasets in a single collection were first obtained for a single GC inducible query gene. An averaged correlation ranking for a single query gene used a single best gene probe for

medRxiv preprint doi: https://doi.org/10.1101/2023.05.10.23289779; this version posted November 4, 2024. The copyright holder for this preprint (which was not certified by peer review) is the author/funder, who has granted medRxiv a license to display the preprint in perpetuity. All rights reserved. No reuse allowed without permission.

each dataset. Results for different suitable query genes were grouped according to cell type bias, and again averaged to obtain multigene expression correlation signatures, namely 2 in the absence of severe inflammation, and 3 signatures in the presence of severe inflammation (Figure 1A and B, Table S1). In case of lymphocyte bias, only a single query gene DDIT4 was used on both collections allowing for a direct comparison of the corresponding signatures (Figure 1B, Table S1). Several query genes such as VSIG4 and ADAMTS2 (both monocyte bias), and OLAH (neutrophil bias) only showed strong GC-driven gene expression correlation in the presence of severe inflammation, whereas other query genes could be used on both collections (Figure 1B). The cell type biased signatures obtained either in the absence of severe inflammation (n =3), or in the presence of severe inflammation (n= 4) are together referred to as GC signatures 1 and 2, respectively. Repeating the procedure on 2 subcollections of 15 datasets each yielded highly similar GC signatures 1 and 2 as shown (Figure 1B, Table S1). Genes PIK3IP1, FBXO32, BTG1, and DUSP2 were typically present in lymphocyte-biased signatures of GC-driven gene expression in whole blood and also in PBMCs in the absence of severe inflammation (Table S1 and S3). Since muscle, skin, and fat represent well known and important tissue targets for GCs, we also applied the procedure to corresponding datasets collections. Distinct but partially overlapping correlation signatures of circadian GC-driven and molecular CLOCK-driven gene expression were readily obtained for these tissues (Table S3). In contrast, CLOCK-driven gene expression was not detected in whole blood and isolated blood cells. High ranking GC signature genes in muscle included transcription factors FOXO3 and FOXO1, and GLUL (encoding Glutamate-Ammonia Ligase) as expected, in skin BCL6 and FOXO1, and in fat, ERRFI1, RHOB, and ITPKC (encoding Inositol-Trisphosphate 3-Kinase C) (Table S3). A good overall signature of GC-driven gene expression in blood and tissues was obtained by ranking genes by frequency of their presence in the first 2000 genes in 16 separate GC signatures (Table S2). More than 1000 candidate GC-regulated genes were indicated by further comparison with *in vitro* upregulated DEGs. Among most frequently upregulated genes were negative regulators of MAPK and NF-kB signaling (DUSP1, TSC22D3, NFKBIA), and transcription factors KLF9, ZBTB16, CEBPD, PER1, and ETS2, as expected (Table S2).

Many high ranking genes in whole blood GC signatures are induced by GC *in vitro*

The signature genes found by correlation search may come from variable differential gene expression due to upregulation by GCs, or more indirectly due to shifts in cell type percentages caused by cortisol in healthy people (GC signature 1), or the appearance of

medRxiv preprint doi: https://doi.org/10.1101/2023.05.10.23289779; this version posted November 4, 2024. The copyright holder for this preprint (which was not certified by peer review) is the author/funder, who has granted medRxiv a license to display the preprint in perpetuity. All rights reserved. No reuse allowed without permission.

specific cell types in severe inflammation (GC signature 2). Therefore, it was important to determine which signature genes could be observed as DEGs *in vitro*, and at the same time determine the cell types involved at basal and induced gene expression levels. A total gene set of high ranking and/or recurrent genes in whole blood GC signatures 1 and 2 was selected to contain best candidate genes for induction by GC as detailed (Table S2, sheet3). Genes in this set (n = 489) were compared with 9 sets of *in vitro* GC-induced DEGs, taken at a cut-off of 2 fold induction and with unadjusted p-value < 0.05, in different immune cells and PBMC preparations (Figure 1C, 1D, and Table S2). Overlap with different DEG sets was in the range of 5-31 % and higher with myeloid cells than with lymphoid cells in experiment GSE112101 (Franco et al., 2019), suggesting a relatively high contribution of monocyte and neutrophil gene expression to the GC signatures-derived gene set (Figure 1C). Frequent DEGs were well represented in whole blood GC signatures (Figure 1D). Genes FKBP5, SESN1, and TSC22D3 were present in all DEG sets (Table S2). The DEG sets excluded 249 potentially GC-induced genes while 86 genes were detected only once in these experiments. Signature genes that were absent in DEGs included a limited number of NK-expressed genes (PRF1, GZMB, etc.). These genes originated from the DDIT4 query-derived signature obtained in the absence of severe inflammation, and were likely due to increased NK percentages. The high proportion of genes in the GC signatures-derived gene set upregulated by GC *in vitro* (49 %) indicated that the signatures largely originated from GC gene induction rather than from accompanying shifts in cellular blood count.

Basal gene expression and induction by GC in different cell types *in vitro*

In a next step, a large number of GC signature genes and different marker genes, used as controls, were directly compared for basal expression levels in separated blood cells, and for their induction by GC *in vitro*. Gene expression was profiled using RNA-seq experiment GSE60424 on separated immune cells from different illnesses, (Linsley et al., 2014) excluding sepsis, RNA-seq experiment GSE112101 which studies GC gene induction *in vitro* in different cell types, including isolated immune cells (Franco et al., 2019), RNA-seq experiment GSE109439 on GC gene induction *in vitro* in monocytes and macrophages (Wang et al., 2019), and microarray experiment GSE100531 on GC gene induction in M1 macrophages (Gharib et al., 2019). Basal level expression data from experiment GSE60424 and GSE112101 were largely similar as expected, although with some differences, e.g. in case of CXCR4, TSC22D3, and FLT3 (Figure S2). A limited number of genes (n= 19) were selected for subsequent expression profiling, including most genes used as queries to obtain

medRxiv preprint doi: https://doi.org/10.1101/2023.05.10.23289779; this version posted November 4, 2024. The copyright holder for this preprint (which was not certified by peer review) is the author/funder, who has granted medRxiv a license to display the preprint in perpetuity. All rights reserved. No reuse allowed without permission.

whole blood GC signatures 1 and 2, as well as additional genes used in 2 gene sets GC-1 and GC-2 drawn up for possible biomarker use (see below) (Figure 2A). Gene ZBTB16 was preferentially expressed in B and NK cells, IRS2 was highly expressed in neutrophils, and KLF9 had low basal expression in neutrophils in both experiments GSE112101 (Franco et al., 2019) and GSE60424 (Linsley et al., 2014) (Figure 2B, and Figure S2). Genes CD163, VSIG4, and ADAMTS2 were specifically expressed in monocytes, FLT3 and MAOA preferentially in monocytes, ADORA3 in both monocytes and neutrophils, while OLAH, DAAM2, and ARG1 were preferentially expressed in neutrophils (Figure 2B). Basal expression of ADAMTS2 and FLT3 was higher in monocytes than in monocyte-derived macrophages, while expression of CD163, VSIG4, MAOA, and ADORA3 genes was higher in macrophages instead. *In vitro* upregulation by GC in different separated immune cells and in macrophages was visible at least once for these 19 genes, sometimes even in cell separations with very low/absent basal expression, as in case of CD163 in B cells and VSIG4 in T cells, probably due to small amounts of contaminating myeloid cells (Figure 2B). Gene ARG1 was upregulated by GC in neutrophils (Figure 2B).

Frequent GC activity in septic plasma in neutrophil reporter assays

GC treatment *in vitro* will result in many upregulated and downregulated genes, also depending on duration of treatment. The 19 selected genes were upregulated by *in vitro* GC treatment of PBMCs in 3 experiments from 6h to 72h (Hu et al., 2018; Maranville et al., 2013; Seah et al., 2022), with the exception of MAOA (Figure 2C left panel). Downregulation of HLA-DR marker gene expression by GC was visible, in agreement with the known transcriptional effect of GC on monocytes *in vitro* (Tulzo et al., 2004). Inhibition by GC of early gene activation in PBMCs (Figure 2C left panel), occurring *in vitro*, agreed with inhibition of pro-inflammatory signal transduction by GC, involving MKP-1 (DUSP1), and GILZ (TSC22D3), as described for monocytes (Ehrchen et al., 2019). Khaenam et al., (2014) reported a set of 30 gene transcripts responsive to septic plasma in neutrophil reporter assays, which they used to predict sepsis severity. This set contained 9 genes also prominently present in the GC signatures reported here, including well-known GC inducible genes such as KLF9 and FKBP5. Many other GC-regulated genes were also induced by sepsis plasma, including 13 out of the 19 pre-selected genes used here for expression profiling (Figure 2C right panel), indicating relatively high concentrations of GC compared to control plasma. Strong induction could be observed at a high frequency of approximately 50 in 73 unique sepsis plasma, above the maximal induction level seen in the healthy control plasma. Since potential GC usage was

medRxiv preprint doi: https://doi.org/10.1101/2023.05.10.23289779; this version posted November 4, 2024. The copyright holder for this preprint (which was not certified by peer review) is the author/funder, who has granted medRxiv a license to display the preprint in perpetuity. All rights reserved. No reuse allowed without permission.

not reported for these experiments (Khaenam et al., 2014), it could not be determined whether this frequent GC activity might also be endogenous, or just always derived from exogenous GC in treatment. Sepsis plasma from neutrophil reporter assay experiment GSE49756 also showed additional immunomodulatory activities corresponding with induction by interferon gamma, as well as NF-kB-dependent induction, as shown by upregulation of marker gene IL1B (Figure 2C right panel).

Circadian GC, and GC in severe inflammation, drive different patterns of gene expression in blood, monocytes, and neutrophils

To examine differential expression correlation of GC signature genes in health and in severe inflammation more precisely, we used reciprocal ranking of genes in expression correlation profiles, directly comparing the 19 preselected genes. Separate collections of monocyte and neutrophil transcriptomic datasets were assembled, also based on the absence or presence of severe inflammation, according to provided metadata and experimental description. Collections of (sub)datasets in the absence of severe inflammation included only healthy controls in case of both monocytes (n= 8), and neutrophils (n= 6), while collections in the presence of severe inflammation included datasets mainly on sepsis for either monocytes (n= 11) or neutrophils (n= 10) (Table S3). Different correlation patterns were present dependent on the presence or absence of severe inflammation in blood, and also in isolated monocytes and neutrophils (Figure 3). In blood, in the absence of severe inflammation, expression of genes MAOA, ADORA3, and CD163 was more correlated with cell type specific expression (reticulocytes, eosinophils, and classical monocytes, respectively), while genes ADAMTS2, and AMPH, failed to yield good average gene expression correlation profiles, due to detection limits (Figure 3A). In the presence of severe inflammation, expression was more correlated, with the exception of the gene encoding CXCR4 (Figure 3B). From this analysis, using additional gene expression correlation, and differential expression data, we selected GC-1 (ZBTB16, KLF9, DDIT4, TSC22D3, PER1, IRS2, CXCR4), and GC-2 (VSIG4, ADAMTS2, FLT3, MAOA, AMPH, ADORA3, MACIR, OLAH, DAAM2) gene sets for possible use as whole blood transcriptomic biomarkers in health, and severe inflammation, respectively, as detailed (Figure S3, and Figure S4). In the absence of severe inflammation, clustering was best visible for set GC-1, and also FKBP5, which was tighter in monocytes than in blood (Figure 3A, 3C), likely due to a lower cellular complexity. Datasets on isolated monocytes and neutrophils often showed evidence of contaminating cells, confounding gene expression correlation results to some extent. ARG1 expression correlated with other high ranking GC

medRxiv preprint doi: https://doi.org/10.1101/2023.05.10.23289779; this version posted November 4, 2024. The copyright holder for this preprint (which was not certified by peer review) is the author/funder, who has granted medRxiv a license to display the preprint in perpetuity. All rights reserved. No reuse allowed without permission.

signature genes in neutrophils in severe inflammation, but not in monocytes (Figure 3D, 3F). High expression correlation between VSIG4 and ADAMTS2 was also visible for neutrophils in severe inflammation (Figure 3F), likely due to monocyte contamination. A comparison of RNA-seq datasets with circadian sampling in health (Braun et al., 2018), and in bacterial infection and sepsis (Herwanto et al., 2021) indicated tighter clustering for genes in set GC-2 in the latter (Figure 3G, 3H). Large differences in relative mRNA abundance (appr. > 1000 x) existed between the 19 genes based on TPM, and normalized count values, with TSC22D3, and CXCR4 mRNA being more abundant, and in severe inflammation, also enhanced expression of IRS2, FKBP5, CD163, and ARG1 mRNA was found (Figure 3G, 3H).

Gene induction in vivo by endogenous GC and experimental GC treatment in health

The presence of 2 signatures of GC-driven gene expression in blood in health and in severe inflamamtion might result from different relative induction levels of GC target genes, primarily depending on the concentration and duration of the GC stimulus, or alternatively, might be more conditional on the absence or presence of severe inflammation, and the accompanying cell types. To first address these alternative possibilities, GC-upregulated gene expression *in vivo* was compared using 3 informative PBMC gene expression datasets. Experiment GDS3704 (Bouwens et al., 2010), using PBMC samples taken 6h apart, did not show large shifts in cell percentages between time points, as indicated by similar NK and monocyte marker gene expression levels (Figure 4A). As a consequence, GC signature genes represented a high proportion of upregulated DEGs at the earlier timepoint (Table S4 sheet 1). Both monocyte and lymphoid cell expressed gene clusters were visible among GC signature DEGs (Figure S5), with tight clustering of set GC-1 genes, and also FKBP5 (Figure 4C). Genes VSIG4, ADAMTS2, CD163, and AMPH were not detectably upregulated, while other monocyte expressed GC-induced genes, such as FLT3, ALOX15B, GPER1, and MARVELD1 could be detected as DEGs in this experiment (Figure 4A, and Table S4 sheet 1). In contrast, experimental *in vivo* GC treatment in health (Carlet et al., 2010; Olnes et al., 2016) caused large shifts in cell percentages in PBMCs with increased NK and decreased monocytes at earlier time points (Figure 4A), as described (Olnes et al., 2016). In these experiments, VSIG4, ADAMTS2, and AMPH were co-upregulated upon *in vivo* GC treatment (Figure 4A, 4D), indicating that detectable induction of these genes in PBMCs was not strictly conditional to severe inflammation, and more a consequence of GC stimulus strength above circadian levels.

medRxiv preprint doi: https://doi.org/10.1101/2023.05.10.23289779; this version posted November 4, 2024. The copyright holder for this preprint (which was not certified by peer review) is the author/funder, who has granted medRxiv a license to display the preprint in perpetuity. All rights reserved. No reuse allowed without permission.

Gene induction *in vivo* by endogenous and therapeutic GC in sepsis and burn shock

Recent blood (cell) transcriptomic data, taken together, describe a large number of GC inducible genes in blood in therapy with GC (see introduction). In case of septic shock, 204 genes expressed in blood were reported to be modulated by GC treatment (Wong et al., 2014), and 175 genes in case of burn shock (Plassais et al., 2017). However, likely GC target genes in upregulated DEGs were not identified by these studies, beyond a limited number (n = about 5) using IPA (Ingenuity pathway analysis) (Plassais et al., 2017). Another dataset GSE106878 on GC treatment of septic shock, was published by Kolte and co-workers (2019), but without full listing or identification of GC upregulated DEGs (Kolte, 2020). Here we compared upregulated DEGs from these 3 whole blood microarray datasets on GC treatment in septic and burn shock, and checked their *in vitro* upregulation by GC in monocytes and neutrophils (Franco et al., 2019), and their ranking in GC signatures 2, and signatures of GC-driven gene expression from isolated neutrophils and monocytes in severe inflammation. Extensive overlap was found, thus extending the number of likely GC-induced genes (n > 150) among upregulated DEGs, including set GC-1 and set GC-2 genes, with the exception of CXCR4 in set GC-1 (Table S4). In GC-treated septic and burn shock, shifts in cell type percentages caused by GC treatment were limited (Figure 4B), likely resulting in a large proportion of GC inducible genes in the upregulated DEGs. As in case of PBMCs in health (Figure 4A), set GC-2 was not useful to monitor circadian GC action in whole blood (Figure 4B). A time course experiment of whole blood gene expression in health (GDS2767 (Baty et al., 2006)), showed upregulation of several GC-1 set genes including CXCR4, but not GC-2 set genes. An increase in NK cell percentages was found in the morning (Figure 4B). To determine whether the presence of GC signature 2 in severe inflammation would always be related exclusively to GC treatment, we examined gene expression correlation patterns in untreated patient groups. Correlation patterns in GC-untreated burn and septic shock data were also indicative for GC signature 2, for example by high ranking of GC-2 set genes in ZBTB16, ADAMTS2, CD163, and ADORA3 profiles (Figure 4E, 4F). This analysis showed a specific effect by endogenous GC before treatment, on blood gene expression in severe inflammation, which might depend on the presence of an increased GC stimulus compared to circadian GC in health.

Using gene set GC-1 as a transcriptional biomarker for circadian cortisol

Major sources of intra-individual variability in cellular blood count in health are circadian rhythm (Ackermann et al., 2012), and exercise (Gustafson et al., 2017). As a result, relative gene expression changed in a circadian fashion, which was in close relation to circadian

medRxiv preprint doi: https://doi.org/10.1101/2023.05.10.23289779; this version posted November 4, 2024. The copyright holder for this preprint (which was not certified by peer review) is the author/funder, who has granted medRxiv a license to display the preprint in perpetuity. All rights reserved. No reuse allowed without permission.

changes in differential (relative) blood counts. Well visible circadian expression in longitudinal respiratory viral challenge experiment GSE73072 (Liu et al., 2016) was used as a co-selection criterion for set GC-1 (Figure S3B), to minimize the confounding effect of circadian change in cell type percentages. This experiment sampled whole blood, during several days, mostly at 3 time points per twenty-four hours for a larger number of individuals, using a microarray platform. C1QA gene expression in non-classical / intermediate monocytes was upregulated during inflammation in influenza, compared to marker genes used for neutrophils (Figure 5, row 1 panels) and classical monocytes (Figure 5, row 2 panels). Gene induction also marked ongoing inflammation, for example, in case of IL1B, interferon alpha inducible genes OASL and IFI27, and interferon gamma inducible GBP1 (Figure 5). Expression of all 7 genes in set GC-1 was visibly circadian (Figure S3B), with highest expression at early day as shown for DDIT4 (mostly expressed in NK cells), and TSC22D3 (mostly neutrophil) (Figure 5). Several GC signature 1 genes were upregulated during inflammation (eg SOCS1, NFIL3, CLEC4E, PELI1, TNFAIP3), but not genes selected in set GC-1 (Figure S3B). A composite value of gene expression in the set (see methods) was used to visualize circadian cortisol action in health, which also continued during mild inflammation, but from a lower basal level. Some variability in mean and range of DDIT4, TSC22D3, and set GC-1 expression between healthy individuals was apparent, which may relate to small individual differences in circadian cortisol phase, longer lasting individual differences in cellular percentages (as a confounder) or to actual individual differences in strength of GC induction (Figure 5). In conclusion, gene set GC-1 was suitable for longitudinal monitoring of circadian GC activity in whole blood, and was not induced by systemic mild inflammation caused by uncomplicated respiratory viral infection.

Specific gene induction in severe inflammation compared to mild inflammation

GC inducible gene expression was upregulated during severe inflammation but not during mild inflammation, as in case of set GC-1 genes which retained circadian expression in experimental respiratory viral infection. For a better view of GC signature gene expression in severe inflammation, it was important to first differentiate gene expression in mild and severe inflammation more generally. Therefore, datasets on mild respiratory viral infection (Zhai et al., 2015), and sepsis (Burnham et al., 2017), were directly compared for gene expression correlation, and differential expression with healthy controls, using identical Illumina gene probes. Longitudinal data on mild seasonal respiratory viral infection, agreed well with experimental viral challenge (GSE73072, (Liu et al., 2016), as visible for interferon alpha

medRxiv preprint doi: https://doi.org/10.1101/2023.05.10.23289779; this version posted November 4, 2024. The copyright holder for this preprint (which was not certified by peer review) is the author/funder, who has granted medRxiv a license to display the preprint in perpetuity. All rights reserved. No reuse allowed without permission.

inducible genes OASL, and IFI27, still upregulated at day 6 after first symptoms, especially in influenza, as reported by Zhai et al., (2015), (Figure 6B). Differential expression correlation between disease days 0-6 in mild respiratory viral infection, and sepsis was determined for marker genes for different cell types and specific inductions. Gene expression correlation clusters originating in inflammation were conserved to different degrees in respiratory viral infection and sepsis. More conserved clustering included marker genes for induction by interferon alpha and gamma, genes CASP1 and CASP4, and other genes indicated in red (Figure 6A). Different or new clustering in severe inflammation included GYG1 with CEACAM1 and MMP8 in neutrophils, and C1QA/B/C genes with PPARG and VSIG4 in monocytes, as indicated in black (Figure 6A right panel). STAT3-dependent inductions of SOCS3, and SBNO2 were associated with inflammation, and development, respectively. Gene expression clusters corresponding to classical monocytes, and non-classical / intermediate monocytes were visible in mild inflammation, and related clusters corresponding to MS1 and MS3 monocyte states (Reyes et al., 2020) in sepsis (Figure 6A). Combined correlation and differential expression analysis of genes AZU1 and MMP8 indicated that neutrophils with banded nuclei were not increased during mild inflammation, while these immature neutrophils were increased in severe inflammation (Figure 6A, 6C, 6D), consistent with emergency granulopoiesis occurring in sepsis (Kwok et al., 2023). Gene GYG1 encoding glycogenin, used as a marker for glucose metabolism mainly in neutrophils, was more upregulated at a higher frequency in sepsis than in mild inflammation (Figure 6C, 6D). Other genes, highly upregulated in severe inflammation, but not in mild inflammation, included GC signature 2 genes OLAH (mainly in neutrophils), ADAMTS2, and VSIG4 (both in monocytes), as well as genes not regulated by GCs such as FAM20A, and METTL7B (Figure 6C, 6D). Inductions involving interferon were also visible in sepsis, but from a relatively lower basal level, possibly due to large shifts in global gene expression.

Gene induction by GC in myeloid cells in health and during severe inflammation

In addition to GC signatures 1 and 2, signatures of GC-driven gene expression were also obtained for monocytes, and neutrophils, in each case distinguishing between the presence or absence of severe inflammation according to description (Table S1, Table S3). These signatures predicted wide ranging effects of GCs on cell biology. Based on gene functional categories, this included modulation of phagocytosis and cell motility, modulation of secretory pathway activity, increased sphingolipid synthesis, and uptake of apoptotic cells (efferocytosis) by monocytes during severe inflammation (Figure S6). Specific gene sets for

medRxiv preprint doi: https://doi.org/10.1101/2023.05.10.23289779; this version posted November 4, 2024. The copyright holder for this preprint (which was not certified by peer review) is the author/funder, who has granted medRxiv a license to display the preprint in perpetuity. All rights reserved. No reuse allowed without permission.

monocytes and neutrophils were derived by combining relevant GC signatures (Table S2) increasing the total number (n = 625) of candidate GC-regulated genes recovered from blood and separated cells (Table S2). Comparing with *in vitro* data showed 50 % of these genes being upregulated by GC at least once in 9 experiments (Table S2). To relate differences in GC-regulated gene expression to inflammation status, we used the monocyte and neutrophil dataset collections, that were aided by data on *in vitro* inducibility in myeloid cells by interferons and interleukins (GSE190594; (Green et al., 2023), GSE131990; (Devlin et al., 2020), GSE146438; (Gorby et al., 2020)), and *in vivo* differential expression in health, interferon treatment in MS, and sepsis (GSE60424; (Linsley et al., 2014), GSE133822; (Washburn et al., 2019), GSE123729; (Coulibaly et al., 2019)). Isolation of monocyte and neutrophils from whole blood generally resulted in early gene activation, as was evident from increased expression of immediate early genes, and the presence of corresponding gene expression correlation clusters (Figure S7, S8, S9, S10). Whole blood gene expression data were used instead to determine *in vivo* expression of such genes in neutrophils, in case of mainly neutrophil-derived gene expression clustering. Gene expression originating from contaminating cells was identified by using suitable marker genes (Figure S7, S8, S9, S10). An overview shows the presence of different myeloid cell types and gene inductions as seen in homeostasis, inflammation, and in severe inflammation (Figure 7). Gene expression correlation clusters corresponding to neutrophils with banded nuclei and (meta)myelocytes were visible in collections of control neutrophils (Figure S9), and neutrophils in severe inflammation (Figure S10), respectively. Intermediate / non-classical monocytes were present in the absence of severe inflammation (Figure S7). A gene expression correlation cluster of C1QA/B/C genes, OLFML2B, SLCO2B1, VSIG4, MSR1, MRC1 (encoding M2 macrophage marker CD206), and LYVE1 (macrophage marker in mononuclear phagocytes), in severe inflammation, indicated the presence of M2 macrophage-like monocytes (Figure S8). Gene induction involving interferons alpha and gamma was well visible in dataset collections of control neutrophils and monocytes (Figure S7, S9), likely due to a low frequency of samples with mild inflammation occurring in the control groups. Gene induction in monocytes and neutrophils during mild inflammation, not involving interferon, included marker gene IL1B (NF-kB-dependent, likely induced by cytokines IL1B and/or TNF), and other genes of which several with known STAT3-dependent induction (eg marker gene SOCS3, likely induced by cytokines G-CSF and/or IL6) (Figure S7, S9). Inductions involving interferon remained present during severe inflammation, for example in case of OASL (IFN alpha), GBP2 (IFN gamma), and CASP1 (possibly both IFN-induced and NF-kB-dependent) (Figure S8, S10).

medRxiv preprint doi: https://doi.org/10.1101/2023.05.10.23289779; this version posted November 4, 2024. The copyright holder for this preprint (which was not certified by peer review) is the author/funder, who has granted medRxiv a license to display the preprint in perpetuity. All rights reserved. No reuse allowed without permission.

Upregulation of C1QA/B/C genes and RGL1 in monocytes, and CEACAM1 in neutrophils, no longer involved induction by interferon (Figure S8, S10), as was also observed for whole blood data (Figure 6A). Broadly correlated expression of genes IL1B, GK, NAMPT, and SOD2 in monocytes and neutrophils, as seen in mild inflammation (Figure S7, S9), was also present in severe inflammation (Figure S8, S10). Changes in gene expression during sepsis, relative to healthy controls, were generally much larger in neutrophils than in monocytes, also in many cases of shared upregulation, as visible in dataset GSE60424 (Linsley et al., 2014). Neutrophils reached higher relative expression levels of genes GYG1, HK3, PGD, and LDHA in glucose metabolism (Figure S10), than did monocytes, whereas monocytes reached higher relative expression levels of PPARG (Figure S8). Specific and strong upregulation in monocytes, only in severe inflammation, occurred for genes OLFML2B, EDNRB and LYVE1, the latter also constitutively expressed in neutrophils (Figure S8). A number of genes with absent / low basal expression in health and mild inflammation was strongly upregulated in both monocytes and neutrophils during severe inflammation, including gene FAM20A (Figure S8, S10). FAM20A is prominently present in an IL-10 driven gene signature *in vitro*, in monocytes ((GSE59184 (Montoya et al., 2014), GSE43700 (Teles et al., 2013), GSE47122 (Italiani et al., 2014), GSE146438 (Gorby et al., 2020); GEO2R, and supporting data (Figure S8)), M2c macrophages (Lurier et al., 2017), and IL-10 induced tolerogenic dendritic cells (GSE44719 (Banchereau et al., 2014), GSE45466 (Braun et al., 2013); GEO2R, (Avancini et al., 2023)). These experiments using IL-10 indicated STAT3-dependent induction of FAM20A *in vitro*, but the relevant inducer(s) *in vivo* remained unknown. Larger clusters of GC-regulated gene expression, beyond the genes shown earlier (Figure 3C, 3D, 3E, 3F), were evident from the data on separated monocytes and neutrophils (Table S7, S8, S9, S10). Genes MFGE8 in monocytes, and PFKFB2 in neutrophils, upregulated in severe inflammation, indicated a regulatory role for GCs in efferocytosis, and glucose metabolism, respectively.

Frequent upregulation of set GC-2 genes early and late after severe injury

In case of severe injury, longitudinal data provide a precise time point for the start of severe inflammation. Such data might show whether start of gene induction by GC would correlate with the ordered appearance of different cell types. From the dataset on genomic storm occurring after critical injury (Xiao et al., 2011), neutrophil bands appeared in circulation immediately after injury, while later, immature neutrophils likely corresponded with myelocytes and metamyelocytes originating from emergency granulopoiesis (Figure 8, upper panels). Longitudinal changes in relative gene expression in neutrophils, and monocyte were

medRxiv preprint doi: https://doi.org/10.1101/2023.05.10.23289779; this version posted November 4, 2024. The copyright holder for this preprint (which was not certified by peer review) is the author/funder, who has granted medRxiv a license to display the preprint in perpetuity. All rights reserved. No reuse allowed without permission.

visible, such as a decrease in expression of MME (CD10), a marker gene for old mature neutrophil, and of CD86, a marker gene for antigen presenting monocyte (Figure 8, row 2 panels). Gene marker PPARG for macrophage-like monocyte became upregulated compared to healthy control (Figure 8, row 2 panels). Induction by GC of genes in set GC-2 was frequently visible before, and after appearance of cells from emergency granulopoiesis, both in monocytes (eg VSIG4, ADAMTS2), and in neutrophils (eg OLAH, DAAM2). Although induction of GC-2 genes was frequently observed, a contribution of GC in treatment remained possible, since GC usage was not reported by Xiao et al (2011). VSIG4 expression peaked earlier than ADAMTS2, suggesting a different course for monocyte subtypes after injury (Figure 8, row 3 panels). Taking a similar approach as in case of selecting gene sets GC-1 and GC-2, several relevant gene sets for monitoring inflammation were selected using whole blood gene expression correlation and differential gene expression data, as detailed (Figure S11, and Figure S12). A gene set SIM (for Severe Inflammatory Myeloid cells, including GYG1, n = 16) was selected from a large group of highly upregulated genes in severe inflammation, especially in neutrophils, unrelated to GC induction (Figure S11). A related set FAM20A (n = 4) consisted of genes co-induced specifically in severe inflammation, also unrelated to GC induction (n = 4) (Figure S11). Gene sets were also used corresponding to induction by interferon gamma (n = 23, including GBP1), and interferon alpha (n = 8, including OASL), which were frequently upregulated in mild and in severe inflammation (Figure S12). Additionally, a gene set corresponding to T cells (n = 13, including LEF1, with bias for naive T cell) (Figure S13), was used to follow decreased percentages of T cells during inflammation. Upregulation of SIM set genes occurred immediately after injury, closely followed by upregulation of the FAM20A set, while relative expression of module T cells in blood was decreased instead. Relative expression of T cell module and SIM set was still different from healthy controls at week 4, indicating continued systemic severe inflammation in a number of patients. Combined expression of genes in set GC-2 was increased in most patient blood samples, expression of gene module interferon gamma was relatively unchanged, while expression of module interferon alpha was decreased (Figure 8, lower panels).

Upregulation of GC-2 biomarker set expression by treatment with exogenous GC

Set GC-2 was tested as a transcriptomic biomarker using whole blood data with documented GC treatment. For a more complete description of systemic inflammation, gene sets T cell, SIM, FAM20A (n = 4), interferon gamma, and interferon alpha were used again as additional

medRxiv preprint doi: https://doi.org/10.1101/2023.05.10.23289779; this version posted November 4, 2024. The copyright holder for this preprint (which was not certified by peer review) is the author/funder, who has granted medRxiv a license to display the preprint in perpetuity. All rights reserved. No reuse allowed without permission.

features. Adequate gene probes were selected for each gene in case of Affymetrix GPL570 and Illumina GPL10558 platforms, (Table S5), confirmed by expression correlation clustering using representative datasets (Figure S13). In case of set GC-1, gene PER1 was not included in gene set expression comparison, because of a single suboptimal probe present on the Illumina microarray platforms. Gene modules / sets were used as transcriptomic biomarkers using a measure of combined gene expression in the set (see methods). Expression value distributions were skewed and often with many outliers in case of the inducible modules (Figure 9). Increased expression of GC-1 and GC-2 sets was visible upon systemic GC treatment in burn- and septic-shock (Figure 9A, 9B). Increases in GC-1 and GC-2 expression in SLE and RA patients being treated with GCs (Figure 9C, 9D) agreed with results by Hu et al. (2018), who used an 8 gene molecular signature to monitor GC responses upon GC treatment. Upregulation of set GC-2 relative to GC-1 was much stronger in GC-treated burn shock and septic shock, than in SLE or RA. Expression of SIM and FAM20A gene sets was high in burn shock and septic shock, but relatively unchanged by GC treatment (Figure 9A, 9B). Interferon alpha and gamma modules were upregulated in SLE as expected (Figure 9C), while a marked decrease was visible in case of burn shock (Figure 9A), possibly related to more general shifts in gene expression in myeloid cells.

Upregulation of GC-2 set by endogenous cortisol during severe inflammation in different diseases.

Next, whole blood transcriptomic data covering many different diseases, and preferably including healthy controls, were examined by plotting gene set expression value distributions for patient groups. To allow a better comparison between datasets, the same adequate probes were used again in case of Affymetrix GPL570 and Illumina V3, and V4 (GPL10558) platforms (Table S5). Value distributions were plotted in the same range of 9 log2 units for all datasets, and datasets were grouped together by assay platform, including RNA-seq (Figures S14, S15, S16, S17, S18). The distributions for different sample groups were ordered within an experiment, and tentatively between experiments using the same platform, and between platforms, for use in an overview (Figure 10). Upregulation of SIM set genes was high in severe injury, sepsis, SIRS, severe COVID-19, Kawasaki disease, severe malaria, infectious diarrhea, lung cancer, active tuberculosis, IBD, and SJIA, very low in mild seasonal respiratory viral infection, and absent in latent tuberculosis, and asthma, with strength of differential expression and frequency of cases depending on disease (Figure 10, and Figures S14, S15, S16, S17, S18). Upregulation of FAM20A (n = 4) set genes generally accompanied

medRxiv preprint doi: https://doi.org/10.1101/2023.05.10.23289779; this version posted November 4, 2024. The copyright holder for this preprint (which was not certified by peer review) is the author/funder, who has granted medRxiv a license to display the preprint in perpetuity. All rights reserved. No reuse allowed without permission.

upregulation of the SIM set genes, and was absent in mild respiratory viral infection, latent tuberculosis, and asthma. Expression of gene module IFN gamma was relatively high during active tuberculosis, active sarcoidosis, and leishmaniasis, while gene induction by IFN alpha was relatively high in acute respiratory viral infection, mild influenza, rotaviral diarrhea, and SLE, as expected (Figure 10). Upregulation of set GC-2 was relatively high in sepsis, and in severe COVID-19, besides GC-treated burn shock, and was also detected in additional diseases that are frequently treated by GC, namely severe asthma (exacerbation), JIA, SJIA, sarcoidosis, and IBD, besides SLE and RA (Figure 10, and Figures S14, S15, S16, S17, S18). Upregulation of set GC-2 was also seen in severe inflammation, in diseases that are not commonly treated with GCs, such as severe malaria, and infectious diarrhea, as well as in examples of diseases with explicitly documented absence of GC treatment, besides burn shock, namely in case of acute Kawasaki disease, and sepsis (Figure 10). Gene expression clustering of 19 GC-induced example genes, including set GC-2 was compared between healthy controls, severe malaria, infectious diarrhea, GC-untreated Kawasaki disease, and another example of GC-untreated septic shock (GSE110487, RNA-seq, (Barcella et al., 2018)), to check co-upregulation of the set. Relatively strong clustering of most GC-2 set genes, depending on disease, (Figure S19) indicated that GC-2 set genes were indeed co-regulated, as in case of GC-untreated septic shock and burn shock (Figure 4B, 4E, and 4F). This analysis showed a transcriptomic signature of endogenous cortisol during severe inflammation for different diseases.

Adjustment of GC biomarker sets for different diseases

Gene sets GC-1 and GC-2 partially overlapped with existing whole blood transcriptomic biomarkers for guiding GC replacement therapy in Addisons disease (Sævik et al., 2021), and pharmacodynamic monitoring of therapeutic GC in SLE, and RA (Hu et al., 2018; Northcott et al., 2021). To adjust biomarker gene sets for application in different diseases, we compared correlation characteristics, and fold upregulation for all reported genes separately, using whole blood RNA-seq datasets. These data encompassed the effect of circadian GC in health (GSE113883 (Braun et al., 2018)), GCs in sepsis (GSE154918 (Herwanto et al., 2021)), and in gastroenteritis (GSE69529 (DeBerg et al., 2018)), systemic GC usage in SLE (GSE72509 (Hung, Pratt, Sundararaman, Townsend, et al., 2015)), RA (GSE117769 by Goldberg and co-workers, 2018), severe asthma (GSE207751 by Ginebaugh and co-workers, 2022), JIA, SJIA, IBD (GSE112057 (Mo et al., 2018)), and severe COVID-19 (GSE171110 (Lévy et al., 2021), GSE157103 (Overmyer et al., 2021), GSE206264 (López-Martínez et al., 2023)), as well as

medRxiv preprint doi: https://doi.org/10.1101/2023.05.10.23289779; this version posted November 4, 2024. The copyright holder for this preprint (which was not certified by peer review) is the author/funder, who has granted medRxiv a license to display the preprint in perpetuity. All rights reserved. No reuse allowed without permission.

the effect of high endogenous GC in GC-untreated severe COVID-19 (GSE168400 (Amado-Rodríguez et al., 2022), GSE197204 (López-Martínez et al., 2023)) (Table S6). Gene expression correlation profiles were obtained (Table S6), compared to each other (Figures S20, S21, S22, S23, S24), and checked for the presence of GC signature genes (Table S6, and Figure S25). Fold induction was determined by comparing with healthy controls, where available, and by examining gene expression value distribution range in disease (Table S6, and Figure S25). This analysis also highlighted inadequate annotation of gene ADORA3 on different assay platforms. Genes ADORA3 and TMIGD3 are chromosomal neighbors, and produce different (hybrid) transcripts and proteins (Ranjan et al., 2017), which are not always detected separately, or named correctly on different platforms. Platforms Affymetrix GPL570 and Illumina GPL10558 each contain 2 ADORA3 probesets and no TMIGD3 annotated probesets. Both platforms detect different transcripts according to Ensemble (Harrison et al., 2024), one corresponding with ADORA3, and expressed in eosinophils, another containing TMIGD3 sequence, and GC inducible. The specific probesets used in set GC-2 for both platforms corresponded to TMIGD3 sequence. Best marker genes for circadian GC action in health included set GC-1, additional genes such as FKBP5 and ECHDC3, and partially overlapped with “time telling” genes used in predicting circadian phase in health (Braun et al., 2018; Hughey, 2017; Laing et al., 2017), (Figure 11). Suitable marker genes for monitoring GC action in asthma, RA, and SLE were ZBTB16 (in set GC-1), set GC-2, and additional genes such as FKBP5, ALOX15B, IL1R2, and ARG1, and included most previously reported GC biomarker genes for SLE and RA (Figure 11). MAOA expression in reticulocytes represented an occasional confounder for GC induction. In general, the occurrence of severe inflammation in disease, and associated variability in neutrophils, limited the choice of biomarker genes, especially in severe COVID-19 and sepsis, e.g. excluding IL1R2 (Figure 11).

DISCUSSION

Aim of study and short summary of results

In this study, we aimed to develop gene expression biomarkers for GC action on blood cells. We obtained gene signatures of GC induction by using correlated expression with several well-known GC target genes, used as queries, in meta-analysis of collections of public blood transcriptomic datasets. Different signatures were found depending on the absence or presence of severe inflammation, as in case of sepsis and critical injury. These 2 signatures, which both showed good overlap with GC upregulated genes in immune cells *in vitro*,

medRxiv preprint doi: https://doi.org/10.1101/2023.05.10.23289779; this version posted November 4, 2024. The copyright holder for this preprint (which was not certified by peer review) is the author/funder, who has granted medRxiv a license to display the preprint in perpetuity. All rights reserved. No reuse allowed without permission.

originated from *in vivo* expression, thereby providing an alternative starting point for selecting biomarker genes. GC signatures 1, with different cell type biases, originated from circadian gene induction by GC in lymphocytes, neutrophils, and monocytes. From this signature, we selected a set of genes (GC-1) as best biomarkers for GC action, for use on whole blood in the absence of severe inflammation. Set GC-1 could be used efficiently, to detect induction by endogenous circadian cortisol, and expression was not upregulated during mild inflammation. GC signatures 2, also with different cell type biases, originated from lymphocytes, and from alternatively activated monocytes and neutrophils in severe inflammation. Upregulation of key signature genes expressed in myeloid cells was visible in whole blood, upon GC treatment in burn shock, and septic shock. We demonstrate that expression of a selected set of GC signature 2 genes (GC-2) was well suited to detect gene induction in blood upon systemic GC treatment in SLE, RA, asthma, in septic shock, and in burn shock. GC signature 2 was found in many more different inflammatory illnesses, including Kawasaki disease, severe malaria, severe COVID-19, and gastroenteritis, resulting from both exogenous and endogenous GC. Use of set GC-2 indicated different frequencies and strength of induction in patients depending on illness. Using meta-analysis, we also provide an overview of gene expression, in homeostasis, inflammation, and severe inflammation in circulating monocytes and neutrophils, more generally.

Meta-analysis of gene expression correlation is a useful method

Differential gene expression in blood upon *in vivo* GC or ACTH treatment has been widely studied in humans and animals. The change in blood cell percentages caused by these treatments enormously complicates the interpretation of the transcriptomic data. Potential GC-regulated DEGs in these experiments are usually identified from existing literature, or by comparing *in vivo* with *in vitro* gene induction results, for example in PBMCs (Hu et al., 2018). More exceptionally, a set of co-expressed GC-induced genes in blood of ACTH injected pigs was directly identified by cluster analysis using a single experiment (Sautron et al., 2015). We noticed induction signals originating from circadian and stress-related changes in endogenous cortisol, and sometimes also from GC usage, leading to gene expression correlation profiles in many blood transcriptomic datasets, which provided a useful starting point for finding candidate GC-regulated genes. It indicated that a search would not necessarily be limited to GC administration experiments or studies with documented GC usage, and that Pearson's correlation might be used in meta-analysis to obtain robust gene expression correlation profiles. In case of the initial GC signatures 1 and 2, datasets were

medRxiv preprint doi: https://doi.org/10.1101/2023.05.10.23289779; this version posted November 4, 2024. The copyright holder for this preprint (which was not certified by peer review) is the author/funder, who has granted medRxiv a license to display the preprint in perpetuity. All rights reserved. No reuse allowed without permission.

selected from a total number of 375+ blood transcriptomic datasets, based on the quality of correlation hits. Subsequent gene expression correlation profiles on whole blood were obtained in meta-analysis using transcriptomic datasets collections based on experimental description, to ensure that GC-driven gene expression was separately observed for circadian GC, and GC in severe inflammation. The recovery of known GR target genes in GC signatures, many recurrent candidate genes, and the large overlap with GC upregulated DEGs in blood cells in different *in vitro* and *in vivo* experiments showed that the approach was generally very effective. Likewise, a large overall signature of GC-driven gene expression in blood and tissues, corresponded well with GC upregulated DEGs in immune cells and cell cultures observed *in vitro*. A general advantage of using correlation is its independence from gene expression range and basal expression levels, or background signals often present in microarray data, allowing easier detection of GC-regulated genes at low-fold induction. A difficulty with correlation analysis was that GC-regulated DEGs may drop down in gene expression correlation profiles due to overriding alternative correlations, and thus escape detection.

Circadian GC-driven gene expression

Circadian gene expression in whole blood has been well documented in experiments on insufficient sleep and mistimed sleep (Archer et al., 2014; Arnardottir et al., 2014; Möller-Levet et al., 2013). Circadian rhythms occurring in differential (relative) blood counts (Ackermann et al., 2012; Lange et al., 2022) can be expected to result in mainly cell type-specific circadian gene expression in whole blood. Neutrophil and NK numbers go up at day time, monocyte numbers remain relatively unchanged, while T and B cell numbers go down at early day time, regulated by cortisol via the HPA axis, and catecholamines via the sympathetic nervous system (Lange et al., 2022). It is likely that higher percentages of NK cells and neutrophils, coinciding with higher gene induction by cortisol, lead to the corresponding cell type biases in blood-based GC signatures 1. Using dataset collections of separated monocytes, neutrophils, and PBMCs allowed detection of circadian GC-driven gene expression in different cell types more precisely. Several methods exist to predict the circadian phase from transcriptomic measurements of whole blood (Braun et al., 2018; Hughey, 2017; Laing et al., 2017) and monocytes (Wittenbrink et al., 2018). A glucocorticoid driven network links many of the top ranked biomarker genes for circadian phase in whole blood, indicating gene induction by circadian GC either via local circadian clocks or directly (Laing et al., 2017). In agreement, among the circadian expressed, best “time telling” genes in these studies were many genes

medRxiv preprint doi: https://doi.org/10.1101/2023.05.10.23289779; this version posted November 4, 2024. The copyright holder for this preprint (which was not certified by peer review) is the author/funder, who has granted medRxiv a license to display the preprint in perpetuity. All rights reserved. No reuse allowed without permission.

present here in GC signatures 1 and 2 (9/15 (Hughey, 2017); e.g. 13/76 (Laing et al., 2017); 3/40 (Braun et al., 2018); e.g. 10/34 (Wittenbrink et al., 2018)).

GC-driven gene expression in monocytes and neutrophils.

It has been argued that a better understanding of cell type and tissue specific effects of GCs, would be important for adjusting or developing new therapies (Quatrini & Ugolini, 2021) . Highly cell type specific gene induction upon *in vitro* GC treatment was reported in isolated immune cells and in proliferating non-immune cell cultures, and the global effects of GC in different cells were compared at the molecular pathway level (Franco et al., 2019). Here, we traced *in vivo* effects of endogenous GC on the transcriptome of lymphocytes, monocytes, neutrophils, muscle, skin, and fat, by using expression correlation with GC-induced query genes in meta-analysis. The focus here was on monocytes and neutrophils, since they contributed most to the GC-driven signatures detected in whole blood. Generally stronger signatures present in severe inflammation compared to health, might reflect higher GC levels and induction in severe inflammation than during circadian rhythm. Circadian GC-driven gene expression in health, which would be laborious to document using alternative approaches, showed differences between monocytes and neutrophils, and mostly represented a subset of genes induced in severe inflammation. Finding VSIR, encoding VISTA, as a novel GC-regulated gene in neutrophils added to the importance given to VISTA as a possible therapeutic target in managing cytokine storms (ElTanbouly et al., 2021), Similarly, finding GPER1, encoding the GPCR estrogen receptor, as induced in monocytes, pointed to the anti-inflammatory activity of estrogen on monocytes (Pelekanou et al., 2016), being modulated by cortisol. Gene expression correlation profiles for monocytes in severe inflammation shared many genes, reported as GR-targeted DEGs in monocytes and macrophages *in vitro* (Wang et al., 2019), or as GC-regulated DEGs *in vivo*, in isolated monocytes from giant cell arteritis patients (Estupiñán-Moreno et al., 2022). GC treatment of isolated monocytes triggers an extensive transcriptional program, directing monocyte to macrophage differentiation to an alternatively activated state with anti-inflammatory phenotype (Ehrchen et al., 2007; Ehrchen et al., 2019; Heideveld et al., 2018; Wang et al., 2019). GC treatment of monocyte-derived macrophages also induces alternatively activated macrophage subtypes with roles in wound repair, tissue remodeling and efferocytosis (Abdelaziz et al., 2020; Desgeorges et al., 2019; Ehrchen et al., 2019; Roszer, 2015). Important genes functional in tissue repair (ADAMTS2), (Ehrchen et al., 2019), and efferocytosis (C1QA/B/C, MFGE8), (Ehrchen et al., 2019) were present in gene expression correlation profiles from monocyte separations in severe

medRxiv preprint doi: https://doi.org/10.1101/2023.05.10.23289779; this version posted November 4, 2024. The copyright holder for this preprint (which was not certified by peer review) is the author/funder, who has granted medRxiv a license to display the preprint in perpetuity. All rights reserved. No reuse allowed without permission.

inflammation. Notable with respect to wound healing was regulation by GC of genes ANG, RNASE1, and RNASE4, encoding angiogenic factors. In this way, the response of blood mononuclear phagocytes to GC in severe inflammation resembled alternative activation. Due to tight gene expression correlation clustering caused by induction by GC, assigning gene expression to specific mononuclear phagocytic cell types, such as MS1 monocytes, non-classical monocytes, macrophage-like monocytes, and/or myeloid dendritic cells remained difficult, and would require precise analysis of single cell RNA sequencing data on sepsis. Gene expression correlation profiles for neutrophils in severe inflammation also shared many genes, reported as upregulated DEGs in neutrophils treated by GC (Franco et al., 2019). The GC signatures from blood and isolated neutrophils indicated important effects of GCs on inflammatory neutrophils during severe inflammation, for example modulation of IL1 and IL18 signaling (e.g. by upregulation of IL1 decoy receptor IL1R2, IL18R1, and IRAK3), modulation of leukotriene chemotaxis and synthesis (upregulation of LTB4R encoding leukotriene B4 receptor, and upregulation of ALOX5AP/FLAP), and prostaglandin breakdown (upregulation of HPGD). Secretion of arginase 1, encoded by ARG1, has been implicated in immunosuppression by low density neutrophils in severe inflammation, and arginase derived from tumor infiltrating myeloid cells is an important factor in suppression of the cancer immune response (Grzywa et al., 2020; Mortaz et al., 2018). As ARG1 is also upregulated in neutrophils by *in vivo* dexamethasone treatment of severe COVID-19 (Sinha et al., 2022), and ARG1 is a GC receptor targeted gene in liver (Okun et al., 2015), our results strongly suggest it might be a GC target gene in neutrophils as well.

Cell biology of monocytes and neutrophils in mild and severe inflammation

A very large quantitative and qualitative difference existed between blood gene expression during inflammation in mild respiratory viral infection, and in severe inflammation. Blood gene expression, specific to severe inflammation, is likely ultimately due to gene induction by systemic DAMPs and MAMPs, as in trauma and sepsis (Raymond et al., 2017; Relja & Land, 2020). Blood transcriptomics, including gene expression in monocytes and neutrophils, has been used to correlate gene expression with degrees of severity in COVID-19 (Wang et al., 2022). Immature neutrophils originating from emergency myelopoiesis are a heightened characteristic in severe COVID-19 and sepsis (Aschenbrenner et al., 2021; Kwok et al., 2023; Schulte-Schrepping et al., 2020). Based on their complete absence, we suggest that data on experimental, and prospective, seasonal respiratory viral infection, may represent a clean example of systemic mild inflammation, without a transition to severe inflammation as

medRxiv preprint doi: https://doi.org/10.1101/2023.05.10.23289779; this version posted November 4, 2024. The copyright holder for this preprint (which was not certified by peer review) is the author/funder, who has granted medRxiv a license to display the preprint in perpetuity. All rights reserved. No reuse allowed without permission.

frequently occurring in COVID-19 patients. Mild inflammation as seen in uncomplicated respiratory viral infection was especially marked by inductions involving interferon, and also by upregulation of NF-kB-dependent IL1B, and STAT3-dependent SOCS3, as expected. Upregulation of GK, encoding glycerol kinase, expressed in correlation with ACSL1 and AQP9, mainly in neutrophils in mild inflammation, might indicate increased triacylglycerol synthesis in support of lipid body biogenesis, which is important in the production of inflammatory mediators from arachidonic acid (Melo & Weller, 2016; Weller, 2016). Upregulated expression of CDKN1C and C1QA/B/C genes was consistent with increased frequencies of intermediate monocytes present in blood in mild respiratory viral infection (Vangeti et al., 2023). Differential expression correlation of highly upregulated genes between inflammation in mild respiratory viral infection and in sepsis (as observed for CEACAM8 in neutrophils, and genes FCGR1A/B/C, and RGL1 in monocytes) indicated that genes may become targets for alternative induction pathways in sepsis, and hypothetically, switching from interferon to relatively strong induction by IL6.

Using single-cell RNA sequencing, 4 different monocyte states have been defined in sepsis including a population similar to non-classical monocytes named MS3, expressing high FCGR3A (CD16), and a CD14 +, HLA-DR low subpopulation named MS1. MS1 expresses RETN, and IL1R2, is expanded in sepsis and COVID-19, and originates from altered myelopoiesis in bone marrow (Reyes et al., 2020; Reyes et al., 2021). Additional marker genes can be found for MS1, and for MS3 (e.g. CDKN1C, C1QA/B/C genes) in the study by Reyes et al. (2020). Here, the existence of different gene expression clusters in monocytes in severe inflammation, with either C1QA/B/C genes or CDKN1C (non-classical-like), suggested important heterogeneity in MS3 cells. Of relevance, a macrophage-like cell type, separate from non-classical monocytes, has been characterized by single cell RNA sequencing of cerebrospinal fluid and PBMCs in tuberculous meningitis, expressing C1QA/B/C genes, SLCO2B1, LYVE1, as well as VSIG4, MSR1, and OLFML2B (Mo et al., 2024). Here, we show upregulated co-expression of these genes in monocyte separations, including VSIG4 and C1QA/B/C genes, and upregulation of macrophage marker genes LYVE1, and PPARG, indicating similar circulating macrophage-like cells, more generally in severe inflammation.

Juss et al. (2016) have described a large number of highly upregulated genes in neutrophil separations in ARDS compared to healthy controls. We found that many of these genes were not at all upregulated during inflammation in mild respiratory viral infection. Other genes such as GYG1 were upregulated in mild inflammation, also, but at lower fold change and

medRxiv preprint doi: https://doi.org/10.1101/2023.05.10.23289779; this version posted November 4, 2024. The copyright holder for this preprint (which was not certified by peer review) is the author/funder, who has granted medRxiv a license to display the preprint in perpetuity. All rights reserved. No reuse allowed without permission.

lower frequency. This qualitative transcriptomic difference indicated the importance of distinguishing between mild and severe inflammation. Low density neutrophils (LDNs) containing immature and mature granulocytes expand in sepsis and COVID-19 (Mortaz et al., 2018; Uhel et al., 2017), (Kwok et al., 2023; Reusch et al., 2021; Schrijver et al., 2019; Schulte-Schrepping et al., 2020). Immature granulocytes were indicated here also, by strong correlated upregulation of proliferation and azurophilic granule marker genes. Neutrophils and monocytes in severe inflammation shared upregulation of many genes, including genes co-expressed with FAM20A, and many GC-regulated genes. Upregulation of CD163 and MERTK seen in gene expression datasets in severe inflammation agreed with flow cytometric data of both monocytes and neutrophils in sepsis (Groselj-Grenc et al., 2008; Guignant et al., 2013), and also indicated similar functional changes occurring in neutrophils and monocytes.

Severe inflammation occurring in different illnesses

Upregulated DEGs in myeloid cells in severe inflammation were analyzed by gene expression correlation analysis, to derive more specific features. A SIM (Severe Inflammatory Myeloid) gene set (n = 16) was selected from a large group of upregulated genes in severe inflammation in myeloid cells, and probably remained more heterogeneous with respect to gene regulation. This gene set was well suited to detect severe inflammation in patient samples for many different diseases. Within the large group of upregulated genes, a small subcluster of genes co-expressed with FAM20A in whole blood was used as a potentially informative biomarker gene set (n= 4). Besides FAM20A, genes METTL7B, and CYP19A1 in the set are also upregulated in IL-10 induced M2c macrophages (Lurier et al., 2017). METTL7B and ITGA7 are neighboring genes on chromosome 12, which might suggest shared regulation of gene expression. It would therefore be interesting to determine if FAM20A (geneset) might qualify as a whole blood IL-10 induction biomarker *in vivo*. Another group of upregulated genes in severe inflammation in myeloid cells were GC inducible genes, from which gene set GC-2 (MACIR/C5orf30, ADORA3, DAAM2, OLAH, ADAMTS2, FLT3, VSIG4, AMPH, MAOA) was selected. GC treatment in septic shock and burn shock induced many genes in GC signatures 1, and 2 above the expression level reached by endogenous GC. Previously, upregulated DEGs in GC treatment in septic shock were not discussed as potential GC target genes, possibly since IPA (Ingenuity Pathway Analysis) at the time showed down-regulation of glucocorticoid signaling pathways instead (Wong et al., 2014). A small number of well-known GC target genes were reported as upregulated DEGs in GC treatment in burn shock (Plassais et al., 2017), but not identified within a larger cluster of co-expressed GC-regulated

medRxiv preprint doi: https://doi.org/10.1101/2023.05.10.23289779; this version posted November 4, 2024. The copyright holder for this preprint (which was not certified by peer review) is the author/funder, who has granted medRxiv a license to display the preprint in perpetuity. All rights reserved. No reuse allowed without permission.

genes. Furthermore, upregulation of set GC-2 was frequent in GC-untreated Kawasaki disease, severe malaria, severe COVID-19, and infectious diarrhea, which indicated induction by endogenous GC, and not just by exogenous GC in treatment. These results were in good agreement, with increased serum cortisol present in critical illness more generally, and also in Kawasaki disease (Aso & Satoh, 2021; Sano et al., 2010), severe malaria (Enwonwu et al., 1999; Vandermosten et al., 2023), COVID-19 (Tan et al., 2020), and gastroenteritis (Rezai et al., 2022). Endogenous GC has been discussed as a possible factor in immunosuppression in sepsis (He et al., 2020; Vandewalle & Libert, 2020), although not commonly so (Fu et al., 2023; Hibbert et al., 2018; Liu et al., 2022; Ono et al., 2018; Padovani & Yin, 2024; Torres et al., 2022; Venet & Monneret, 2018). On the other hand, myeloid cells have been widely implicated in immunosuppression in severe inflammation, in case of monocytes (Avendaño-Ortiz et al., 2018; Mengos et al., 2019; Shalova et al., 2015), neutrophils (Darcy et al., 2014; Demaret et al., 2015; Hesselink et al., 2019; Mortaz et al., 2018; Reusch et al., 2021; Silvestre-Roig et al., 2019; Sinha et al., 2022), or both cell types (Reyes et al., 2021; Schrijver et al., 2019; Schulte-Schrepping et al., 2020; Uhel et al., 2017; Venet et al., 2021). Low expression of HLA-DR is typical for monocytes in sepsis, and is an important biomarker for immunosuppression (Cajander et al., 2013; Hibbert et al., 2018; Monneret & Venet, 2014; Torres et al., 2022). Low monocyte HLA-DR expression in septic shock, and after surgery was found to correlate with high serum cortisol in earlier reports, while treatment by GC *in vitro* downregulated HLA-DR (Kim et al., 2010; Tulzo et al., 2004). Here, we find a wide functional range of genes induced by GCs in circulating monocytes and neutrophils in severe inflammation. This likely pointed to an important role for endogenous GCs in immunosuppression in sepsis, via myeloid cells, which would be worthwhile to explore.

Transcriptional biomarkers

Blood gene transcriptional modules of co-expression can be used as a basis for biomarker discovery (Chaussabel & Baldwin, 2014; Chaussabel et al., 2008). Here, we selected 2 gene sets GC-1, and GC-2 for use as blood transcriptomic biomarkers for GC action on cells, based on expression correlation and differential expression analysis of many public datasets. Different sets of GC-induced genes have recently been selected for monitoring the response of blood cells to GC treatment in SLE, RA and Addison's disease (Hu et al., 2018; Northcott et al., 2021; Sævik et al., 2021). Set GC-1 might represent a set suitable for use on whole blood in the absence of severe inflammation, similar to a set of 3 genes (TSC22D3, DDIT4, and FKBP5) proposed for guiding GC replacement therapy in Addison's disease (Sævik et al.,

medRxiv preprint doi: https://doi.org/10.1101/2023.05.10.23289779; this version posted November 4, 2024. The copyright holder for this preprint (which was not certified by peer review) is the author/funder, who has granted medRxiv a license to display the preprint in perpetuity. All rights reserved. No reuse allowed without permission.

2021). Set GC-1 genes are among the high ranking DEGs in PBMCs in GC therapy of Addison's disease reported in a separate study (Chantzichristos et al., 2021), supporting their potential use as biomarkers. In case of inflammatory illnesses, GC-1 set genes would become less suitable for straightforward use on whole blood or PBMCs due to changes in cell percentages, and large shifts in differential gene expression in specific cell types, especially neutrophils, which tend to obscure the existing induction signal. Hu and coworkers developed a set of 8 biomarker genes for GC activity (FKBP5, ECHDC3, IL1R2, ZBTB16, IRS2, IRAK3, ACSL1, DUSP1), based on differential expression seen upon GC treatment both in health and in SLE, which can be applied to whole blood using qPCR (Hu et al., 2018). An alternative set of 5 genes (VSIG4, ALOX15B, CD163, AMPH, IL1R2), based on expression correlation with GC usage in both PBMC and whole blood datasets on SLE, was also tested for biomarker potential (Northcott et al., 2021). These selections apparently originated from induction by GC, in neutrophils and monocytes, respectively. Here, set GC-2 combined several genes highly induced by GC in monocytes and neutrophils in severe inflammation, and was adequate for detecting effects of GC usage in both autoimmune diseases, and in sepsis and burn shock. If required, the present data analysis would also allow a precise selection of GC biomarker genes expressed in either monocytes or predominantly in neutrophils, as well as extension of set GC-2 depending on disease. The more limited choice of suitable genes in sepsis compared to SLE, RA, and asthma might be a consequence of strong additional inductions, besides by GC, occurring in sepsis, e.g. in case of genes IL1R2, IRAK3, and ARG1.

Specific blood transcriptional endotypes in septic shock are associated with increased patient mortality in GC treatment, suggesting it would be important to account for heterogeneity using transcriptomics (Antcliffe et al., 2019; Wong et al., 2015; Wong et al., 2021). Serum IFN gamma / IL-10 ratio has also been proposed as a biomarker to help decide on GC treatment in septic shock (König et al., 2021). As impaired corticosteroid metabolism in sepsis is thought to be a factor in the outcomes of GC treatment (Annane et al., 2019), GC inducible genes TSC22D3 (encoding GILZ), and DUSP1 (encoding MKP1) are included with other biomarkers for stratification in clinical trial RECORDS on corticosteroid (GC + MC) sensitivity in sepsis (Fleuriet et al., 2023). In case of using whole blood transcriptomic data, set GC-2 would represent a more robust alternative biomarker, also in retrospective analysis, and for determining the transcriptomic effects of combined hydrocortisone (GC) and fludrocortisone (MC) treatment. In general, it would be worthwhile to relate set GC-2

medRxiv preprint doi: https://doi.org/10.1101/2023.05.10.23289779; this version posted November 4, 2024. The copyright holder for this preprint (which was not certified by peer review) is the author/funder, who has granted medRxiv a license to display the preprint in perpetuity. All rights reserved. No reuse allowed without permission.

expression to other measurements and clinical data, such as possibly immunosuppression by endogenous GC in sepsis, as well as by exogenous GC in treatment.

Relevant gene module / biomarker combinations have been used for patient stratification in subclasses, for example in SLE, bacterial infection, severe RSV infection, and sepsis (Altman et al., 2021; Banchereau et al., 2016; Banchereau et al., 2012; Northcott et al., 2021; Rinchai et al., 2020). In contrast, gene modules have not been applied in most other studies on stratification of sepsis in endotypes as reviewed (Komorowski et al., 2022; Pelaia et al., 2023; Tsakiroglou et al., 2023). A smart combination of biomarker features, closely corresponding to gene transcriptional modules, would allow a basic description of patient immunological status in different inflammatory illnesses. Gene induction by GC will likely be a relevant feature, as well as, for example, inductions by interferon alpha and gamma in a larger biomarker panel. In future, such panels might then be used for initial classification, and for immune status monitoring, building on more easily understandable features, than in case of existing sepsis endotypes.

LIMITATIONS

GC-driven gene expression correlation profiles were determined here by the transcriptomic datasets present in a collection, and the GC-induced query genes used for obtaining a combined profile, both of which are choices, that can be made differently. Gene expression correlation offers an integral view of cellular processes, which are often not known to be connected. We were most interested in expression correlations with query genes directly caused by gene induction by GC, which necessitated a great deal of cross-checking of different gene expression profiles and comparison with *in vitro* and *in vivo* GC upregulated genes. In case of DEGs a common rule for cut-off is 2 fold change and adjusted p-value below 0.05, whereas selecting best candidate genes for GC induction from GC signatures remained difficult.

Changing percentages of cell types in blood hugely complicates blood transcriptomic analysis, as noted by many authors. Here, we developed biomarker gene sets for use on whole blood, since whole blood is easier obtained than separated cells in clinical practice, and because many datasets on whole blood are already deposited in public databases and available for analysis. Expression levels of these biomarker sets, especially set GC-1 for circadian GC action likely remain sensitive to changes in cell percentages, limiting their usefulness. It

medRxiv preprint doi: https://doi.org/10.1101/2023.05.10.23289779; this version posted November 4, 2024. The copyright holder for this preprint (which was not certified by peer review) is the author/funder, who has granted medRxiv a license to display the preprint in perpetuity. All rights reserved. No reuse allowed without permission.

would be more accurate, and also easier, to develop GC transcriptomic biomarkers for use on data of separated cell (sub) types instead.

Clearly, there is a limit to novel insights that can be gained from analysis of bulk transcriptomics as performed here, regarding monocyte and neutrophil cell biology in homeostasis and during inflammation. Analysis of public single cell sequencing data would have allowed mapping (abundant) expression of GC-induced genes and marker genes to specific cell subtypes more precisely. It might also reveal whether different inductions can co-exist in the same cell, and infer trajectories. The main intention here was to place inductions by GC in a broader framework of gene expression in homeostasis, mild, and severe inflammation.

LEGENDS

Figure 1

Obtaining GC-driven gene signatures and comparison with *in vitro* DEGs

A work diagram for obtaining GC-driven gene expression correlation signatures using defined collections of transcriptomic datasets, as illustrated for a single whole blood collection. Datasets were selected by experimental description. Scrolls symbolize gene lists ordered by Pearson correlation values with query genes. **B** GC-driven gene expression correlation signatures obtained on 2 whole blood dataset collections and subcollections thereof, using appropriate query genes as indicated in grey. **C** Venn diagrams of total gene set derived from whole blood GC signatures 1 and 2, with 9 upregulated DEG sets from GC treatment of immune cells *in vitro*. PBMC (GSE110156, 6h, 1 mM prednisolone (Hu et al., 2018)), PBMC b (GSE33649 , 8h, 500 nM dexamethasone (Maranville et al., 2013)), macrophage (GSE61880, time series 1-24h, 100 nM dexamethasone (Jubb et al., 2016)), macrophage b, monocyte (GSE109439, 4h, 1 mM, triamcinolone acetonide (Wang et al., 2019)), monocyte b, neutrophil, CD4 T cell, and B cell (GSE112101, 2h and 6h, 22.7 microM methylprednisolone (Franco et al., 2019)). **D** frequency distribution of all GC-induced DEGs as present in total of 9 DEG sets. Overlap of DEGs with total gene set derived from whole blood GC signatures as indicated.

Figure 2

In vitro gene induction by GC

medRxiv preprint doi: https://doi.org/10.1101/2023.05.10.23289779; this version posted November 4, 2024. The copyright holder for this preprint (which was not certified by peer review) is the author/funder, who has granted medRxiv a license to display the preprint in perpetuity. All rights reserved. No reuse allowed without permission.

Overview of selected genes used for expression profiling, and *in vitro* induction by GC in PBMCs and immune cells. **A** Overview of 19 genes selected from GC-signatures. Query: genes used as expression correlation queries to obtain GC signatures 1 and 2 from 2 whole blood dataset collections. High in GC-sign.: high ranking of gene in GC signatures. Biomarker set: genes selected in GC-1 and GC-2 biomarker sets. **B** Induction in isolated immune cells (GSE112101, (Franco et al., 2019)). Ratio: ratio of total expression at time 0h comparing 4 types of blood cells (B, B cells; T, CD4 T cells; M, monocytes; N, neutrophils). Log2 FC: fold change after GC treatment; methylprednisolone 22.7 microM, 2h, and 6h versus vehicle control (pairwise for 4 donors). NS: pairwise p-value > 0.05 (left panel). Induction in monocytes (M), and macrophages (Mf) (GSE109439, (Wang et al., 2019)). Ratio: ratio of total expression at time 0h in monocytes and macrophages. Log2 FC: fold change after GC treatment; triamcinolone 1 mM, 4h versus vehicle control (right panel). **C** Induction by GC in PBMCs; GSE217320, (Seah et al., 2022) (a), GSE110156, (Hu et al., 2018) (b), GSE33649, (Maranville et al., 2013) (c). Log 2FC: treatment versus vehicle controls; dexamethasone 2.5nM, 5nM, 50nM combined, 72h (a); prednisolone 1mM 6h (b); dexamethasone 0.5 mM 8h, and 24h (c) (left panel). Induction by sepsis plasma in isolated neutrophils; GSE49755 (d), GSE49756 (e), GSE49757 (f), (Khaenam et al., 2014) (right panel). Unadjusted p-values as indicated. Marker genes for antigen presentation (Ag. Pr.), NF-kB-dependent expression (NF-kB), and early gene expression (early) are also included.

Figure 3

Differential expression correlation of genes induced by GC in health and severe inflammation

Reciprocal ranking in gene expression correlation profiles for 6 dataset collections and 2 separate RNA-seq datasets. **A-B** profiles for whole blood. Number of datasets with gene (SETS), and consistent gene expression correlation hits (CONS. H.), as indicated. Genes selected as biomarker sets GC-1, and GC-2 as shown. **A** whole blood in the absence of severe inflammation (40 sets in collection). **B** whole blood in the presence of severe inflammation (38 sets in collection). **C-F** profiles for myeloid cells. Genes in grey; expression below detection limit in all or most datasets, genes in red; profile originating from other contaminating cell types, or *in vitro* activation. **C** monocytes in the absence of severe inflammation (8 (sub)sets in collection). **D** monocytes in the presence of severe inflammation (11 (sub)sets in collection). **E** neutrophils / granulocytes in the absence of severe inflammation (6 (sub)sets in collection). **F** neutrophils / granulocytes in the presence of severe inflammation (10 (sub)sets in collection). **G** whole blood, healthy, circadian sampling

medRxiv preprint doi: https://doi.org/10.1101/2023.05.10.23289779; this version posted November 4, 2024. The copyright holder for this preprint (which was not certified by peer review) is the author/funder, who has granted medRxiv a license to display the preprint in perpetuity. All rights reserved. No reuse allowed without permission.

(GSE113883, (Braun et al., 2018)), excluding one outlier individual no. 14. Genes MAOA and AMPH in grey; at detection limit. Log10 TPM: log of mean TPM values in all samples. **H** whole blood, sepsis, and uncomplicated infections (GSE154918, (Herwanto et al., 2021)). Log10 N. C.; log of mean normalized counts in all samples for ill patients. Gene rankings in profiles color-coded in green from 1 (high) to 400 (low). Gene expression correlation profiles for each of 19 genes in Figure 2A shown in rows.

Figure 4

In vivo gene induction by GC.

Gene expression changes due to endogenous and exogenous GC in health, and in septic and burn shock. **A** DEGs in PBMCs by endogenous GC, and by experimental GC treatment in health. DEGs in 6h time difference, due to endogenous, circadian cortisol (GDS3704, (Bouwens et al., 2010)), (left panel). DEGs after dexamethasone (DEX) injection, compared with time 0h (GDS3864, (Carlet et al., 2010)) (middle panel). DEGs after hydrocortisone (HC) injection (GSE67255, (Olnes et al., 2016)). Doses 50 and 250 mg combined, and compared with time 0h (right panel). Gene names in red: tight correlation clustering observed with gene VSIG4 in dataset. Selected genes as also shown in Figure 2A, biomarker sets GC-1, and GC-2 as indicated, with added marker genes for expression in NK cells (NK), neutrophils (N), and monocytes (M). **B** DEGs in whole blood by endogenous GC in health, and by exogenous GC in burn shock and septic shock. DEGs between morning compared with rest of day, due to endogenous, circadian cortisol (GDS2767, (Baty et al., 2006)) (left panel). DEGs due to hydrocortisone treatment in burn shock (GSE77791, (Plassais et al., 2017)), comparing 24h and 120h continuous GC treatment, with 24h and 120h placebo, and in septic shock (GSE106878, (Kolte, 2020)), comparing 24h GC treatment with 24h placebo (middle panels). DEGs due to GC treatment in septic shock as reported by Wong et al. (2014) (right panel). Marker genes added for expression in NK cells (NK), neutrophils (N), and monocytes (M). **C-F** reciprocal gene expression ranking in profiles from 4 single data (sub) sets. **C** PBMCs in health, effect of endogenous GC (GDS3704, (Bouwens et al., 2010)), **D** PBMCs in health, effect of exogenous GC (GSE67255, (Olnes et al., 2016)), **E** whole blood, burn shock, subset no GC treatment, endogenous GC (GSE77791, (Plassais et al., 2017)). **F** whole blood, septic shock, subset no GC treatment, endogenous GC (GSE106878, (Kolte, 2020)). Gene rankings in profiles color-coded in green from 1 (high) to 200 (low). Gene expression correlation profiles for each of 19 genes in Figure 2A shown in rows.

medRxiv preprint doi: https://doi.org/10.1101/2023.05.10.23289779; this version posted November 4, 2024. The copyright holder for this preprint (which was not certified by peer review) is the author/funder, who has granted medRxiv a license to display the preprint in perpetuity. All rights reserved. No reuse allowed without permission.

Figure 5

Circadian cortisol action detected using biomarker gene set GC-1

Gene expression in time series of experimental respiratory viral infection, showing marker genes for cell type and inflammation, GC inducible genes DDIT4 and TSC22D3, and set GC-1. Panels rows 1 -5) Gene expression in 2 nonresponding (Nos 22 and 24) and 2 responding (Nos 12 and 13) individuals infected with H1N1 from experiment GSE73072 (Liu et al., 2016). X-axis, time (h) relative to viral challenge at 0h. Y-axis, expression value at log 2 scale. Row 1) marker genes for neutrophil-specific expression. Row 2) marker genes for classical monocyte-specific expression. Row 3) marker genes for non-classical / intermediate monocyte-specific expression. Row 4) marker genes for ongoing inflammation. Row 5) genes DDIT4 and TSC22D3, and combined value for 7 genes in set GC-1. Row 6) Gene expression in all 24 individuals infected with H1N1 from experiment GSE73072, nonresponding (n= 13), and responding (n= 11), showing C1QA, used as marker gene for inflammation, and set GC-1. X-axis, 24h interval ticks in phase with maximal expression of GC-1. Y-axis, expression value at log 2 scale.

Figure 6

Specific gene expression in mild and severe inflammation

Differential correlation and differential gene expression in whole blood in mild and severe inflammation. **A**) reciprocal gene ranking in 48 gene expression correlation profiles (rows) for mild seasonal respiratory viral infection (GSE68310, (Zhai et al., 2015) , subset days 0, 2, 4, and 6 after reporting ill), and for sepsis (E-MTAB-5273, (Burnham et al., 2017), subset sepsis and bacterial infection). Linear scale was used in obtaining correlation profiles, only shared gene probes for both datasets, and in case of 48 query genes, only single adequate gene probes. Genes profiles were put in same order, for easier comparison. Gene rankings in profiles shaded in green (high) to white (low). Marker genes for cell types and inductions as shown, including monocyte states MS1 and MS3 according to Reyes et al. (2020), PPARG (M2 monocyte / macrophage), IL1B (NF-kB-dependent expression), and SOCS3 (STAT3-dependent expression). Origin of different correlation clusters in inflammation and in severe inflammation as indicated (origin, see main text). Genes (co)-induced by interferon, genes likely dependent on STAT3, and genes induced by GC as indicated (induction). **B**) longitudinal expression of interferon alpha inducible genes OASL and IFI27 in dataset GSE68310 on prospective, seasonal respiratory viral infection, either influenza, or not

medRxiv preprint doi: https://doi.org/10.1101/2023.05.10.23289779; this version posted November 4, 2024. The copyright holder for this preprint (which was not certified by peer review) is the author/funder, who has granted medRxiv a license to display the preprint in perpetuity. All rights reserved. No reuse allowed without permission.

influenza (B; baseline, D0, D2, D4, D6, D21; days after reporting ill, S; spring). **C**, **D**) gene expression distributions in ill and healthy sample groups for a selection of genes used in correlation comparison, and several additional relevant genes (e.g. IL10 en FAM20A). **C**) gene expression in dataset GSE68310 on prospective, seasonal respiratory viral infection, using ill sample groups; 0, 2, 4, and 6 days (ill) and healthy sample groups; baseline, 21 days, and spring (H). **D**) gene expression in dataset E-MTAB-5273 on sepsis in sample groups sepsis or bacterial infection (ill), and healthy (H). **B**, **C**, **D**) Y-axis values at log-2 scale, with interval of 12 log-2 units for each panel. A partial BG subtraction of 150 units at linear scale was performed for GSE68310. Genes PRKY and RPS4Y were used as 2 controls showing signal in male samples, and BG noise level and distribution in female samples. Shown are box plots with added binned dot plots. Identical gene probes from platform GPL10558 used in C and D.

Figure 7

Comparing gene induction in myeloid cells, in homeostasis, inflammation, and severe inflammation.

Gene induction in homeostasis, mild inflammation, and severe inflammation, in monocytes and neutrophils, shown for GC-induced genes (including biomarker sets GC-1 and GC-2), and for relevant marker genes induced during inflammation. The schematic combines results from correlation and differential expression analysis using different informative datasets (see main tekst). Circadian GC-induced gene expression was found during homeostasis in monocytes and neutrophils but with some differences, such as no detection of KLF9 and ZBTB16 in neutrophils, or IRAK3 in monocytes. Inflammation caused by mild respiratory viral infection, results in elevated blood cytokines, which induce gene expression in monocytes and neutrophils. Induction of marker gene IL1B is NF-kB-dependent, while induction of other genes involved interferon or known STAT3-dependent expression. Induction of IL1B, SOCS3, and OSM, as seen in separated monocytes and neutrophils was due to early gene activation by cell isolation procedure (marked: **? E**). In case of neutrophils, *in vivo* induction could be seen for these genes using whole blood datasets, instead (marked: *****). Gene induction involving interferon was visible in intermediate / non-classical monocytes (**I/NC**), e.g. for C1QA/B/C genes. Less frequent upregulation, and upregulation much lower than in severe inflammation, occurred for a number of genes (eg GYG1) as indicated by a dashed vertical arrow. Severe inflammation in trauma or sepsis results in systemic release of DAMPs and MAMPs, and cytokines, which broadly induced 2 patterns of gene expression, one more

medRxiv preprint doi: https://doi.org/10.1101/2023.05.10.23289779; this version posted November 4, 2024. The copyright holder for this preprint (which was not certified by peer review) is the author/funder, who has granted medRxiv a license to display the preprint in perpetuity. All rights reserved. No reuse allowed without permission.

similar to mild inflammation (**A**), the other more specific to severe inflammation (**B**). Macrophage-like monocytes (MFL) and immature neutrophils (IMM) were cell types characteristic for severe inflammation. Several genes were highly upregulated in severe inflammation, including FAM20A, due to a unknown inducer (combination) marked **X**. Elevated GC resulted in strong gene induction depending on cell type. Genes expressed in monocyte state MS1, and in macrophage-like monocytes (MFL) in sepsis as indicated.

Figure 8

Longitudinal gene expression during severe inflammation after trauma.

Expression of marker genes, GC inducible genes, and relevant gene sets in whole blood, after trauma, and compared to healthy controls (GSE36809 (Xiao et al., 2011)). Cell type specific expression and inductions of different genes as indicated in panels. Gene sets include SIM (severe inflammatory myeloid, n= 16), FAM20A_4 (n = 4), naive T cell (T cell, n= 13) , GC-2 (GC- inducible, n= 9), induction by interferon gamma (IFN gamma, n= 23), and induction by interferon alpha (IFN alpha, n = 8). Expression values and time after injury shown at log 2 scales (h, hours; d, days; w, weeks). Mean value for healthy controls (H) was set at zero. In case of GC- induced genes OLAH, DAAM2, VSIG4, and ADAMTS2, maximal expression values in healthy controls, which possibly still correspond to gene probe background levels, are indicated by horizontal lines. Expression values for gene sets were calculated using adequate gene probes, with subtraction of background / basal expression, and adjusting for different gene expression ranges as detailed in methods.

Figure 9

Distribution of gene sets expression in severe inflammation and autoimmune disease

Increase of GC-1 and GC-2 gene set expression upon GC treatment in patients with burn shock, septic shock, systemic lupus erythematosus (SLE), and rheumatoid arthritis (RA). Included for comparison are gene sets T cell, set severe inflammatory myeloid (SIM), set FAM20A, (4 genes including FAM20A), and sets interferon gamma (IFN gamma), and interferon alpha (IFN alpha). Datasets used different assay platforms, and log fold change between expression values in one dataset are not directly comparable to log fold changes in other datasets. Y-axis values on log-2 scale, with interval of 9 log 2 units for each panel. Shown are box plots with added binned dot plots. **A** GSE77791 (Plassais et al., 2017), healthy

medRxiv preprint doi: https://doi.org/10.1101/2023.05.10.23289779; this version posted November 4, 2024. The copyright holder for this preprint (which was not certified by peer review) is the author/funder, who has granted medRxiv a license to display the preprint in perpetuity. All rights reserved. No reuse allowed without permission.

(H), severe burn shock (1-5 days, excluding 7 days samples (no GC), severe burn shock with hydrocortisone treatment (1-5 days, excluding 7 days samples (+ GC). **B** GSE106878 (Kolte, 2020), septic shock placebo 0h (P0), septic shock hydrocortisone 0h (GC0), septic shock placebo 24h (P24), septic shock hydrocortisone 24h (GC24). **C** GSE110174 (Hu et al., 2018), healthy (H), SLE low and medium prednisone usage (l/m GC), SLE high prednisone usage (hGC), SLE unknown prednisone usage (uGC). **D** GSE117769 published by Goldberg and co-workers (2018), healthy control (H), RA without GC treatment (no GC), RA with GC treatment (+ GC).

Figure 10

GC-2 gene expression is upregulated by endogenous and exogenous GC depending on disease

Overview of gene expression in whole blood during different diseases and upon treatment with GCs using 5 relevant features; a gene set for severe inflammatory myeloid (SIM), a gene set of 4 induced genes including FAM20A (FAM (4)), a gene set GC-2 for induction by GC during severe inflammation (GC-2), and gene sets for induction by either interferon gamma (IFN-G), or interferon alpha (IFN-A). Gene set expression values were plotted in ranges of 9 log 2 units and distributions compared within, and between experiments for platforms GPL570, GPL10558, and RNA sequencing data, and tentatively ordered according to deviation from healthy controls. Red arrows indicate maximal upregulation from healthy control for each gene set. Decreases in basal gene set expression, as frequently seen in case of interferon gamma and alpha induction in severe inflammation, may occur because of shifts in cell percentages, and do not necessarily indicate gene repression. Datasets, different platforms, and supporting figure panels as shown.

Figure 11

Evaluating biomarker genes of GC action in whole blood in different diseases

Left panel, scoring suitable biomarker genes of GC action in whole blood in health, and different diseases, based on induction strength and correlation analysis using relevant RNA-seq datasets (see main text). Included are all genes in set GC-1 and set GC-2, gene ARG1, and additional genes present in published GC biomarker gene sets. Grey marking, genes absent in single dataset, and taken from supplementary datasets; GSE69683 (asthma), GSE120178, and GSE129705 (both RA), GSE139940, and GSE110685 (both SLE), and GSE161731 (subset bacterial pneumonia and sepsis). Asterisk for ADORA3, and MAOA; see main text. Middle

medRxiv preprint doi: https://doi.org/10.1101/2023.05.10.23289779; this version posted November 4, 2024. The copyright holder for this preprint (which was not certified by peer review) is the author/funder, who has granted medRxiv a license to display the preprint in perpetuity. All rights reserved. No reuse allowed without permission.

panel, genes present in whole blood transcriptomic sets of "time telling" genes identified by machine learning. In a 15 genes set for monitoring the circadian clock in blood (Hughey, 2017), (TT-1), in 234 genes identified as phase markers by Laing et al. (2017), (TT-2), and in a a set of 41 predictive genes for circadian state (Braun et al., 2018), (TT-3). Relative strength indicated from 1 to 4, based on coefficients in 2 principal components used for prediction (TT-1), number of times identified as circadian phase marker using 4 different methods (TT-2), and high frequency of selection in predictor in different training samples (TT-3). Right panel, genes present in whole blood transcriptomic biomarker sets for guiding GC replacement therapy in Addison's disease (Sævik et al., 2021), and monitoring response to GC treatment in SLE and RA (Hu et al., 2018), (SLE-1), and SLE (Northcott et al., 2021), (SLE-2).

SUPPLEMENTAL INFORMATION

Figure S1

Different expression correlation clusters of cortisol-induced genes in health and severe inflammation.

A, hierarchical clustering of a 20 gene expression correlation matrix from combined, related datasets GSE11761 and GSE14642 on PBMCs and exercise in healthy people (Radom-Aizik et al., 2009a, 2009b). Signal quality as indicated, with several probesets not (3) or barely (4) above background level. B, hierarchical clustering of a 20 gene expression correlation matrix from dataset GSE9960 on PBMCs of critically ill and sepsis patients (Tang et al., 2009). Adjusted differential gene expression comparing to GSE11761 and GSE14642 as indicated. C, same from dataset GSE57065 on whole blood of septic shock patients, subsetted for healthy controls (Cazalis et al., 2014). Signal quality as indicated with 6 probesets barely above background level. D, same from dataset GSE57065 subsetted for septic shock patients. Differential gene expression in blood from septic shock patients and healthy controls as indicated. Cluster 1, genes clearly present in an expression correlation cluster in health. Cluster 2, genes not (clearly) present in cluster 1 in health, and present in an expression correlation cluster in severe inflammation. Cell type of main gene expression as indicated. All

medRxiv preprint doi: https://doi.org/10.1101/2023.05.10.23289779; this version posted November 4, 2024. The copyright holder for this preprint (which was not certified by peer review) is the author/funder, who has granted medRxiv a license to display the preprint in perpetuity. All rights reserved. No reuse allowed without permission.

datasets are obtained from the same platform (GPL570, Affymetrix Human Genome U133 Plus 2.0 Array), with good and identical probesets used for the correlation matrices.

Figure S2

Cell type specific expression and *in vitro* induction by GC of whole blood GC signature genes.

Genes selected for profiling (n =227) were derived from an exploratory signature of GC-driven gene expression in whole blood (see sheet 1 supporting table 2). Basal and upregulated gene expression by GC treatment of immune cells *in vitro*. GSE60424 basal, relative base level expression for different immune cell types as a ratio of total expression in 6 cell types shown (B cell, CD4 T, CD8 T, monocyte, neutrophil, NK, excluding sepsis samples; GSE60424, (Linsley et al., 2014). GSE112101 basal, relative base level expression in 4 cell types shown (B cell, CD4 T, monocyte, neutrophil; GSE112101, (Franco et al., 2019). GSE112101 induced, differential expression (Log2 FC, pairwise for 4 donors, NS: pairwise p-value > 0.05) upon GC treatment for different cell types in experiment GSE112101 (4 cell types, 22.7 microM methylprednisolone, 2h and 6h, (Franco et al., 2019). GSE109439 basal, relative base level gene expression in monocytes and macrophages (GSE109439, (Wang et al., 2019). GSE109439 induced, differential expression upon GC treatment of monocytes and macrophages (GSE109439, 1 mM triamcinolone acetonide, 4h, (Wang et al., 2019). GSE100521 induced, differential expression of M1 macrophages repolarized to M2 with methylprednisolone, 100nM, 24h (GSE100521, (Gharib et al., 2019). Basal expression ratios are shaded blue. DEG values are log2 fold change of induced and base expression levels, with table cells shaded red (up regulation) and green (down regulation), accordingly. NS, not significant (p > 0.05); NA, gene not detected/absent from platform, or absent p-value. Log2 fold change, and unadjusted p-values used for experiment GSE109439 according to Wang et al., (2019). Genes in exploratory GC signature 1, signature 2 or both as indicated, marker genes (32) included as expression controls.

Figure S3

Selection of gene set GC-1 for use as whole blood transcriptomic biomarker of GC action in health.

Main criteria: 1) genes belonging to a “core” cluster of correlated expression of GC inducible genes in whole blood in the absence of severe inflammation. 2) balanced set between genes

medRxiv preprint doi: https://doi.org/10.1101/2023.05.10.23289779; this version posted November 4, 2024. The copyright holder for this preprint (which was not certified by peer review) is the author/funder, who has granted medRxiv a license to display the preprint in perpetuity. All rights reserved. No reuse allowed without permission.

preferentially expressed in neutrophil and lymphoid cells. 3) strong circadian upregulation of genes. 4) no upregulating during mild inflammation. **A** Reciprocal ranking in 56 gene expression correlation profiles (rows) obtained using an exploratory collection of 62 blood transcriptomic datasets excluding severe inflammation (see sheet 16 in supporting table 1). Gene rankings as derived from minimally 25 contributing datasets, except for gene AREG (11 datasets), approximately 50-55 contributing datasets on average. Gene rankings in profiles color-coded in green from 1 (high) to 400 (low). A pre-selection of 31 genes from whole blood exploratory GC signature 1, and 25 relevant marker genes for cell type and inflammation as indicated. Gene IL1B with NF-kB-dependent induction (NF-kB), genes IL1RN and TNFAIP6, both with NF-kB-dependent induction and induction by interferon (NF-kB + IFN), 2 interferon alpha (IFN alpha), and 2 interferon gamma (IFN gamma) inducible genes were used together as different markers for inflammation. Gene CIRBP (cold inducible RNA-binding protein) was added as a marker for circadian expression. A "core group" of GC inducible genes, with some subclustering related to differential expression in lymphoid cells or myeloid cells was visible. Marker genes upregulated in inflammation indicated in red. Several exploratory GC signature 1 genes (TNFAIP3, SOCS1, NFIL3) showed correlated expression with inflammation markers. **B** Circadian expression seen by plotting datasets GSE73072 on mild respiratory viral infection (Liu et al., 2016), and GSE56931 on sleep deprivation (Arnardottir et al., 2014) (Circadian). Upregulation during mild inflammation using dataset GSE73072 (Up in inflam). **C** Differential expression of 31 genes from exploratory signature GC 1, mild respiratory viral infection (GSE68310, GPL10558, (Zhai et al., 2015)), ill days 0 and 2 (n= 258) versus baseline and spring (n= 243) (Log2 FC mild 1), and sepsis (E-MTAB-5273, GPL10558, (Burnham et al., 2017)), sepsis (n= 221) versus control (n = 10) (Log 2FC sev 1) with corresponding p-values (Log10 pval mild 1, Log10 pval sev 1). Differential expression of same 31 selected genes in sepsis (GSE154918, RNA-seq, (Herwanto et al., 2021)), sepsis and bacterial infection (n = 65) versus healthy (n= 40) (Log 2FC sev 2) with corresponding p-values (Log10 pval sev 2). Log2 FC values color-coded from red (upregulation) to blue (downregulation), NA gene absent. Log10 p-values color-coded from green (more significant) to white, not significant (yellow), NA, gene absent. **D** Expression ratios of 31 genes in isolated cells (GSE60424, RNA-seq, (Linsley et al., 2014)), all monocyte samples excluding IFN-treated MS, and sepsis (Mo control, n= 14), all neutrophil samples excluding IFN-treated MS, and sepsis (Ne control, n= 14), monocytes IFN-treated MS (Mo IFN, n= 3), neutrophils IFN-treated MS (Ne IFN, n= 3), monocytes sepsis (Mo sepsis, n= 3), and neutrophils sepsis (Ne sepsis, n= 3). In RNA-seq

medRxiv preprint doi: https://doi.org/10.1101/2023.05.10.23289779; this version posted November 4, 2024. The copyright holder for this preprint (which was not certified by peer review) is the author/funder, who has granted medRxiv a license to display the preprint in perpetuity. All rights reserved. No reuse allowed without permission.

table, 1 count added, and made cpm, before calculating ratios. Ratio values color-coded in grey, NA, gene absent. **E** Correlation, hierarchical clustering of gene expression correlation matrix of 31 genes derived from whole blood exploratory GC signature 1, using the collection of 62 blood transcriptomic datasets excluding severe inflammation, genes selected in biomarker set GC-1 as indicated.

Figure S4

Selection of gene set GC-2 for use as whole blood transcriptomic biomarker of GC action in severe inflammation.

Main criteria: 1) genes belonging to a group of correlated expression of GC inducible genes in whole blood in the presence of severe inflammation. 2) no strong correlation with other genes upregulated in severe inflammation more generally. 3) balanced set between genes preferentially expressed in neutrophils and monocytes. 4) strong upregulation during severe inflammation in whole blood, and in isolated monocytes or neutrophils. **A** Reciprocal ranking in 63 gene expression correlation profiles (rows) obtained using a collection of 38 blood transcriptomic datasets on severe inflammation (see sheet 15 in supporting table 1). Gene rankings as derived from minimally 20 contributing datasets, except for genes CPM, SRGAP1, INSR, DNASE4, SIGLEC16, and MARVELD1 (15 datasets), approximately 30-35 contributing datasets on average. Gene rankings in profiles color-coded in green from 1 (high) to 400 (low). A pre-selection of 41 genes from exploratory GC signature 2 (see sheet 1 in supporting table 2), genes in biomarker set GC-1, and 18 relevant marker genes for cell type and inflammation used as indicated. Genes that were selected as biomarker GC-2 set as indicated. Gene IL1B (NF-kB), genes GK and NAMPT which are upregulated mainly in neutrophils during inflammation, genes IL1RN and CASP1 (NF-kB + IFN), 2 interferon alpha (IFN alpha), and 2 interferon gamma (IFN gamma) inducible genes were used together as different markers for inflammation. Also included are marker genes mainly expressed in neutrophils during severe inflammation such as GYG1 and LDHA. Gene groups related to differential expression in monocytes or neutrophils were visible. Several exploratory GC signature 2 genes (eg IRAK3, IL1R2), mainly expressed in neutrophils, showed strong correlated expression with marker genes for severe inflammation. Genes that were also strongly upregulated in mild inflammation indicated in red (inflammation A, eg interferon-induced), genes more strongly or exclusively upregulated in severe inflammation indicated in brown (inflammation B, GC inducible genes, and gene expression related to increased

medRxiv preprint doi: https://doi.org/10.1101/2023.05.10.23289779; this version posted November 4, 2024. The copyright holder for this preprint (which was not certified by peer review) is the author/funder, who has granted medRxiv a license to display the preprint in perpetuity. All rights reserved. No reuse allowed without permission.

neutrophil glucose metabolism). **B** Differential expression of 41 genes from exploratory GC signature 2, and 4 biomarker GC-1 set genes, mild respiratory viral infection (GSE68310, GPL10558, (Zhai et al., 2015)), ill days 0 and 2 (n= 258) versus baseline and spring (n= 243) (Log2 FC mild 1), and sepsis (E-MTAB-5273, GPL10558, (Burnham et al., 2017)), sepsis (n= 221) versus control (n = 10) (Log 2FC sev 1) with corresponding p-values (Log10 pval mild 1, Log10 pval sev 1). Differential expression of same 45 selected genes in sepsis (GSE154918, RNA-seq, (Herwanto et al., 2021)), sepsis and bacterial infection (n = 65) versus healthy (n= 40) (Log 2FC sev 2) with corresponding p-values (Log10 pval sev 2). Log2 FC values color-coded from red (upregulation) to blue (downregulation), NA gene absent. Log10 p-values color-coded from green (more significant) to white, not significant (yellow), NA, gene absent. **C** Expression ratios of 45 genes in isolated cells, (GSE60424, RNA-seq, (Linsley et al., 2014)), all monocyte samples excluding IFN-treated MS, and sepsis (Mo control, n= 14), all neutrophil samples excluding IFN-treated MS, and sepsis (Ne control, n= 14), monocytes IFN-treated MS (Mo IFN, n= 3), neutrophils IFN-treated MS (Ne IFN, n= 3), monocytes sepsis (Mo sepsis, n= 3), and neutrophils sepsis (Ne sepsis, n= 3). In RNA-seq table, 1 count added, and made cpm, before calculating ratios. Ratio values color-coded in grey, NA, gene absent. **D** Correlation, hierarchical clustering of gene expression correlation matrix of same 41 genes in whole blood exploratory GC signature 2 and genes in biomarker set GC-1 using the collection of 38 blood transcriptomic datasets on severe inflammation, genes selected in set GC-2 as indicated.

Figure S5

Cluster analysis of upregulated DEGs in PBMCs sampled with 6 h time difference

Hierarchical clustering of an expression correlation matrix of 34 upregulated DEGs (p-values unpaired < 0.05) from dataset GDS3704 (PBMC, fatty acids consumption, 0h and 6h time points, 21 individuals (Bouwens et al., 2010)). DEGs shown from experiment were selected as follows: 1) based on log2 fold change > 0.2, and adding top 20 upregulated DEGs with lowest p-values (see sheet 1 supporting table 4). 2) visible upregulation by GC *in vitro* in one or more immune cells in experiment GSE112101 (Franco et al., 2019). 3) high ranking (cut-off about 200) in correlation signatures of GC-driven gene expression in PBMCs, using 2 signatures either with bias for lymphocytes, or bias for monocytes (see sheets 5,6 supporting table 3, and sheet 1 supporting table 4). 4) excluding gene CDK5R1 because of poor clustering with other DEGs and marker genes. Marker genes specifically expressed in different immune cells or upon early cell activation *in vitro* were also included. Circadian

medRxiv preprint doi: https://doi.org/10.1101/2023.05.10.23289779; this version posted November 4, 2024. The copyright holder for this preprint (which was not certified by peer review) is the author/funder, who has granted medRxiv a license to display the preprint in perpetuity. All rights reserved. No reuse allowed without permission.

cortisol-regulated DEGs were found in 3 larger clusters, broadly corresponding with expression in monocytes, expression mostly in NK cells, and expression in naive T cells.

Figure S6

Functional comparison of GC-driven gene expression profiles in myeloid cells

Comparing ranking of selected genes in GC- driven gene expression profiles obtained on dataset collections of monocytes in the absence of severe inflammation (MoH), monocytes in the presence of severe inflammation (MoS), neutrophils in the absence of severe inflammation (NeH), and neutrophils in the presence of severe inflammation (NeS), as described (see sheet 13, supporting table 3). Gene ranking in profiles color-coded in green (1, high) to white (500), to blue (10000, low). Genes were tentatively grouped according to functional categories, using gene summaries provided by GeneCards (Stelzer et al., 2016), and additional literature search. RNA-seq dataset GSE60424 (Linsley et al., 2014) was used to compare correlation profiles with expression levels in monocytes, neutrophils, separated lymphoid cells combined (B cells, CD4 T cells, CD8 T cells, NK cells), and myeloid cells combined (monocytes and neutrophils). Expression ratios between monocytes in the absence of severe inflammation (MoH), monocytes in sepsis (MoS), neutrophils in the absence of severe inflammation (NeH), and neutrophils in sepsis (NeS). Expression ratios also shown between lymphoid cells in the absence of severe inflammation (LyH), lymphoid cells in sepsis (LyS), myeloid cells in the absence of severe inflammation (MyH), and myeloid cells in sepsis (MyS). Sample groups used for the absence of severe inflammation, excluded sepsis samples, and interferon-treated MS samples. Ratio values shaded in grey. Differences in gene ranking in correlation profiles, generally corresponded to relative expression levels in separated myeloid cells.

Figure S7

Gene induction by GC in a broader framework of gene expression in monocytes in the absence of severe inflammation

Reciprocal ranking in gene expression correlation profiles for monocytes, in the absence of severe inflammation, compared with gene induction occurring during isolation of myeloid cells from blood, and gene induction by interferons and IL-10. Green matrix; reciprocal gene ranking using a dataset collection (n= 8) of monocytes in the absence of severe inflammation (see sheet 13 supporting table 3). Genes include GC-regulated genes and relevant marker genes for describing inflammation, cell type, and several cellular processes. GC-regulated

medRxiv preprint doi: https://doi.org/10.1101/2023.05.10.23289779; this version posted November 4, 2024. The copyright holder for this preprint (which was not certified by peer review) is the author/funder, who has granted medRxiv a license to display the preprint in perpetuity. All rights reserved. No reuse allowed without permission.

genes that were chosen for obtaining a combined GC-driven gene profile (see sheet 3 supporting table 3) are shown in red. Gene rankings in profiles are color-coded in green from 1 (high) to 500 (low), high gene rankings (< 10) as indicated. N in grey; insufficient supporting datasets for gene in profile. Visible gene expression correlation (sub) clusters are indicated by black boxes. Visible gene groups, and gene induction involving interferon as annotated (vertical). Gene clusters originating from *in vitro* activation, *in vivo* inflammation, and contamination as indicated (horizontal). GSE60424 monocytes and neutrophils versus blood source (DEGs); Differential gene expression between separated cell preparations, and corresponding whole blood samples due to enrichment from source material, and *in vitro* activation (RNA-seq dataset GSE60424, one count added to table, made cpm (Linsley et al., 2014)). Sepsis samples and samples from *in vivo* interferon treatment of MS were excluded from the group comparisons. Log2 fold change between monocyte samples (n= 14), and blood samples (n= 14) (Log2FC Mo), and log2 fold change between neutrophil samples (n= 14), and blood samples (n= 14) (Log2FC Ne). Log2 fold change color-coded in red to blue, NA; gene absent in dataset. Genes not expressed in either monocytes or neutrophils indicated in red. GSE60424 IFN treatment monocytes and neutrophils (expression ratio); Expression ratios between control monocytes (MO control, n= 14), control neutrophils (NE control, n= 14), and monocytes (MO IFN, n= 3), and neutrophils (NE IFN, n=3) isolated from MS patients treated with interferon. Sepsis samples for monocytes (n = 3) and neutrophils (n= 3) were excluded from the control sample groups. Expression ratios shaded in blue, NA; gene absent in dataset. Genes not expressed in either monocytes or neutrophils indicated in red. GSE146438 IL10 Monocytes (DEGs); differential gene expression between monocytes treated *in vitro* with IL-10 or IL-10 variants, and untreated control monocytes. Monocytes were rested 2 days in M-CSF media and subsequently stimulated for 24h with different concentrations of IL-10 or IL-10 variants (RNA-seq dataset GSE146438 (Gorby et al., 2020)). Log2 fold change between IL-10 treated monocyte samples (n= 18), and untreated samples (n= 3) (Log2FC). Log2 fold change color-coded in red to blue. Log10 of unadjusted p-values color-coded in green to white, yellow not significant (Log10P). NA; gene absent in dataset. GSE190594 interferon monocytes (DEGs); differential gene expression between monocytes treated *in vitro* with either IFN alpha or IFN gamma for 24h, and untreated control monocytes (GSE190594, (Green et al., 2023)). Illumina GPL10558 gene probes used for different genes as indicated. Log2 fold change between IFN alpha treated monocyte samples (n= 9), and untreated samples (n= 8) (Log2FC IFNA), and between IFN gamma treated monocyte samples (n= 9), and untreated samples (n= 8) (Log2FC IFNG). Log2 fold change color-coded

medRxiv preprint doi: https://doi.org/10.1101/2023.05.10.23289779; this version posted November 4, 2024. The copyright holder for this preprint (which was not certified by peer review) is the author/funder, who has granted medRxiv a license to display the preprint in perpetuity. All rights reserved. No reuse allowed without permission.

in red to blue. Corresponding log10 of unadjusted p-values color-coded in green to white, yellow not significant (Log10P IFNA, Log10P IFNG). NA; gene absent in dataset.

Figure S8

Gene induction by GC in a broader framework of gene expression in monocytes in the presence of severe inflammation

Reciprocal ranking in gene expression correlation profiles for monocytes, in the presence of severe inflammation, compared with differential expression occurring in isolated myeloid cells in sepsis, and gene induction *in vitro* by IL-10 and interferons. Green matrix; reciprocal gene ranking using a dataset collection (n= 11) of monocytes in the presence of severe inflammation (see sheet 13 supporting table 3). Genes include GC-regulated genes and relevant marker genes for describing inflammation, cell type such as macrophage-like monocyte, and several cellular processes. GC-regulated genes that were chosen for obtaining a combined GC-driven gene profile (see sheet 4 supporting table 3) are shown in red. Gene rankings in profiles are color-coded in green from 1 (high) to 500 (low), high gene rankings (< 10) as indicated. Visible gene expression correlation (sub) clusters are indicated by black boxes. Visible gene groups, and gene induction involving interferon, NF-kB-dependent induction, and STAT3-dependent induction as annotated (vertical). Gene clusters originating from *in vitro* activation, *in vivo* inflammation A (more similar to clustering seen also in mild inflammation), *in vivo* inflammation B (clustering more specific to severe inflammation), and contamination as indicated (horizontal). GSE60424 sepsis monocytes and neutrophils (expression ratio); Expression ratios between control monocytes (MO control, n= 14), control neutrophils (NE control, n= 14), and monocytes (MO sepsis n= 3), and neutrophils (NE sepsis, n=3) isolated from sepsis patients. Samples for monocytes (n = 3), and neutrophils (n= 3) isolated from IFN-treated MS patients were excluded from the control sample groups. Expression ratios shaded in blue, NA; gene absent in dataset. Genes not expressed in either monocytes or neutrophils, or expressed in unseparated neutrophil bands, indicated in red. GSE133822 sepsis monocytes (DEGs); differential gene expression between CD14 monocytes from sepsis patients, and healthy control CD14 monocytes (RNA-seq dataset GSE133822 (Washburn et al., 2019)). Log2 fold change color-coded in red to blue (Log2FC). Log10 of unadjusted p-values color-coded in green to white, yellow not significant (Log10P). NA; gene absent in dataset. GSE146438 IL10 Monocytes (DEGs); differential gene expression between monocytes treated *in vitro* with IL-10 or IL-10 variants, and untreated control monocytes. Monocytes were rested 2 days in M-CSF media and subsequently

medRxiv preprint doi: https://doi.org/10.1101/2023.05.10.23289779; this version posted November 4, 2024. The copyright holder for this preprint (which was not certified by peer review) is the author/funder, who has granted medRxiv a license to display the preprint in perpetuity. All rights reserved. No reuse allowed without permission.

stimulated for 24h with different concentrations of IL-10 or IL-10 variants (RNA-seq dataset GSE146438 (Gorby et al., 2020)). Log2 fold change between IL-10 treated monocyte samples (n= 18), and untreated samples (n= 3) (Log2FC). Log2 fold change color-coded in red to blue. Log10 of unadjusted p-values color-coded in green to white, yellow not significant (Log10P). NA; gene absent in dataset. GSE190594 interferon monocytes (DEGs); differential gene expression between monocytes treated *in vitro* with either IFN alpha or IFN gamma for 24h, and control monocytes (GSE190594, (Green et al., 2023)). Illumina GPL10558 gene probes used for different genes as indicated. Log2 fold change between IFN alpha treated monocyte samples (n= 9), and untreated samples (n= 8) (Log2FC IFNA), and between IFN gamma treated monocyte samples (n= 9), and untreated samples (n= 8) (Log2FC IFNG). Log2 fold change color-coded in red to blue. Corresponding log10 of unadjusted p-values color-coded in green to white, yellow not significant (Log10P IFNA, Log10P IFNG). NA; gene absent in dataset.

Figure S9

Gene induction by GC in a broader framework of gene expression in neutrophils in the absence of severe inflammation

Reciprocal ranking in gene expression correlation profiles for neutrophils, in the absence of severe inflammation, compared with gene induction occurring during isolation of myeloid cells from blood, and gene induction by interferons. Green matrix; reciprocal gene ranking using a dataset collection (n= 6) of neutrophils in the absence of severe inflammation (see sheet 13, supporting table 3). Genes include GC-regulated genes and relevant marker genes for describing inflammation, cell type, and several cellular processes. GC-regulated genes that were chosen for obtaining a combined GC-driven gene profile (see sheet 1 supporting table able 3) are shown in red. Gene rankings in profiles are color-coded in green from 1 (high) to 500 (low), high gene rankings (< 10) as indicated. Visible gene expression correlation (sub) clusters are indicated by black boxes. Visible gene groups, and gene induction involving interferon, and STAT3-dependent induction as annotated (vertical). Gene clusters originating from *in vitro* activation, *in vivo* inflammation, and contamination as indicated (horizontal). GSE60424 monocytes and neutrophils versus blood source (DEGs); Differential gene expression between separated cell preparations, and corresponding blood samples due to enrichment from source material, and *in vitro* activation (RNA-seq dataset GSE60424, one count added to table, made cpm (Linsley et al., 2014)). Sepsis samples and samples from *in vivo* interferon treatment of MS were excluded from the group comparisons. Log2 fold

medRxiv preprint doi: https://doi.org/10.1101/2023.05.10.23289779; this version posted November 4, 2024. The copyright holder for this preprint (which was not certified by peer review) is the author/funder, who has granted medRxiv a license to display the preprint in perpetuity. All rights reserved. No reuse allowed without permission.

change between monocyte samples (n= 14), and blood samples (n= 14) (Log2FC Mo), and log2 fold change between neutrophil samples (n= 14), and blood samples (n= 14) (Log2FC Ne). Log2 fold change color-coded in red to blue, NA; gene absent in dataset. Genes not expressed in either monocytes or neutrophils indicated in red. GSE60424 IFN treatment monocytes and neutrophils (expression ratio); Expression ratios between control monocytes (MO control, n= 14), control neutrophils (NE control, n= 14), and monocytes (MO IFN, n= 3), and neutrophils (NE IFN, n=3) isolated from MS patients treated with interferon. Sepsis samples for monocytes (n = 3) and neutrophils (n= 3) were excluded from the control sample groups. Expression ratios shaded in blue, NA; gene absent in dataset. Genes not expressed in either monocytes or neutrophils indicated in red. GSE145648 IFN treatment in vitro neutrophils (expression ratio); Expression ratios between control neutrophils (PMN control, n= 3), and neutrophils treated with either type 1 IFN (PMN IFN B1a, n= 3) or IFN gamma (PMN IFN gam. , n = 3) for 4 h (RNA-seq dataset GSE145648, subseries GSE131990, made cpm (Devlin et al., 2020)). Expression ratios shaded in blue, NA; gene absent in dataset.

Figure S10

Gene induction by GC in a broader framework of gene expression in neutrophils in the presence of severe inflammation

Reciprocal ranking in gene expression correlation profiles for neutrophils, in the presence of severe inflammation, compared with differential expression occurring in isolated myeloid cells in sepsis. Green matrix; reciprocal gene ranking using a dataset collection (n= 10) of neutrophils in the presence of severe inflammation (see sheet 13 supporting table 3). Genes include GC-regulated genes and relevant marker genes for describing inflammation, cell type such as (meta) myelocytes, and several cellular processes. GC-regulated genes that were chosen for obtaining a combined GC-driven gene profile (see sheet 2 supporting table 3) are shown in red. Gene rankings in profiles are color-coded in green from 1 (high) to 500 (low), high gene rankings (< 10) as indicated. N in grey; insufficient supporting datasets for gene in profile. Visible gene expression correlation (sub) clusters are indicated by black boxes. Visible gene groups, and gene induction involving interferon, and STAT3-dependent induction as annotated (vertical). Gene clusters originating from *in vitro* activation, *in vivo* inflammation A (more similar to clustering seen also in mild inflammation), *in vivo* inflammation B (clustering more specific to severe inflammation), and contamination as indicated (horizontal). GSE60424 sepsis monocytes and neutrophils (expression ratio); Expression ratios between control monocytes (MO control, n= 14), control neutrophils (NE

medRxiv preprint doi: https://doi.org/10.1101/2023.05.10.23289779; this version posted November 4, 2024. The copyright holder for this preprint (which was not certified by peer review) is the author/funder, who has granted medRxiv a license to display the preprint in perpetuity. All rights reserved. No reuse allowed without permission.

control, n= 14), and monocytes (MO sepsis n= 3), and neutrophils (NE sepsis, n=3) isolated from sepsis patients. Samples for monocytes (n = 3), and neutrophils (n= 3) isolated from IFN-treated MS patients were excluded from the control sample groups. Expression ratios shaded in blue, NA; gene absent in dataset. Genes not expressed in either monocytes or neutrophils, or expressed in unseparated neutrophil bands, indicated in red. GSE123729 sepsis + SIRS granulocytes versus control (DEGs); differential gene expression between granulocytes from sepsis and SIRS patients, and control granulocytes (GSE123729 (Coulibaly et al., 2019)). Log2 fold change color-coded in red to blue (Log2FC). Log10 of unadjusted p-values color-coded in green to white, yellow not significant (Log10P). NA; gene absent in dataset.

Figure S11

Selection of gene set SIM (Severe Inflammatory Myeloid) and set FAM20A (4) used as whole blood transcriptomic biomarkers of severe inflammation.

Main criteria: 1) genes in a large group of correlated expression in myeloid cells in whole blood in the presence of severe inflammation (SIM group). 2) no strong correlation with genes upregulated in severe inflammation by GC. 3) strong upregulation during severe inflammation in whole blood, in isolated monocytes or neutrophils. 4) in case of set FAM20A (n= 4), detectable subclustering of genes within larger SIM group. **A** Reciprocal ranking in 78 gene expression correlation profiles (rows) obtained using a collection of 38 blood transcriptomic datasets on severe inflammation (see sheet 15 supporting table 1). Gene rankings as derived from minimally 20 contributing datasets, approximately 30-35 contributing datasets on average. Gene rankings in profiles color-coded in green from 1 (high) to 400 (low). A pre-selection of highly upregulated genes in severe inflammation as compared to mild inflammation, with additional relevant marker genes for cell type and inflammation as shown. Genes that were selected in SIM and FAM20A-4 sets as indicated. Marker genes include GC-induced genes in severe inflammation (5 genes in biomarker set GC-2), PPARG (M2c monocytes), and genes expressed in immature neutrophils. Genes selected in SIM set include LDHA (in severe inflammation, marker for anaerobic glycolysis in neutrophils). Gene profiles with high ranking of FAM20A, and gene profiles with high ranking of SOCS3 (marker for STAT3-dependent expression) as shown. A stronger expression correlation of genes in cell proliferation with genes expressed in immature neutrophils than with genes expressed in plasmablasts, lower expression correlation of genes expressed in immature neutrophils (clusters AZU1 and MMP8), and a correlated expression of LDHA with genes upregulated in

medRxiv preprint doi: https://doi.org/10.1101/2023.05.10.23289779; this version posted November 4, 2024. The copyright holder for this preprint (which was not certified by peer review) is the author/funder, who has granted medRxiv a license to display the preprint in perpetuity. All rights reserved. No reuse allowed without permission.

neutrophils, instead of marker genes in biogenesis, were indicative for severe inflammation in the dataset collection. Genes that were also strongly upregulated in mild inflammation indicated in red (inflammation A, eg IL1B, and interferon-induced genes OASL and GBP1), genes more strongly or exclusively upregulated in severe inflammation indicated in brown (inflammation B; GC inducible genes, SIM group). **B** Differential expression of genes in SIM set, FAM20A-4 set, and 2 additional genes, which were not selected in sets; mild respiratory viral infection (GSE68310, GPL10558, (Zhai et al., 2015)), ill days 0 and 2 (n= 258) versus baseline and spring (n= 243) (Log2 FC mild 1), and sepsis (E-MTAB-5273, GPL10558, (Burnham et al., 2017)) sepsis (n= 221) versus control (n = 10) (Log 2FC sev 1) with corresponding p-values (Log10 pval mild 1, Log10 pval sev 1). Differential expression of same 22 genes in sepsis (GSE154918, RNA-seq, (Herwanto et al., 2021)), sepsis and bacterial infection (n = 65) versus healthy (n= 40) (Log 2FC sev 2) with corresponding p-values (Log10 pval sev 2). Log2 FC values color-coded from red (upregulation) to blue (downregulation), NA gene absent. Log10 p-values color-coded from green (more significant) to white, not significant (yellow), NA, gene absent. **C** Expression ratios of genes in isolated cells, (GSE60424, RNA-seq, (Linsley et al., 2014)), all monocyte samples excluding IFN treated MS, and sepsis (Mo control, n= 14), all neutrophil samples excluding IFN treated MS, and sepsis (Ne control, n= 14), monocytes IFN treated MS (Mo IFN, n= 3), neutrophils IFN treated MS (Ne IFN, n= 3), monocytes sepsis (Mo sepsis, n= 3), and neutrophils sepsis (Ne sepsis, n= 3). In RNA-seq table, 1 count added, and made cpm, before calculating ratios. Ratio values color-coded in grey. **D** Correlation, hierarchical clustering of gene expression correlation matrix of same 22 genes using the collection of 38 blood transcriptomic datasets on severe inflammation, genes selected in set SIM and set FAM20A-4 as indicated.

Figure S12

Selection of gene sets induction by interferon gamma and induction by interferon alpha.

Main criteria: 1) genes belonging to either interferon alpha or interferon gamma related (sub) clusters of correlated expression in whole blood in the absence of severe inflammation. 2) upregulation during mild inflammation, and 3) upregulation in isolated cells from IFN treated MS. **A** Reciprocal ranking in 80 gene expression correlation profiles (rows) obtained using a exploratory collection of 62 blood transcriptomic datasets excluding severe inflammation (see sheet 16 supporting table 1). Gene rankings as derived from minimally 25 contributing datasets, approximately 50-55 contributing datasets on average. Gene rankings in profiles

medRxiv preprint doi: https://doi.org/10.1101/2023.05.10.23289779; this version posted November 4, 2024. The copyright holder for this preprint (which was not certified by peer review) is the author/funder, who has granted medRxiv a license to display the preprint in perpetuity. All rights reserved. No reuse allowed without permission.

color-coded in green from 1 (high) to 400 (low). Interferon regulated genes, and relevant marker genes for cell types, cellular process, and inflammation as indicated. Genes IL1RN, TNFAIP6, CASP1 and AIM2 were used as additional markers for inflammation with involvement of interferon in gene induction. Gene markers exclusively induced in monocytes during inflammation (TCN2, C2, C1Qs), and genes markers IL1B (NF-kB) and SOCS3 (STAT3) mainly induced in neutrophils during inflammation were also included. A stronger correlated expression of genes in proliferation with genes expressed in plasmablasts than in neutrophil bands, a tight correlated expression of genes expressed in neutrophil bands (clusters AZU1 and MMP8), and a correlated expression of LDHA with genes in biogenesis, indicated a relative absence of severe inflammation in the dataset collection. Marker genes upregulated in inflammation indicated in red**. B** Differential expression of 23 genes in set interferon gamma, and 8 genes in set interferon alpha, mild respiratory viral infection (GSE68310, GPL10558, (Zhai et al., 2015)), ill days 0 and 2 (n= 258) versus baseline and spring (n= 243) (Log2 FC mild 1), and sepsis (E-MTAB-5273, GPL10558, (Burnham et al., 2017)) sepsis (n= 221) versus control (n = 10) (Log 2FC sev 1) with corresponding p-values (Log10 pval mild 1, Log10 pval sev 1). Differential expression of same 31 genes in sepsis (GSE154918, RNA-seq, (Herwanto et al., 2021)), sepsis and bacterial infection (n = 65) versus healthy (n= 40) (Log 2FC sev 2) with corresponding p-values (Log10 pval sev 2). Log2 FC values color-coded from red (upregulation) to blue (downregulation), NA gene absent. Log10 p-values color-coded from green (more significant) to white, not significant (yellow), NA, gene absent. **C** Expression ratios of same 31 genes in isolated cells (GSE60424, RNA-seq, (Linsley et al., 2014)), all monocyte samples excluding IFN treated MS, and sepsis (Mo control, n= 14), all neutrophil samples excluding IFN treated MS, and sepsis (Ne control, n= 14), monocytes IFN treated MS (Mo IFN, n= 3), neutrophils IFN treated MS (Ne IFN, n= 3), monocytes sepsis (Mo sepsis, n= 3), and neutrophils sepsis (Ne sepsis, n= 3). In RNA-seq table, 1 count added, and made cpm, before calculating ratios. Ratio values color-coded in grey. **D** Correlation, hierarchical clustering of gene expression correlation matrix of 31 genes in interferon modules, using the collection of 62 blood transcriptomic datasets excluding severe inflammation, genes selected in sets interferon gamma and alpha as indicated.

Figure S13

Expression correlation clustering of genes and corresponding gene probes used in comparing gene module / set expression values between different inflammatory illnesses.

medRxiv preprint doi: https://doi.org/10.1101/2023.05.10.23289779; this version posted November 4, 2024. The copyright holder for this preprint (which was not certified by peer review) is the author/funder, who has granted medRxiv a license to display the preprint in perpetuity. All rights reserved. No reuse allowed without permission.

Hierarchical clustering of genes in expression correlation matrices for 3 different datasets on severe inflammation, each from a different platform. Genes in set T cell (bias naive T cell, n= 13), SIM set (Severe Inflammatory Myeloid, n= 16), FAM20A set (n= 4), GC-2 set (n= 9), interferon gamma induced gene set (IFN gamma, n= 23), and interferon alpha induced gene set (IFN alpha, n= 8) as indicated. **A** dataset GSE66099, (Sweeney et al., 2015), samples SIRS, sepsis and septic shock (n total = 229), GPL570, Affymetrix Human Genome U133 Plus 2.0 Array. **B** dataset E-MTAB-5273, (Burnham et al., 2017), samples sepsis (n total = 221), GPL10558, Illumina HumanHT-12 V4.0 expression beadchip. **C** dataset GSE154918, (Herwanto et al., 2021), samples sepsis, septic shock, and uncomplicated bacterial infection (n total = 65), GPL20301, Illumina HiSeq 4000 (Homo sapiens). Gene expression correlation clusters corresponding to T cells and SIM set are well separated, with negative correlation. GC-2 clusters, corresponding to GC-induced genes in severe inflammation, and genes from the SIM set are positively correlated, and well separated, while the existence of a cluster for FAM20A genes, separate from other SIM genes, is not as clear from individual datasets. Gene expression clusters corresponding to either induction by interferon gamma, or interferon alpha are positively correlated and well separated. Experiment E-MTAB-5273 only provided a subset of available probes for platform GPL10558 with 7 selected gene probes missing. The clustering results indicated that selected genes, and selected gene probes used for Affymetrix, Illumina, and RNA-seq platforms (see supporting table 5) were generally adequate.

Figure S14

Distribution of gene set expression in health and during inflammatory illnesses (Affymetrix)

GC-1 and GC-2 gene set expression in whole blood samples from sepsis, severe injury, systemic JIA, sarcoidosis, systemic sclerosis, rheumatoid arthritis, and asthma patients. Included for comparison are expression values for gene sets T cell, severe inflammatory myeloid (SIM), FAM20A, (4 genes including FAM20A), interferon gamma (inf gamma), and interferon alpha (inf alpha). All datasets are obtained using Affymetrix Human Genome U133 Plus 2.0 Array (GPL570), and identical probesets (see supporting table 5) were used to calculate gene set expression values for each dataset. **A**; GSE66099 (Sweeney et al., 2015), healthy, SIRS, sepsis and septic shock (s-shock). **B**; GSE36809 (Xiao et al., 2011), healthy, blunt trauma till 99 h (trauma<99h), from 99 h till 28 days (trauma>99h). **C**; GSE77791 (Plassais et al., 2017), healthy, severe burn shock (1-5 days, excluding 7 days samples; b.shock), severe burn shock with hydrocortisone treatment (1-5 days, excluding 7 days samples; b.shock GC). **D**; GSE80060 (Brachat et al., 2017), healthy, systemic juvenile

medRxiv preprint doi: https://doi.org/10.1101/2023.05.10.23289779; this version posted November 4, 2024. The copyright holder for this preprint (which was not certified by peer review) is the author/funder, who has granted medRxiv a license to display the preprint in perpetuity. All rights reserved. No reuse allowed without permission.

idiopathic arthritis (SJIA),with or withour canakinumab (can.mab) treatment on day 3 (all samples batch 1). **E**; GSE19314, (Koth et al., 2011), healthy and sarcoidosis. **F**; GSE65336 (Guo et al., 2015) systemic sclerosis (SSc) before (SSC d0) and after 56 days of anifrolumab treatment (SSc anifrolumab, d56). **G**; GSE93272 (Tasaki et al., 2018) healthy, and rheumatoid arthritis, both drugs treated and untreated (RA). **H**; GSE69683, platform GPL13158 (GPL570-like), (Bigler et al., 2017) healthy, moderate asthma, and severe asthma. Y-axis values on log-2 scale, with interval of 9 log 2 units for each panel. Shown are box plots with added binned dot plots.

Figure S15

Distribution of gene set expression in health and during inflammatory illnesses (Illumina)

GC-1 and GC-2 gene set expression in whole blood samples from patients with SIRS, sepsis, sepsis/ARDS, febrile bacterial and viral infection, Kawasaki disease, children's malaria, mild respiratory viral infection, and systemic lupus erythematosus (SLE), as well as from large healthy populations. Included for comparison are expression values for gene sets T cell, severe inflammatory myeloid (SIM), FAM20A, (4 genes including FAM20A), interferon gamma (inf gamma), and interferon alpha (inf alpha). All datasets are obtained using Illumina HumanHT-12 V4.0 or V3.0 expression beadchips (GPL10558 and GPL6947, respectively), and identical V4.0 probesets, which are also mostly present on V3.0, were used to calculate gene set expression values for each dataset (see supporting table 5). **A**; E-MTAB-5273, GPL10558 (Burnham et al., 2017), healthy, sepsis due to pneumonia (pneumonia), sepsis due to faecal peritonitis (f. peritonitis). **B**; E-MTAB-5273, GPL10558 (Burnham et al., 2017), healthy (none), sepsis response signature 1 (SRS1), sepsis response signature 2 (SRS2). **C**; GSE32707, GPL10558 (Dolinay et al., 2012), SIRS day 0 (SIRS), sepsis + ARDS day 0 (se/ARDS), sepsis alone day 0 (seps.), sepsis alone day 7 (seps.d7). **D**; GSE72829, only GPL10558, (Herberg et al., 2016), febrile children with bacterial infection (bacterial), febrile childeren with viral infection (viral), febrile children with unknown infection (unknown). **E**; GSE73463, GPL10558 (Wright et al., 2018), convalescent Kawasaki disease (kawasaki conv), acute Kawasaki disease (kawasaki acute). **F**: GSE34404, GPL10558 (Idaghdour et al., 2012), children without symptomatic malaria (control), children with symptomatic *P. falciparum* malaria (Pf malaria). **G**; GSE117613, GPL10558 (Nallandhighal et al., 2019), children without *P. falciparum* infection (no Pf), children with severe malarial anemia (m. anemia), children with cerebral malaria (c. malaria). **H**; GSE138458, GPL10558 (Guthridge et al.,

medRxiv preprint doi: https://doi.org/10.1101/2023.05.10.23289779; this version posted November 4, 2024. The copyright holder for this preprint (which was not certified by peer review) is the author/funder, who has granted medRxiv a license to display the preprint in perpetuity. All rights reserved. No reuse allowed without permission.

2020), SLE with low SLEDAI (SLE low), SLE with high SLEDAI (SLE high), control (control), (7 lower quality samples left out). **I**; GSE83456, GPL10558 (Blankley et al., 2016), healthy control (healthy), sarcoidosis (Sarcoid), extra pulmonary TB (EPTB), pulmonary TB (PTB). **J**; GSE42834, GPL10558 (Bloom et al., 2013), healthy control (healthy), non active Sarcoidosis (n act S), active Sarcoidosis (act Sarc), Tuberculosis (TB), lung cancer (lung Ca). **K**; GSE135304, GPL10558 (Kossenkov et al., 2019), benign pulmonary nodules (N benign), malign pulmonary nodules (N malign). **L**; GSE68310, GPL10558 (Zhai et al., 2015), healthy, mild respiratory influenza viral infection (ill). **M**; GSE68310, GPL10558 (Zhai et al., 2015), healthy, mild respiratory non-influenza viral infection (ill). **N**; GSE48348, GPL6947 (Westra et al., 2013), healthy individuals (n= 734). **O**; datasets E-MTAB-1708, E-TABM-1036, and GSE36382, each GPL6947 (Inouye et al., 2010; Mayerle et al., 2013; Schramm et al., 2014), healthy individuals (n= 993, 518, and 991, respectively), only box plot with outliers shown. Y-axis values on log-2 scale, with interval of 9 log 2 units for each panel. Shown are box plots with added binned dot plots.

Figure S16

Distribution of gene set expression in health and during inflammatory illnesses (RNA-seq) number 1

GC-2 gene set expression in whole blood samples from patients with SIRS, acute kidney injury, COVID-19, infectious diarrhea, brucellosis, leishmaniasis, adults malaria, inflammatory bowel disease (IBD), (systemic) juvenile idiopathic arthritis (SJIA and JIA), systemic lupus erythematosus (SLE), and mild respiratory viral infection, as well as from physically healthy populations. Included for comparison are expression values for gene sets T cell, severe inflammatory myeloid (SIM), FAM20A, (4 genes including FAM20A), interferon gamma (inf gamma), and interferon alpha (inf alpha). All datasets are obtained using mRNA sequencing and all genes, as present in different datasets, were used to calculate gene set expression values for each dataset (see supporting table 5). **A**; GSE67401 (Tsalik et al., 2015), SIRS, SIRS with acute kidney injury (SIRS-AKI), SIRS with hemodialysis (Hemodialysis), units 2 log rpm. **B**; GSE157103 (Overmyer et al., 2021), non COVID-19 patients not in ICU (ill), or in ICU (ill ICU), COVID-19 patients not in ICU (C19), or in ICU (C19 ICU), units 2 log tpm. **C**; GSE152641 (Thair et al., 2021), healthy control (healthy), Covid-19 hospital patients (S Covid-19), units 2 log cpm. **D**; GSE69529 (DeBerg et al., 2018), healthy, infectious diarrhea with either bacterial (bact_drr), or rotaviral infection (rota_drr), units 2 log

medRxiv preprint doi: https://doi.org/10.1101/2023.05.10.23289779; this version posted November 4, 2024. The copyright holder for this preprint (which was not certified by peer review) is the author/funder, who has granted medRxiv a license to display the preprint in perpetuity. All rights reserved. No reuse allowed without permission.

cpm. **E**; GSE69597 (Dufort et al., 2016), healthy, brucellosis, leishmaniasis, units 2 log cpm. **F**; GSE52166 (Tran et al., 2016), healthy adults (healthy), adults with febrile *Plasmodium falciparum* malaria (Pf malaria), units 2 log fpkm. **G**; GSE112057 (Mo et al., 2018), healthy, ulcerative colitis (UC), Crohn disease (Crohn), juvenile idiopathic arthritis (JIA), systemic juvenile idiopathic arthritis (SJIA), units 2 log cpm. **H**; GSE72509 (Hung, Pratt, Sundararaman, Townsend, et al., 2015), healthy, systemic lupus erythematosus (SLE), units 2 log rpkm. **I**; GSE107994 (Singhania et al., 2018), control, LTBI (latent TB), LTBI Progressor (l prog TB), active TB, units 2 log cpm. **J;** GSE107793 (Singhania et al., 2018), control, LTBI (latent TB), units 2 log cpm. **K**; GSE97356 (Kuan et al., 2017), healthy and post traumatic stress disorder (PTSD), no PTSD, (no ptsd) , past PTSD (past ptsd), and actual PTSD (ptsd), units 2 log cpm. Shown are box plots with added binned dot plots.

Figure S17

Distribution of gene set expression in health and during inflammatory illnesses (RNA-seq) number 2

GC-1 and GC-2 gene set expression in whole blood samples from acute fungal, bacterial and viral infection, sepsis, severe Covid-19, rheumatoid arthritis (RA), asthma, septic shock, Kawasaki disease, mild coronaviral infection, health, and additionally, gene set expression also in PBMC samples for severe Covid-19. Included for comparison are expression values for gene sets T cell, severe inflammatory myeloid (SIM), FAM20A, (4 genes including FAM20A), interferon gamma (inf gamma), and interferon alpha (inf alpha) (see supporting table 5). **A**; GSE176260, (Steinbrink et al., 2021), healthy control (Health), acute bacterial infection (Bact), acute candidemia (Cand), acute non infectious illness labeled SIRS (SIRS), acute viral infection (vir), units 2 log TMM normalized counts. **B**; GSE60424 (Linsley et al., 2014), diseases excluding sepsis patients and interferon-treated MS patients (other), and sepsis patients (3 samples, sepsis), units 2 log TMM normalized counts. **C**; GSE171110 (Lévy et al., 2021), healthy control (healthy), and severe Covid-19 patients (Sev. Covid-19), units 2 log cpm. **D**; GSE117769 published by Goldberg and co-workers (2018), healthy control (healthy), rheumatoid arthritis without GC treatment (RA-GC), rheumatoid arthritis with GC treatment (RA+GC), units made 2 log cpm. **E**; GSE115823 (Altman et al., 2019), asthmatic children with cold (cold), asthmatic children with cold, asthma exacerbation and systemic GC use (cold/asthmaX/GC), units made 2 log cpm. **F**; GSE161918 (C. Liu et al., 2021), PBMC from healthy control (healthy), and severe Covid-19 patients (Sev. Covid-19), units made 2

medRxiv preprint doi: https://doi.org/10.1101/2023.05.10.23289779; this version posted November 4, 2024. The copyright holder for this preprint (which was not certified by peer review) is the author/funder, who has granted medRxiv a license to display the preprint in perpetuity. All rights reserved. No reuse allowed without permission.

log cpm. **G**; GSE154918 (Herwanto et al., 2021), healthy control (healthy), bacterial infection (bact. inf.), and sepsis, units 2 log normalized value. **H**; GSE110487 (Barcella et al., 2018), septic shock within 16h (septic shock T1), and within 48h (septic shock T2) of admission to ICU. At T1 no patients, at T2 one in 31 patients with hydrocortisone treatment, units made 2 log cpm **I**; GSE207751 (published by Ginebaugh and colleagues, 2022), healthy, moderate asthma, and severe asthma, units 2 log normalized value. **J**; GSE161731 (McClain et al., 2021), healthy control from student cohort (H), mixed severity influenza (Influ.), seasonal corona and other non-influenza respiratory viral infection, mainly prospective from healthy student cohort, and mild (Cor.), mixed severity COVID-19 (C-19), and severe (septic) bacterial pneumonia (Bact. Pn.), units, 2 log tpm, 0.1 tpm added. **K**; GSE196117 (Karakike et al., 2022), healthy control (healthy), sepsis, no recent high dose cortisol intake, with or without clarithromycin treatment (sepsis), units made 2 log cpm **L**; GSE178491 (Ghosh et al., 2022), convalescent Kawasaki (Kawa. conval.), acute Kawasaki before initiation of treatments (Kawa. acute), febrile non-Kawasaki control (febr. acute), 10 samples below 5 million total counts not used, units made 2 log cpm. **M;** GSE113883 (Braun et al., 2018), circadian experiment, using timepoints 13h, 15h, 17h, 19h (T down), and timepoints 1h, 3h, 25h, 27h (T up), outlier individual labeled nr14 removed, units 2 log tpm, 0.1 tpm added**.** Y-axis values on log-2 scale, with interval of 9 log 2 units for each panel. Shown are box plots with added binned dot plots.

Figure S18

Distribution of gene set expression in health and during inflammatory illnesses (other platforms)

GC-1 and GC-2 gene set expression in whole blood samples in health, septic shock, SLE, rheumatoid arthritis (RA), Crohn disease, and ulcerative colitis (UC). Included for comparison are expression values for gene sets T cell, severe inflammatory myeloid (SIM), FAM20A, (4 genes including FAM20A), interferon gamma (inf gamma), and interferon alpha (inf alpha) (see supporting table 5). **A**; GSE110160 (platform GPL3921 taking probesets with highest mean expression) (Hu et al., 2018), healthy, and healthy 2-8 h after prednisolone intake (GC 2-8h). **B**; GSE106878 (platform GPL10295 taking probesets with highest mean expression) (Kolte, 2020), septic shock placebo 0 h (Ssh P0), septic shock hydrocortisone 0 h (Ssh GC0), septic shock placebo 24 h (Ssh P24), septic shock hydrocortisone 24 h (Ssh GC 24). **C**; GSE110174 (platform GPL13158 taking probesets with highest mean expression) (Hu

medRxiv preprint doi: https://doi.org/10.1101/2023.05.10.23289779; this version posted November 4, 2024. The copyright holder for this preprint (which was not certified by peer review) is the author/funder, who has granted medRxiv a license to display the preprint in perpetuity. All rights reserved. No reuse allowed without permission.

et al., 2018), healthy, SLE low and medium prednisone usage (SL l/m GC), SLE high prednisone usage (SL hGC), SLE unknown prednisone usage (SL uGC). **D**; GSE110169 (platform GPL13667 taking probesets with highest mean expression), batches 1 and 3 (Hu et al., 2018), healthy, RA without GC treatment (RA-GC), RA with GC treatment (RA+GC), SLE without GC treatment (SLE-GC), SLE with GC treatment (SLE+GC). **E**; GSE110169 (platform GPL13667 taking probesets with highest mean expression), batches 2 and 4 (Hu et al., 2018), healthy, RA without GC treatment (RA-GC), RA with GC treatment (RA+GC), SLE without GC treatment (SLE-GC), SLE with GC treatment (SLE+GC). **F**; GSE126124 (platform GPL6244, taking probes with highest mean expression) (Palmer et al., 2019), non inflammatory bowel disease (IBD) control (control), Crohn disease without GC use (Crohn), ulcerative colitis without GC use (UC).

Figure S19

Checking gene expression clustering in set GC-1 and GC-2 for selected datasets

Reciprocal ranking in 19 gene expression correlation profiles obtained on 10 single data (sub) sets. **A** health (GSE48348, GPL6947 (Westra et al., 2013)), **B** health (GSE36382, GPL6947 (Mayerle et al., 2013)), **C** control (GSE34404, GPL10558 (Idaghdour et al., 2012)), **D** children's severe malaria, symptomatic (GSE34404, GPL10558 (Idaghdour et al., 2012)), **E** convalescent Kawasaki's disease (GSE73463, GPL10558 (Wright et al., 2018)), **F** acute Kawasaki's disease, GC-untreated (GSE73463, GPL10558 (Wright et al., 2018)), **G** infectious bacterial diarrhea (GSE69529, RNA-seq (DeBerg et al., 2018)), **H** rotaviral diarrhea (GSE69529, RNA-seq (DeBerg et al., 2018)), **I** health, data subset never PTSD (GSE97356, RNA-seq (Kuan et al., 2017)), **J** Septic shock, GC-untreated (except for one sample), timepoints 1 and 2 (GSE110487, RNA-seq (Barcella et al., 2018)). Genes in set GC-1 and set GC-2 as indicated. Gene rankings in profiles color-coded in green from 1 (high) to 200 (low). Gene expression correlation profiles for each of 19 example genes shown in rows.

Figure S20

Gene expression correlation analysis for evaluation of possible GC biomarker genes number 1

A,C, E : Overlap of first 50 genes in gene expression correlation profiles (see sheets 1,2,3 supporting table 6), color-coded in green (50-0). B, D. F : Reciprocal ranking of genes in profiles, color-coded in green (1-200). A ,B : health, GSE113883 (Braun et al., 2018), (n = 140, excluding samples for outlier individual 14). Gene names in grey : at or below detection.

medRxiv preprint doi: https://doi.org/10.1101/2023.05.10.23289779; this version posted November 4, 2024. The copyright holder for this preprint (which was not certified by peer review) is the author/funder, who has granted medRxiv a license to display the preprint in perpetuity. All rights reserved. No reuse allowed without permission.

C , D : SLE, GSE72509 (Hung, Pratt, Sundararaman, Towsend, et al., 2015), (all SLE samples, n = 99). E, F : sepsis, GSE154918 (Herwanto et al., 2021), (all sepsis samples, n = 53). Black square : indicative for severe inflammation. Possible GC biomarker genes indicated by red square, relevant marker genes used as indicated.

Figure S21

Gene expression correlation analysis for evaluation of possible GC biomarker genes number 2

Whole blood gene expression correlation in Rheumatoid Arthritis, asthma, and JIA. A,C, E : Overlap of first 50 genes in gene expression correlation profiles (see sheets 4,5,7 supporting table 6), color-coded in green (50-0). B, D. F : Reciprocal ranking of genes in profiles, color-coded in green (1-200). A ,B : Rheumatoid Arthritis , GSE117769 (Goldberg and co-workers), (all RA samples, n = 52). D : Asthma, GSE207751 (Ginebaugh and co-workers), (all asthma samples, n = 42). E, F : JIA, GSE112057 (Mo et al., 2018), (all JIA samples, n = 89). Possible GC biomarker genes indicated by red square, relevant marker genes used as indicated.

Figure S22

Gene expression correlation analysis for evaluation of possible GC biomarker genes number 3

Whole blood gene expression correlation in SJIA, IBD, and rotaviral gastroenteritis. A,C, E : Overlap of first 50 genes in gene expression correlation profiles (see sheets 7,6 supporting table 6), color-coded in green (50-0). B, D. F : Reciprocal ranking of genes in profiles, color-coded in green (1-200). A ,B : SJIA , GSE112057 (Mo et al., 2018), (all SJIA samples, n = 26). D : IBD, GSE112057 (Mo et al., 2018), (all Crohn and UC samples, n = 75). E, F : rotaviral gastroenteritis, GSE69529 (DeBerg et al., 2018), (all rotavirus samples, n = 55). Possible GC biomarker genes indicated by red square, relevant marker genes used as indicated.

Figure S23

Gene expression correlation analysis for evaluation of possible GC biomarker genes number 4

Whole blood gene expression correlation in bacterial gastroenteritis, and frequently GC-treated severe COVID-19. A,C, E : Overlap of first 50 genes in gene expression correlation profiles (see sheets 6,8,9 supporting table 6), color-coded in green (50-0). B, D. F : Reciprocal ranking of genes in profiles, color-coded in green (1-200). A ,B : bacterial

medRxiv preprint doi: https://doi.org/10.1101/2023.05.10.23289779; this version posted November 4, 2024. The copyright holder for this preprint (which was not certified by peer review) is the author/funder, who has granted medRxiv a license to display the preprint in perpetuity. All rights reserved. No reuse allowed without permission.

gastroenteritis, GSE69529 (DeBerg et al., 2018), (bacterial samples, n = 124). D : Severe COVID-19 , GSE171110 (Lévy et al., 2021), (all COVID-19 samples, n = 44). E, F : Severe COVID-19, GSE157103 (Overmyer et al., 2021), (all COVID-19, ICU and not ICU, samples, n = 100). Possible GC biomarker genes indicated by red square, relevant marker genes used as indicated. Black squares : indicative for severe inflammation.

Figure S24

Gene expression correlation analysis for evaluation of possible GC biomarker genes number 5

Whole blood gene expression correlation in GC-treated, and GC-untreated COVID-19. A,C, E : Overlap of first 50 genes in gene expression correlation profiles (see sheets 10,11,12 supporting table 6), color-coded in green (50-0). B, D. F : Reciprocal ranking of genes in profiles, color-coded in green (1-200). A ,B : Severe COVID-19, GSE206264 ((López-Martínez et al., 2023), (both GC-treated and GC-untreated, n = 27). D : Severe COVID-19, GSE168400 (Amado-Rodríguez et al., 2022), (GC-untreated COVID-19, n = 42). E, F : Severe COVID-19, GSE197204 (López-Martínez et al., 2023), (GC-untreated COVID-19, n = 56, with sample overlap with GSE168400). Possible GC biomarker genes indicated by red square, relevant marker genes used as indicated.

Figure S25

Comparing GC-inducible genes for use as whole blood transcriptomic biomarkers in health and in different diseases.

Differential expression between different circadian phase in health (A), and between disease and healthy control (B-H). In addition, a measure of gene expression distribution range in disease (B-L) was used as a proxy for DEGs to account for absence of healthy control groups, and gene expression below or at detection limit in health in different datasets. Overlap of first 50 highest ranking genes in gene expression correlation profiles with exploratory GC signature genes was used to indicate relative strength of induction by GC. The figure is a visualization of analysis presented in supporting table 6 on 12 RNA-seq datasets. **A** : Circadian in health, GSE113883 (Braun et al., 2018), log10 of mean expression (tpm) in all samples (Log10 H); mean of all individual log2 ratios (n = 11) of expression between T1 timepoints (1h, 3h, 25h, 27h), and T2 timepoints (13h, 15h, 17h, 19h), (Log2FC T1/T2); log10 of corresponding p-values (Log10 pval); overlap of first 50 genes in expression correlation profiles, with genes present in exploratory GC signatures 1 and 2, correlation

medRxiv preprint doi: https://doi.org/10.1101/2023.05.10.23289779; this version posted November 4, 2024. The copyright holder for this preprint (which was not certified by peer review) is the author/funder, who has granted medRxiv a license to display the preprint in perpetuity. All rights reserved. No reuse allowed without permission.

profiles obtained on 140 samples excluding outlier individual labelled nr14 in dataset (GC signature H). 0.1 tpm unit was added to GSE113883 (table in tpm), before calculations (see sheet 1 supporting table 6). **B** : SLE , GSE72509 (Hung, Pratt, Sundararaman, Towsend, et al., 2015), log10 of mean expression (rpkm) in healthy control samples (Log10 H), Log2 fold change in SLE (n = 99), and healthy controls (n = 18), (Log2FC SLE/H) ; log10 of corresponding p-values (Log10 pval); Log2 of ratio of mean value above 9th decile, and mean value below first quartile in distribution for SLE samples (Log2 D10m/Q1m SLE) ; overlap of first 50 genes in expression correlation profiles, obtained on SLE samples, with genes present in exploratory GC signature 1 and 2 (GC signature SLE) (see sheet 2 supporting table 6). **C** : Sepsis, GSE154918 (Herwanto et al., 2021), log10 of mean expression (normalized value) in healthy control samples (Log10 H), Log2 fold change in sepsis (n = 53), and healthy controls (n = 40), (Log2FC SEPSIS /H) ; log10 of corresponding p-values (Log10 pval); Log2 of ratio of mean value above 9th decile, and mean value below first quartile in distribution for sepsis samples (Log2 D10m/Q1m SEPS.) ; overlap of first 50 genes in expression correlation profiles, obtained on sepsis samples, with genes present in exploratory GC signature 1 and 2 (GC signature SEPSIS) (see sheet 3 supporting table 6). **D** : Rheumatoid Arthritis (RA) , GSE117769 (Goldberg and co-workers, 2018), log10 of mean expression (cpm) in healthy control samples (Log10 H), Log2 fold change in GC-treated RA (n = 29), and healthy controls (n = 50), (Log2FC RA+GC/H) ; log10 of corresponding p-values (Log10 pval); Log2 fold change in GC-treated RA (n = 29), and GC-untreated RA (n = 23), (Log2FC +GC/-GC) ; log10 of corresponding p-values (Log10 pval) ; Log2 of ratio of mean value above 9th decile, and mean value below first quartile in distribution for RA samples (Log2 D10m/Q1m RA); overlap of first 50 genes in expression correlation profiles, obtained on RA samples, with genes present in exploratory GC signature 1 and 2 (GC signature RA). 1 count was added to GSE117769 (table in counts), and values cpm normalized, before calculations (see sheet 4 supporting table 6). **E** : Asthma, GSE207751 (Ginebaugh and co-workers, 2022), log10 of mean expression (normalized value) in healthy control samples (Log10 H), Log2 fold change in severe asthma (n = 23), and healthy controls (n = 14), (Log2FC AST. SEV. /H) ; log10 of corresponding p-values (Log10 pval); Log2 fold change in severe asthma (n = 23), and moderate asthma (n = 19), (Log2FC SEV./MOD.); log10 of corresponding p-values (Log10 pval) ; Log2 of ratio of mean value above 9th decile, and mean value below first quartile in distribution for all (n = 42) asthma samples (Log2 D10m/Q1m AST.); overlap of first 50 genes in expression correlation profiles, obtained on all asthma samples, with genes present in exploratory GC signature 1 and 2 (GC signature AST.)

medRxiv preprint doi: https://doi.org/10.1101/2023.05.10.23289779; this version posted November 4, 2024. The copyright holder for this preprint (which was not certified by peer review) is the author/funder, who has granted medRxiv a license to display the preprint in perpetuity. All rights reserved. No reuse allowed without permission.

(see sheet 5 supporting table 6). **F** : Gastroenteritis, GSE69529 (DeBerg et al., 2018), log10 of mean expression (cpm) in healthy control samples (Log10 H), Log2 fold change in rotaviral gastroenteritis (n = 55), and healthy controls (n = 24), (Log2FC ROTAVIRUS/H) ; log10 of corresponding p-values (Log10 pval); Log2 of ratio of mean value above 9th decile, and mean value below first quartile in distribution for rotaviral gastroenteritis samples (Log2 D10m/Q1m ROTA); overlap of first 50 genes in expression correlation profiles, obtained on rotaviral gastroenteritis samples, with genes present in exploratory GC signature 1 and 2 (GC signature ROTA). Log2 fold change in bacterial gastroenteritis (n = 124), and healthy controls (n = 24), (Log2FC BACTERIAL/H) ; log10 of corresponding p-values (Log10 pval) ; Log2 of ratio of mean value above 9th decile, and mean value below first quartile in distribution for bacterial gastroenteritis samples (Log2 D10m/Q1m BACT.); overlap of first 50 genes in expression correlation profiles, obtained on bacterial gastroenteritis samples, with genes present in exploratory GC signature 1 and 2 (GC signature BACT.). 1 count was added to GSE69529 (table in counts), and values cpm normalized, before calculations (see sheet 6 supporting table 6). **G** : JIA, SJIA, and IBD, GSE112057 (Mo et al., 2018), log10 of mean expression (cpm) in healthy control samples (Log10 H), Log2 fold change in JIA (n = 89), and healthy controls (n = 12), (Log2FC JIA/H) ; log10 of corresponding p-values (Log10 pval); Log2 of ratio of mean value above 9th decile, and mean value below first quartile in distribution for JIA samples (Log2 D10m/Q1m JIA); overlap of first 50 genes in expression correlation profiles, obtained on JIA samples, with genes present in exploratory GC signature 1 and 2 (GC signature JIA). Log2 fold change in SJIA (n = 26), and healthy controls (n = 12), (Log2FC SJIA/H) ; log10 of corresponding p-values (Log10 pval); Log2 of ratio of mean value above 9th decile, and mean value below first quartile in distribution for SJIA samples (Log2 D10m/Q1m SJIA); overlap of first 50 genes in expression correlation profiles, obtained on SJIA samples, with genes present in exploratory GC signature 1 and 2 (GC signature SJIA). Log2 fold change in IBD (n = 75), and healthy controls (n = 12), (Log2FC IBD/H) ; log10 of corresponding p-values (Log10 pval); Log2 of ratio of mean value above 9th decile, and mean value below first quartile in distribution for IBD samples (Log2 D10m/Q1m IBD); overlap of first 50 genes in expression correlation profiles, obtained on IBD samples, with genes present in exploratory GC signature 1 and 2 (GC signature IBD). 1 count was added to GSE112057 (table in counts), and values cpm normalized, before calculations (see sheet 7 supporting table 6). **H** : Severe COVID-19, frequent GC treatment, GSE171110 (Lévy et al., 2021), log10 of mean expression (cpm) in healthy control samples (Log10 H), Log2 fold change in severe COVID-19 (n = 44), and healthy controls (n = 10), (Log2FC C-19/H) ; log10

medRxiv preprint doi: https://doi.org/10.1101/2023.05.10.23289779; this version posted November 4, 2024. The copyright holder for this preprint (which was not certified by peer review) is the author/funder, who has granted medRxiv a license to display the preprint in perpetuity. All rights reserved. No reuse allowed without permission.

of corresponding p-values (Log10 pval); Log2 of ratio of mean value above 9th decile, and mean value below first quartile in distribution for COVID-19 samples (Log2 D10m/Q1m C-19); overlap of first 50 genes in expression correlation profiles, obtained on COVID-19 samples, with genes present in exploratory GC signature 1 and 2 (GC signature C-19). 1 count was added to GSE171110 (table in counts), and values cpm normalized, before calculations. (see sheet 8 supporting table 6) **I** : Severe COVID-19, frequent GC treatment, GSE157103 (Overmyer et al., 2021), Log2 fold change in severe COVID-19 in ICU (n = 50), and severe COVID-19 not in ICU (n = 50), (Log2FC ICU/not ICU) ; log10 of corresponding p-values (Log10 pval); Log2 of ratio of mean value above 9th decile, and mean value below first quartile in distribution for all (n = 100) severe COVID-19 samples (Log2 D10m/Q1m C-19); overlap of first 50 genes in expression correlation profiles, obtained on all severe COVID-19 samples, with genes present in exploratory GC signature 1 and 2 (GC signature C-19). 0.1 tpm unit was added to GSE157103 (table in tpm), before calculations (see sheet 9 supporting table 6). **J** : Severe COVID-19, GSE206264 (López-Martínez et al., 2023), Log2 fold change in GC-treated severe COVID-19 (n = 11), and GC-untreated severe COVID-19 (n = 16), (Log2FC +GC/-GC) ; log10 of corresponding p-values (Log10 pval); Log2 of ratio of mean value above 9th decile, and mean value below first quartile in distribution for all (n = 27) severe COVID-19 samples (Log2 D10m/Q1m C-19); overlap of first 50 genes in expression correlation profiles, obtained on all severe COVID-19 samples, with genes present in exploratory GC signature 1 and 2 (GC signature C-19). 1 count was added to GSE206264 (table in counts), and values cpm normalized, before calculations (see sheet 10 supporting table 6). **K** : Severe COVID-19, no GC treatment, GSE168400 (Amado-Rodríguez et al., 2022), Log2 of ratio of mean value above 9th decile, and mean value below first quartile in distribution for all (n = 42) severe COVID-19 samples (Log2 D10m/Q1m C-19); overlap of first 50 genes in expression correlation profiles, obtained on all severe COVID-19 samples, with genes present in exploratory GC signature 1 and 2 (GC signature C-19). 1 count was added to GSE168400 (table in counts), and values cpm normalized, before calculations (see sheet 11 supporting table 6). **L** : Severe COVID-19, no GC treatment, GSE197204 (López-Martínez et al., 2023), (some samples shared with GSE168400), Log2 of ratio of mean value above 9th decile, and mean value below first quartile in distribution for all (n = 56) severe COVID-19 samples (Log2 D10m/Q1m C-19); overlap of first 50 genes in expression correlation profiles, obtained on all severe COVID-19 samples, with genes present in exploratory GC signature 1 and 2 (GC signature C-19). 1 count was added to GSE197204 (table in counts), and values cpm normalized, before calculations (see sheet 12 supporting

medRxiv preprint doi: https://doi.org/10.1101/2023.05.10.23289779; this version posted November 4, 2024. The copyright holder for this preprint (which was not certified by peer review) is the author/funder, who has granted medRxiv a license to display the preprint in perpetuity. All rights reserved. No reuse allowed without permission.

table 6). **A-L** Relative gene expression in healthy controls color-coded from blue (maximal) to white (minimal), for each dataset separately. Genes expressed at or below detection limit (in health) shaded in grey. Log2 fold change in differential expression color-coded in red (maximal upregulation) to blue (maximal downregulation), for each comparison separately. Corresponding p-values color-coded from green (minimal value in comparison) to white, shaded yellow at p-value above 0.05 (not significant). Log2 of ratio of mean value above 9th decile and mean value below first quartile color-coded in red (maximal) to white (minimal), for each dataset (or subset) separately, to indicate range in distribution. Overlap of highest 50 ranking genes in expression correlation profiles with exploratory GC signatures 1 and 2 coded in grey (50) to white (0). NA: gene absent in dataset. GC biomarker gene sets GC-1 (lightgreen), and GC-2 (darkgreen), possible GC biomarker genes (red), and relevant marker genes as indicated (B and M, antigen presentation by B cell and monocyte; NF-kB, NF-kB dependent gene induction; immature neutrophil, neutrophil bands or (meta) myelocytes in case of severe inflammation; NK/C-TOX, natural killer cell and cytotoxic T cell. Upregulated marker genes in severe inflammation include PPARG (monocytes), MERTK (monocytes and neutrophils), and genes GYG1, HK3, LDHA (mainly neutrophil). Downregulated marker genes in severe inflammation include genes ALDH1A1, PLA2G7, and ARHGEF10L (in monocytes), and genes MME, HAL, and NOV (downregulated in neutrophil compartment).

Figure S26

Graphical abstract

Table S1

Signatures of GC-driven gene expression in whole blood

14 gene expression correlation signatures of GC-driven gene expression obtained on 4 whole blood dataset (sub) collections combining different GC-induced genes as correlation queries. Gene ranking in gene expression correlation profiles color-coded in green from 1 (high) to 500 (low). Lists are cut off at 2000 genes. Average correlation value (cor), number of contributing datasets (nr), and ranking (rank) in single gene profile. Mean of rankings in different profiles (mean.rank), sum of contributing datasets (sumof supportingdatasets), and final ranking in signature (rank.mean). #N/B; number of contributing datasets for a gene in a profile below a set threshold.

medRxiv preprint doi: https://doi.org/10.1101/2023.05.10.23289779; this version posted November 4, 2024. The copyright holder for this preprint (which was not certified by peer review) is the author/funder, who has granted medRxiv a license to display the preprint in perpetuity. All rights reserved. No reuse allowed without permission.

Sheet 1) circadian cortisol 15 nonsevere; Gene expression correlation signature from circadian cortisol with little cell type bias obtained on a collection of 15 datasets excluding severe inflammation, using GC-induced query genes, PER1, ZBTB16, DDIT4, TSC22D3, KLF9, IRS2.

Sheet 2) circ cort 15 nonsev bias Lympho; Gene expression correlation signature from circadian cortisol with bias for lymphocytes (mostly NK) obtained on a collection of 15 datasets excluding severe inflammation, using GC-induced query gene DDIT4. Several high ranking genes more generally expressed in NK cells and NK/T cells as indicated (bold, red, orange).

Sheet 3) circ cort 15 nonsev bias Neutro; Gene expression correlation signature from circadian cortisol with bias for neutrophils obtained on a collection of 15 datasets excluding severe inflammation, using GC-induced query genes, TSC22D3, IRS2, FKBP5, ECHDC3, TPST1. Several genes more generally expressed in neutrophils as indicated (bold, red).

Sheet 4) inflam. GC 15 sev bias Lympho; Gene expression correlation signature from GC in severe inflammation with bias for lymphocytes obtained on a collection of 15 datasets on severe inflammation using GC-induced query gene DDIT4.

Sheet 5) inflam. GC 15 sev bias Myelo; Gene expression correlation signature from GC in severe inflammation with bias for neutrophils and monocytes obtained on a collection of 15 datasets on severe inflammation using GC-induced query genes, FLT3, ADORA3, CD163, OLAH, DAAM2, ADAMTS2, VSIG4. Several genes more generally upregulated in neutrophils during severe inflammation as indicated (bold, red).

Sheet 6) inflam. GC 15 sev bias Neutro; Gene expression correlation signature from GC in severe inflammation with bias for neutrophil obtained on a collection of 15 datasets on severe inflammation using GC-induced query genes, OLAH, IL1R2, IL18R1, FKBP5, ECHDC3. Several genes more generally upregulated in neutrophils during severe inflammation as indicated (bold, red).

Sheet 7) inflam. GC 15 sev bias Mono; Gene expression correlation signature with bias for monocyte obtained on a collection of 15 datasets on severe inflammation using GC-induced query genes, FLT3, ADAMTS2, VSIG4, AMPH, GPER1. Several genes more generally upregulated in neutrophils during severe inflammation as indicated (bold, red).

medRxiv preprint doi: https://doi.org/10.1101/2023.05.10.23289779; this version posted November 4, 2024. The copyright holder for this preprint (which was not certified by peer review) is the author/funder, who has granted medRxiv a license to display the preprint in perpetuity. All rights reserved. No reuse allowed without permission.

Sheet 8) circadian cortisol 40 nonsevere; Gene expression correlation signature from circadian cortisol with little cell type bias obtained on a collection of 40 datasets excluding severe inflammation, using GC-induced query genes, PER1, ZBTB16, DDIT4, TSC22D3, KLF9, IRS2.

Sheet 9) circ cort 40 nonsev bias Lympho; Gene expression correlation signature from circadian cortisol with bias for lymphocytes (mostly NK) obtained on a collection of 40 datasets excluding severe inflammation, using GC-induced query gene DDIT4. Several high ranking genes more generally expressed in NK cells and NK/T cells as indicated (bold, red, orange).

Sheet 10) circ cort 40 nonsev bias Neutro; Gene expression correlation signature from circadian cortisol with bias for neutrophils obtained on a collection of 40 datasets excluding severe inflammation, using GC-induced query genes, TSC22D3, IRS2, FKBP5, ECHDC3, TPST1. Several genes more generally expressed in neutrophils as indicated (bold, red).

Sheet 11) inflam. GC 38 sev bias Lympho; Gene expression correlation signature from GC in severe inflammation with bias for lymphocytes obtained on a collection of 38 datasets on severe inflammation using GC-induced query gene DDIT4.

Sheet 12) inflam. GC 38 sev bias Myelo; Gene expression correlation signature from GC in severe inflammation with bias for neutrophils and monocytes obtained on a collection of 38 datasets on severe inflammation using GC-induced query genes, FLT3, ADORA3, CD163, OLAH, DAAM2, ADAMTS2, VSIG4. Several genes more generally upregulated in neutrophils during severe inflammation as indicated (bold, red).

Sheet 13) inflam. GC 38 sev bias Neutro; Gene expression correlation signature from GC in severe inflammation with bias for neutrophil obtained on a collection of 38 datasets on severe inflammation using GC-induced query genes, OLAH, IL1R2, IL18R1, FKBP5, ECHDC3. Several genes more generally upregulated in neutrophils during severe inflammation as indicated (bold, red).

Sheet 14) inflam. GC 38 sev bias Mono; Gene expression correlation signature from GC in severe inflammation with bias for monocyte obtained on a collection of 38 datasets on severe inflammation using GC-induced query genes, FLT3, ADAMTS2, VSIG4, AMPH, GPER1. Several genes more generally upregulated in neutrophils during severe inflammation as indicated (bold, red).

medRxiv preprint doi: https://doi.org/10.1101/2023.05.10.23289779; this version posted November 4, 2024. The copyright holder for this preprint (which was not certified by peer review) is the author/funder, who has granted medRxiv a license to display the preprint in perpetuity. All rights reserved. No reuse allowed without permission.

Sheet 15) **dataset collections**; Lists of datasets in 4 collections used to obtain GC-driven gene expression profiles. Dataset collection blood no severe inflammation (n=15), and collection blood severe inflammation (n= 15) are subcollections of collection blood no severe inflammation (n= 40), and collection blood severe inflammation (n= 38), respectively. GEO and ArrayExpress dataset accessions (dataset), data subset used and edits performed (comment 1), and health or type of disease (comment 2) as indicated.

Sheet 16) **exploratory dataset collection**; Dataset collection blood no severe inflammation (n=62), also containing several PBMC datasets and whole blood datasets on MS and tuberculosis. Datasets from this larger collection were used to assemble collection blood no severe inflammation (n= 40, sheet 12), which excludes PBMC, tuberculosis, and MS datasets, among others.

Table S2

Overall signature of GC-driven gene expression *in vivo*, 7 gene sets derived from GC signatures in blood, and 9 DEG sets of *in vitro* GC induction in immune cells.

Candidate gene sets for regulation by GC were derived from expression correlation signatures of GC-driven gene expression *in vivo* from different dataset (sub) collections covering whole blood, PBMCs, isolated monocytes, and neutrophils, either in the absence or presence of severe inflammation. Gene sets were selected by combining related GC signatures, taking into account recurrent genes and top ranking genes. Upregulated DEG sets came from *in vitro* experiments on GC treatment of PBMCs, monocytes, macrophages, neutrophils, CD4 T cells, and B cells. A threshold of 2 fold upregulation and unadjusted p-values below 0.05 was used for upregulated DEGs. Sheets 3-11; Log2 fold change, and corresponding p-values all from two tailed, unpaired t tests.

Sheet 1) **exploratory GC sign. cut off**; top ranking genes (n = 272) in earlier GC signatures 1 and 2 obtained in the exploratory phase by programmatic selection of datasets from a collection of 375+ whole blood and PBMC transcriptomic datasets, using either GC inducible gene query 1 (PER1, ZBTB16, DDIT4, TSC22D3, KLF9, IRS2), or query 2 (FLT3, ADORA3, CD163, OLAH, DAAM2, ADAMTS2, VSIG4). **Sheet 2**) **all GC signatures 2000;** an overall signature of GC-driven gene expression in blood and tissues obtained by ranking genes by frequency of occurrence in first 2000 genes in 16 separate GC signatures (see supporting tables S1 and S3), and a comparison with upregulated DEGs by GC *in vitro* in different immune cells and human cell cultures from experiment GSE112101 (Franco et al.,

medRxiv preprint doi: https://doi.org/10.1101/2023.05.10.23289779; this version posted November 4, 2024. The copyright holder for this preprint (which was not certified by peer review) is the author/funder, who has granted medRxiv a license to display the preprint in perpetuity. All rights reserved. No reuse allowed without permission.

2019). Frequency, mean ranking and top ranking in positive signatures, and signature with highest ranking as indicated (GC signatures *in vivo* correlation). Log10 of unadjusted p-values < 0.05 (paired, two-tailed t-test) were calculated for DEGs in 9 sample groups of different cells in experiment GSE112101. Mean and minimal Log10 was calculated only for p-values corresponding with upregulated DEGs not using a threshold for fold upregulation. Sample group with lowest p-value as indicated. NA in pink, no sample group with significant upregulation; in grey, gene not present on platform or gene present with different alias (GC *in vitro* upregulated DEGs). **Sheet 3**) **gene sets from GC sign.;** drafting of 7 sets of candidate GC-regulated genes using combinations of overlap and high ranking in different GC signatures as indicated. Contributing GC signatures were from whole blood, PBMCs, monocytes and neutrophils. **Sheet 4**) **comparison GC sign. gene sets.**; comparison of candidate GC-regulated genes (n= 625 in total) in 7 gene sets selected from whole blood GC signatures 1 and 2, PBMC-based GC signatures, and from GC signatures in monocytes and neutrophils, either in health or in severe inflammation. Genes present in set 1, that were expressed in NK cells more generally and that originated from lymphocyte-biased circadian GC signatures, are marked in bold red. Set 1 ; from whole blood GC signatures 1 bias lymphocyte, little cell type bias, and bias neutrophil (WB GC signature circadian). Set 2 ; from whole blood GC signatures 2 bias myeloid cells, bias monocyte, and bias neutrophil (WB GC sign. Sev. Inflam. bias Myeloid cells). Set 3 ; from whole blood GC signatures 2 bias lymphocyte (WB GC sign. Sev. Inflam. bias Lymphocyte). Set 4; from circadian GC signature of isolated monocytes and circadian GC signature PBMC bias monocyte (mono GC signature circadian). Set 5; from GC signature of isolated monocytes in severe inflammation and whole blood GC signatures 2 bias monocyte (mono GC signature sev. inflam.). Set 6; from circadian GC signature of isolated neutrophils and whole blood circadian GC signatures 1 bias neutrophil (neutro GC signature circadian). Set 7; from GC signature of isolated neutrophils / granulocytes in severe inflammation and whole blood GC signatures 2 bias neutrophil (neutro GC signature sev. inflam.). All candidate GC-regulated genes in 7 sets were scored for their presence in 7 separate sets, to give a corresponding frequency distribution (frequency Signature sets). Number of times present in 9 DEG sets as tabled in sheet 14 also shown (frequency DEGs). **Sheet 5**) **PBMC_GSE100156**; GC upregulated DEGs in PBMCs (GSE110156; (Hu et al., 2018)). **Sheet 6**) **PBMC_GSE33649_8h**; GC upregulated DEGs in 8h dexamethasone treated, PHA activated PBMCs compared to 8h ethanol control treated, PHA activated PBMCs (GSE33649 subset, (Maranville et al., 2013)). **Sheet 7**) **MDMacro_GSE61880**; GC upregulated DEGs in monocyte derived macrophages

medRxiv preprint doi: https://doi.org/10.1101/2023.05.10.23289779; this version posted November 4, 2024. The copyright holder for this preprint (which was not certified by peer review) is the author/funder, who has granted medRxiv a license to display the preprint in perpetuity. All rights reserved. No reuse allowed without permission.

(GSE61880; (Jubb et al., 2016)), using time points corresponding with highest fold change as indicated. **Sheets 8, and 9**) GC upregulated DEGs in monocyte derived macrophages (**MDMacro_GSE109439**) and monocytes (**monocyte_GSE109439**) (GSE109439; (Wang et al., 2019)). **Sheets 10, 11, 12, 13**) GC upregulated DEGs in monocytes (**monocyte_GSE112101**), neutrophils (**neutrophil_GSE112101**), CD4 T cells (**T_CD4_GSE112101**), and B cells (**B-Cell_GSE112101**) (GSE112101; (Franco et al., 2019)). **Sheet 14**) **GC DEGs frequency distribution**; all genes in 9 DEG sets (n = 1725) scored for their presence in 9 separate DEG sets, and corresponding frequency distribution (frequency DEGs). Number of times present in 7 GC signature gene sets as tabled in sheet 4 also shown (frequency Signature sets).

Table S3

Signatures of GC-driven gene expression in blood cells and tissues

9 gene expression correlation signatures of GC-driven gene expression obtained on 8 transcriptomic dataset collections of monocytes, neutrophils, PBMC, muscle, skin, and fat, combining different GC-induced genes as correlation queries. In case of monocytes and neutrophils, dataset collections were specific for either health or presence of severe inflammation, based on experimental description. Also, 3 gene expression correlation signatures of CLOCK- driven gene expression in tissues. In case of tissues, CLOCK-driven gene profiles showed some overlap with GC-driven profiles. Gene ranking in gene expression correlation profiles color-coded in green from 1 (high) to 500 (low). Lists are cut off at 2000 genes. Average correlation value (cor), number of contributing datasets (nr), and ranking (rank) in single gene profile. Mean of rankings in different profiles (mean.rank), sum of contributing datasets (sumof supportingdatasets), and final ranking in signature (rank.mean). #N/B; number of contributing datasets for a gene in a profile below a set threshold.

Sheet 1) circadian cortisol neutrophil; Gene expression correlation signature from circadian cortisol obtained on a collection of 6 neutrophil datasets on health, using GC-induced query genes CCND3, CEBPD, ECHDC3, FKBP5, IL1R2, IRS2, TOB1.

Sheet 2) inflammatory GC neutrophil; Gene expression correlation signature from GC in severe inflammation obtained on a collection of 10 neutrophil / granulocyte datasets on severe inflammation, using GC-induced query genes CLEC4E, ECHDC3, FKBP5, CD163, MACIR, OLAH, DAAM2.

medRxiv preprint doi: https://doi.org/10.1101/2023.05.10.23289779; this version posted November 4, 2024. The copyright holder for this preprint (which was not certified by peer review) is the author/funder, who has granted medRxiv a license to display the preprint in perpetuity. All rights reserved. No reuse allowed without permission.

Sheet 3) circadian cortisol monocyte; Gene expression correlation signature from circadian cortisol obtained on a collection of 8 monocyte datasets on health, using GC-induced query genes ZBTB16, KLF9, TSC22D3, PER1, IRS2, FKBP5, FLT3, ALOX15B, GPER1, TPST1.

Sheet 4) inflammatory GC monocyte; Gene expression correlation signature from GC in severe inflammation obtained on a collection of 11 monocyte datasets on severe inflammation, using GC-induced query genes IL1R2, FKBP5, TPST1, FLT3, ADAMTS2, VSIG4.

Sheet 5) PBMC circ cort bias lympho; Gene expression correlation signature from circadian cortisol with a bias for lymphocytes obtained on a collection of 7 PBMC datasets on health and vaccination, using GC-induced query genes DDIT4, KLF9, BTG1.

Sheet 6) PBMC circ cort bias mono; Gene expression correlation signature from circadian cortisol with a bias for monocytes obtained on a collection of 7 PBMC datasets on health and vaccination, using GC-induced query genes GPER1, FLT3, ECHDC3, FKBP5, ADORA3, SMAP2, RNF144B.

Sheet 7) muscle circadian cortisol; Gene expression correlation signature from circadian cortisol obtained on a collection of 11 muscle datasets on health and sarcopenia, using GC-induced query genes DDIT4, TSC22D3, PER1, CEBPB, CEBPD, KLF9, FKBP5, ZBTB16, GLUL, FOXO3, FOXO1.

Sheet 8) skin circadian cortisol; Gene expression correlation signature from circadian cortisol obtained on a collection of 6 skin datasets on health and nonlesional skin in psoriasis, using GC-induced query genes TSC22D3, PER1, KLF9, FKBP5, ZBTB16, BCL6, IRS2.

Sheet 9) fat circadian cortisol; Gene expression correlation signature from circadian cortisol obtained on a collection of 5 fat tissue datasets on health and obesity, using GC-induced query genes TSC22D3, PER1, KLF9, ZBTB16, ITPKC, RHOB, ERFFI1.

Sheet 10) muscle CLOCK; Gene expression correlation signature from CLOCK-driven gene expression obtained on a collection of 11 muscle datasets on health and sarcopenia, using selected CLOCK:BMAL1-regulated core clock query genes PER3, HLF, TEF, DBP.

Sheet 11) skin CLOCK; Gene expression correlation signature from CLOCK-driven gene expression obtained on a collection of 6 skin datasets on health and nonlesional skin in psoriasis, using selected CLOCK:BMAL1-regulated core clock query genes PER2, PER3, HLF, TEF, DBP, NR1D2.

medRxiv preprint doi: https://doi.org/10.1101/2023.05.10.23289779; this version posted November 4, 2024. The copyright holder for this preprint (which was not certified by peer review) is the author/funder, who has granted medRxiv a license to display the preprint in perpetuity. All rights reserved. No reuse allowed without permission.

Sheet 12) fat CLOCK; Gene expression correlation signature from CLOCK-driven gene expression obtained on a collection of 5 fat tissue datasets on health and obesity, using selected CLOCK:BMAL1-regulated core clock query genes PER2, PER3, HLF, TEF, DBP.

Sheet 13) **dataset collections**; overview of datasets in 8 separate collections used to obtain gene expression correlation profiles (datasets), sample groups according to cell type, tissue, or disease (comment 1; disease, subset, cells/tissue), assay type, (microarray platform with GEO accession, or RNA-seq), value type, and scale (comment 2; scale, platform), number of samples used with each data (sub)set (nr.samples).

Table S4

Circadian DEGs in health, and GC treatment induced DEGs in septic shock and burn shock

Upregulated DEGs in whole blood of septic shock and burn shock patients upon GC treatment were compared with each other, with data on upregulation in monocytes and neutrophils in sepsis compared to controls, with data on *in vitro* induction by GC, and with correlation signatures of GC-driven gene expression in severe inflammation. The comparison was made to help identify direct gene targets of GC treatment in shock. DEGs induced by circadian GC in health were added for comparison.

Sheet 1) **6h circadian DEGs GDS3704**; DEGs in PBMCs at 0h and 6h time points after fatty acid consumption (GDS3704, 84 samples, dietary unsaturated and saturated fatty acid consumption, (Bouwens et al., 2010)), experiment added to compare DEGs induced by circadian GC in health, and by GC treatment in shock. Expression of circadian, GC-induced genes is higher at 0h time point in the experiment. Log2 fold change and p-values given for unpaired and paired two-sided t-tests of highest 2000 upregulated DEGs. **Sheet 2**) **GC DEGs septic shock GSE106878**; Upregulated DEGs in whole blood of septic shock patients beween either 24h GC or 24h placebo treatment (GSE106878, sequential hydrocortisone injections, 24 GC treated patients, 23 placebo treated patients, (Kolte, 2020)). Log2 fold change and p-values given for unpaired two sided t-tests of highest 2000 upregulated DEGs. **Sheet 3**) **GC DEGs burn shock GSE77791**; Upregulated DEGs in whole blood of burn shock patients treated with GC, comparing one day and 120h time points with placebo treatment at one day and at 120h time points (GSE77791, priming dose and continuous infusion of hydrocortisone, time series, 15 GC treated individuals, 15 placebo treated individuals, (Plassais et al., 2017)). Log2 fold change and p-values given for unpaired two sided t-tests of highest 2000

medRxiv preprint doi: https://doi.org/10.1101/2023.05.10.23289779; this version posted November 4, 2024. The copyright holder for this preprint (which was not certified by peer review) is the author/funder, who has granted medRxiv a license to display the preprint in perpetuity. All rights reserved. No reuse allowed without permission.

upregulated DEGs. **Sheet 4**) **GC DEGs sepsis (Wong, 2014)**; Upregulated and downregulated DEGs in whole blood of GC-treated pediatric septic shock. Differentially expressed Affymetrix probe sets with provided gene annotation (256) after corticosteroid treatment of pediatric septic shock (Wong et al., 2014). Probe sets corresponding with genes present in gene sets based on whole blood GC 1 (circadian) and GC 2 (severe inflammation) gene expression correlation signatures as indicated, and marked in red. Additional DEGs found in GSE106878 and GSE77791 marked in orange. **Sheet 5**) **comparison GC DEGs shock**; A comparison of GC treatment induced DEGs in septic shock (GSE106878, (Kolte, 2020)), and in burn shock (GSE77791, (Plassais et al., 2017)). The highest 2000 upregulated DEGs in GC treatment of either septic shock or burn shock, with p-values less than 0.05, were profiled together for expression in monocytes and neutrophils during sepsis (GSE60424, (Linsley et al., 2014)), inducibility by GC *in vitro* in monocytes and neutrophils (GSE112101, (Franco et al., 2019)), as well as for ranking in signatures of GC-driven gene expression in severe inflammation in whole blood, monocytes, and neutrophils / granulocytes. DEGs GSE106878 septic shock and GSE77791 burn shock; A large proportion of DEGs are shared between both experiments, including several genes with different gene symbols on both platforms (eg OLAH and THEDC1). HUGO approved gene symbols are provided where necessary. Log2 fold change (log GC/-) color-coded in red to green and corresponding p-values given for unpaired two sided t-tests, shaded in green to white, in yellow; p-value > 0.05 (not significant). #N/B in logGC/- columns; gene missing from platform. #N/B in p-value columns; gene missing from platform, or gene not with first 2000 upregulated DEGs. DEGs GSE60424 monocytes and neutrophils sepsis; Several highly induced genes in GC treatment of septic shock and burn shock are also upregulated in monocytes, neutrophils or in both cell types during sepsis (3 samples for each cell type) compared with controls (healthy, type 1 diabetes, amyotrophic lateral sclerosis, and multiple sclerosis excluding interferon beta treatment, 14 samples for each cell type in total) in experiment GSE60424 (Linsley et al., 2014). Ratios of gene expression in monocytes (M) and neutrophils (N) in controls and sepsis as indicated, and color-coded in grey. Log2 of gene expression ratio between monocytes and neutrophils during sepsis added separately (log M seps/ N seps), and color-coded from yellow (more in monocytes) to blue (more in neutrophils). ##### in blue; no detection in monocytes, ##### in yellow; no detection in neutrophils. #N/B; gene missing from platform. DEGs GSE112101 healthy monocytes and neutrophils in vitro GC treatment; Gene inducibility by GC *in vitro* in monocytes and in neutrophils isolated from healthy people (GSE112101, (Franco et al., 2019)) broadly agrees with a direct effect of GC on DEGs seen *in vivo*. Log2 of

medRxiv preprint doi: https://doi.org/10.1101/2023.05.10.23289779; this version posted November 4, 2024. The copyright holder for this preprint (which was not certified by peer review) is the author/funder, who has granted medRxiv a license to display the preprint in perpetuity. All rights reserved. No reuse allowed without permission.

gene expression ratio between GC treated monocytes and GC treated neutrophils (log M GC/N GC) color-coded from yellow (more in monocytes) to blue (more in neutrophils). ##### in blue; no detection in monocytes, ##### in yellow; no detection in neutrophils. Log2 fold change between GC-treated and untreated control samples color-coded in red to blue, and unadjusted p-values given for unpaired and paired two sided t-tests of differential expression in monocytes (MGC) and neutrophils (NGC), shaded in green to white, in yellow; p-value > 0.05 (not significant). #N/B; gene missing from platform. ##### in blue; no detection in samples with GC, ##### in red; no detection in samples without GC. COR blood severe (n= 38); Ranking of DEGs in whole blood GC signatures 2 (severe inflammation), bias lymphocyte, bias myeloid cells, bias neutrophil, and bias monocyte. COR datasets collection cells; Ranking of DEGs in correlation signatures of GC-driven gene expression in severe inflammation in dataset collections of isolated neutrophils / granulocytes, and isolated monocytes. High ranking of DEGs in signatures from GC-driven gene expression *in vivo* indicated a direct effect of GC treatment on such DEGs seen *in vivo*. #N/B; gene not present in GC signatures, which may also be due to different gene alias used in DEGs. Gene rankings 1-500 in signatures shaded in green (1 high) to white (500 low).

Table S5

Gene sets and gene probe identifiers used in screening different illnesses

Gene composition for gene sets T cell, SIM (severe inflammatory myeloid), FAM20A (n= 4), biomarker gene sets GC-2, GC-1, interferon gamma, and interferon alpha as provided. For determining gene set expression values in microarray experiments, genes were represented by a single adequate probe identifier chosen for microarray platforms GPL570 (Affymetrix Human Genome U133 Plus 2.0 array), GPL10558 (Illumina HumanHT-12 V4.0 expression beadchip), and GPL6947 (Illumina HumanHT-12 V3.0 expression beadchip) as given. Illumina platforms GPL10558 and GPL6947 share probe identifiers, but with a small number of specific gene probes absent from GPL6947 compared to GPL10558. Gene set expression values were calculated according to methods**.**

Table S6

Comparing GC-inducible genes for use as whole blood transcriptomic biomarkers in health and in different diseases.

medRxiv preprint doi: https://doi.org/10.1101/2023.05.10.23289779; this version posted November 4, 2024. The copyright holder for this preprint (which was not certified by peer review) is the author/funder, who has granted medRxiv a license to display the preprint in perpetuity. All rights reserved. No reuse allowed without permission.

Differential expression, and gene expression correlation analysis, using 12 whole blood RNA-seq datasets on health and different diseases. Potential GC biomarker genes (n= 26), including genes in biomarker sets GC-1, GC-2, and in 3 existing GC biomarker sets for Addison's disease (Sævik et al., 2021), and SLE (Hu et al., 2018; Northcott et al., 2021) were tested for health, and for different diseases. Results for several marker genes for cell type and inflammation are also provided. Basal expression for different genes in health is included for each dataset, where available, as well as differential expression between disease and healthy controls. A ratio of mean of values above 9th decile, and below first quartile in a given distribution was calculated as a measure of induction strength, in case of inducible genes. Correlation analysis shows first 50 genes in gene expression correlation profiles, and their overlap with exploratory GC signature genes 1 and 2 (see sheet 1 in supporting table 2).

Sheet 1) GSE113883 health; Circadian in health, GSE113883 (Braun et al., 2018). 0.1 tpm unit was added to GSE113883 (table in tpm), before calculations. **columns 1** , IDENTIFIER (gene name); **2,** mean H (mean expression (tpm) in all samples); **3**, Log10 H (log10 of mean expression (tpm) in all samples); **4**, Log2FC T1/T2 (mean of all individual log2 ratios (n = 11) of expression between T1 timepoints (1h, 3h, 25h, 27h), and T2 timepoints (13h, 15h, 17h, 19h); **5**, pval (corresponding p-values); **6**, Log10 pval (log10 of corresponding p-values); **7** GC signature hit health (overlap of first 50 genes in expression correlation profiles, with genes present in exploratory GC signatures 1 and 2, correlation profiles obtained on 140 samples excluding outlier individual labelled nr14 in dataset); **8**, COR50 H (first 50 genes in expression correlation profiles obtained on 140 samples excluding outlier individual labelled nr14 in dataset).

Sheet 2) GSE72509 SLE; SLE with healthy controls, GSE72509 (Hung, Pratt, Sundararaman, Towsend, et al., 2015). **columns 1** , IDENTIFIER (gene name); **2,** mean H (mean expression (rpkm) in healthy control samples); **3**, Log10 H (log10 of mean expression (rpkm) in healthy control samples) ; **4**, Log2FC SLE/H (Log2 fold change in SLE (n = 99), and healthy controls (n = 18)) ; **5**, pval (corresponding p-values); **6**, Log10 pval (log10 of corresponding p-values); **7**, Q1m SLE (mean of values below first quartile in distribution for SLE samples); **8**, D10m SLE (mean of values above 9th decile in distribution for SLE samples); **9** , Log2 D10m/Q1m SLE (Log2 of ratio of mean value above 9th decile, and mean value below first quartile in distribution for SLE samples); **10**, GC signature hit SLE (overlap of first 50 genes in expression correlation profiles, obtained on SLE samples, with genes

medRxiv preprint doi: https://doi.org/10.1101/2023.05.10.23289779; this version posted November 4, 2024. The copyright holder for this preprint (which was not certified by peer review) is the author/funder, who has granted medRxiv a license to display the preprint in perpetuity. All rights reserved. No reuse allowed without permission.

present in exploratory GC signature 1 and 2); **11**, COR50 SLE (first 50 genes in expression correlation profiles obtained on SLE samples)

Sheet 3) GSE154918 sepsis; Sepsis, bacterial infection, healthy controls, GSE154918 (Herwanto et al., 2021). **columns 1**, IDENTIFIER (gene name); **2** mean H (mean expression (normalized value) in healthy control samples); **3** Log10 H (log10 of mean expression (normalized value) in healthy control samples) ; **4**, Log2FC SEPSIS /H (Log2 fold change in sepsis (n = 53), and healthy controls (n = 40); **5**, pval (corresponding p-values); **6** Log10 pval (log10 of corresponding p-values); **7**, Q1m SEPSIS (mean of values below first quartile in distribution for sepsis samples); **8**, D10m SEPSIS (mean of values above 9th decile in distribution for sepsis samples); **9,** Log2 D10m/Q1m SEPSIS (Log2 of ratio of mean value above 9th decile, and mean value below first quartile in distribution for sepsis samples); **10**, GC signature hit SEPSIS (overlap of first 50 genes in expression correlation profiles, obtained on sepsis samples, with genes present in exploratory GC signature 1 and 2); **11**, COR50 SEPSIS (first 50 genes in expression correlation profiles obtained on sepsis samples).

Sheet 4) GSE117769 RA; rheumatoid arthritis +/- GC treatment, healthy controls, GSE117769. 1 count was added to GSE117769 (table in counts), and values cpm normalized, before calculations. **columns 1**, IDENTIFIER (gene name); **2**, mean H (mean expression (cpm) in healthy control samples); **3**, Log10 H (log10 of mean expression (cpm) in healthy control samples); **4**, Log2FC RA+GC/H (Log2 fold change in GC-treated RA (n = 29), and healthy controls (n = 50); **5**, pval (corresponding p-values); **6**, Log10 pval (log10 of corresponding p-values); **7**, Log2FC +GC/-GC (Log2 fold change in GC-treated RA (n = 29), and GC-untreated RA (n = 23); **8**, pval (corresponding p-values); **9**, Log10 pval (log10 of corresponding p-values); **10**, Q1m RA (mean of values below first quartile in distribution for all RA samples); **11**, D10m RA (mean of values above 9th decile in distribution for all RA samples); **12**, Log2 D10m/Q1m RA (Log2 of ratio of mean value above 9th decile, and mean value below first quartile in distribution for all RA samples); **13**, GC signature hit RA (overlap of first 50 genes in expression correlation profiles, obtained on all RA samples, with genes present in exploratory GC signature 1 and 2); **14**, COR50 RA (first 50 genes in expression correlation profiles obtained on all RA samples).

Sheet 5) GSE207751 asthma; moderate and severe asthma, healthy controls, GSE207751. **columns 1**, IDENTIFIER (gene name); **2**, mean H (mean expression (normalized value) in healthy control samples); **3**, Log10 H (log10 of mean expression (normalized value) in healthy control samples); **4**, Log2FC AST. SEV. /H (Log2 fold change in severe asthma (n =

medRxiv preprint doi: https://doi.org/10.1101/2023.05.10.23289779; this version posted November 4, 2024. The copyright holder for this preprint (which was not certified by peer review) is the author/funder, who has granted medRxiv a license to display the preprint in perpetuity. All rights reserved. No reuse allowed without permission.

23), and healthy controls (n = 14)); **5**, pval (corresponding p-values); **6**, Log10 pval (log10 of corresponding p-values); **7**, Log2FC SEV./MOD. (Log2 fold change in severe asthma (n = 23), and moderate asthma (n = 19)); **8**, pval (corresponding p-values); **9**, Log10 pval (log10 of corresponding p-values); **10**, Q1m ASTHMA (mean of values below first quartile in distribution for all asthma samples); **11**, D10m ASTHMA (mean of values above 9th decile in distribution for all asthma samples); **12**, Log2 D10m/Q1m ASTHMA (Log2 of ratio of mean value above 9th decile, and mean value below first quartile in distribution for all (n = 42) asthma samples); **13**, GC signature hit ASTHMA (overlap of first 50 genes in expression correlation profiles, obtained on all asthma samples, with genes present in exploratory GC signature 1 and 2); **14**, COR50 ASTHMA (first 50 genes in expression correlation profiles obtained on all asthma samples).

Sheet 6) GSE69529 gastroenteritis; infectious bacterial diarrhea, rotaviral diarrhea, healthy controls, GSE69529 (DeBerg et al., 2018). 1 count was added to GSE69529 (table in counts), and values cpm normalized, before calculations. **columns 1**, IDENTIFIER (gene name); **2**, mean H (mean expression (cpm) in healthy control samples); **3**, Log10 H (log10 of mean expression (cpm) in healthy control samples); **4**, Log2FC ROTAVIRUS/H (Log2 fold change in rotaviral gastroenteritis (n = 55), and healthy controls (n = 24)); **5**, pval (corresponding p-values); **6**, Log10 pval (log10 of corresponding p-values); **7**, Log2FC BACTERIAL/H (Log2 fold change in bacterial gastroenteritis (n = 124), and healthy controls (n = 24)); **8**, pval (corresponding p-values); **9**, Log10 pval (log10 of corresponding p-values); **10**, Q1m ROTA (mean of values below first quartile in distribution for rotaviral gastroenteritis samples); **11**, D10m ROTA (mean of values above 9th decile in distribution for rotaviral gastroenteritis samples), 1**2**, Log2 D10m/Q1m ROTA (Log2 of ratio of mean value above 9th decile, and mean value below first quartile in distribution for rotaviral gastroenteritis samples); **13**, Q1m BACT. (mean of values below first quartile in distribution for bacterial gastroenteritis samples); **14**, D10m BACT. (mean of values above 9th decile in distribution for bacterial gastroenteritis samples); 1**5**, Log2 D10m/Q1m BACT. (Log2 of ratio of mean value above 9th decile, and mean value below first quartile in distribution for bacterial gastroenteritis samples); 1**6**, GC signature hit ROTA (overlap of first 50 genes in expression correlation profiles, obtained on rotaviral gastroenteritis samples, with genes present in exploratory GC signature 1 and 2); 1**7**, COR50 ROTA (first 50 genes in expression correlation profiles obtained on rotaviral gastroenteritis samples); 1**8**, GC signature hit BACT. (overlap of first 50 genes in expression correlation profiles, obtained on bacterial gastroenteritis samples, with

medRxiv preprint doi: https://doi.org/10.1101/2023.05.10.23289779; this version posted November 4, 2024. The copyright holder for this preprint (which was not certified by peer review) is the author/funder, who has granted medRxiv a license to display the preprint in perpetuity. All rights reserved. No reuse allowed without permission.

genes present in exploratory GC signature 1 and 2); 1**9**, COR50 BACT. (first 50 genes in expression correlation profiles obtained on bacterial gastroenteritis samples).

Sheet 7) GSE112057 JIA, SJIA, IBD; JIA (oligo, poly), SJIA, IBD (Crohn, Ulcerative Colitis), healthy controls, GSE112057 (Mo et al., 2018). 1 count was added to GSE112057 (table in counts), and values cpm normalized, before calculations. **columns 1**, IDENTIFIER (gene name); **2**, mean H (mean expression (cpm) in healthy control samples); **3**, Log10 H (log10 of mean expression (cpm) in healthy control samples); **4**, Log2FC JIA/H (Log2 fold change in JIA (n = 89), and healthy controls (n = 12)); **5**, pval (corresponding p-values); **6**, Log10 pval (log10 of corresponding p-values); **7**, Log2FC SJIA/H (Log2 fold change in SJIA (n = 26), and healthy controls (n = 12)); **8**, pval (corresponding p-values); **9**, Log10 pval (log10 of corresponding p-values); **10**, Log2FC IBD/H (Log2 fold change in IBD (n = 75), and healthy controls (n = 12)); **11**, pval (corresponding p-values); 1**2**, Log10 pval (log10 of corresponding p-values); 1**3**, Q1m JIA (mean of values below first quartile in distribution for JIA samples); 1**4**, D10m JIA (mean of values above 9th decile in distribution for JIA samples); 1**5**, Log2 D10m/Q1m JIA (Log2 of ratio of mean value above 9th decile, and mean value below first quartile in distribution for JIA samples); **16,** Q1m SJIA (mean of values below first quartile in distribution for SJIA samples); 1**7**, D10m SJIA (mean of values above 9th decile in distribution for SJIA samples); 1**8**, Log2 D10m/Q1m SJIA (Log2 of ratio of mean value above 9th decile, and mean value below first quartile in distribution for SJIA samples); **19,** Q1m IBD (mean of values below first quartile in distribution for IBD samples); **20**, D10m IBD (mean of values above 9th decile in distribution for IBD samples); **21** Log2 D10m/Q1m IBD (Log2 of ratio of mean value above 9th decile, and mean value below first quartile in distribution for IBD samples); **22**, GC signature hit JIA (overlap of first 50 genes in expression correlation profiles, obtained on JIA samples, with genes present in exploratory GC signature 1 and 2); **23**, COR50 JIA (first 50 genes in expression correlation profiles obtained on JIA samples); **24**, GC signature hit SJIA (overlap of first 50 genes in expression correlation profiles, obtained on SJIA samples, with genes present in exploratory GC signature 1 and 2); **25**, COR50 SJIA (first 50 genes in expression correlation profiles obtained on SJIA samples); **26**, GC signature hit IBD (overlap of first 50 genes in expression correlation profiles, obtained on IBD samples, with genes present in exploratory GC signature 1 and 2); **27**, COR50 IBD (first 50 genes in expression correlation profiles obtained on IBD samples)

medRxiv preprint doi: https://doi.org/10.1101/2023.05.10.23289779; this version posted November 4, 2024. The copyright holder for this preprint (which was not certified by peer review) is the author/funder, who has granted medRxiv a license to display the preprint in perpetuity. All rights reserved. No reuse allowed without permission.

Sheet 8) GSE171110 severe COVID-19; severe COVID19, frequent GC treatment, healthy controls, GSE171110 (Lévy et al., 2021). 1 count was added to GSE171110 (table in counts), and values cpm normalized, before calculations. **columns 1**, IDENTIFIER (gene name); **2**, mean H (mean expression (cpm) in healthy control samples); **3**, Log10 H (log10 of mean expression (cpm) in healthy control samples); **4**, Log2FC severe COVID-19/H (Log2 fold change in severe COVID-19 (n = 44), and healthy controls (n = 10)); **5**, pval (corresponding p-values); **6**, Log10 pval (log10 of corresponding p-values); **7**, Q1m COVID-19 (mean of values below first quartile in distribution for severe COVID-19 samples); **8**, D10m COVID19 (mean of values above 9th decile in distribution for severe COVID-19 samples); **9** Log2 D10m/Q1m COVID-19 (Log2 of ratio of mean value above 9th decile, and mean value below first quartile in distribution for severe COVID-19 samples); **10**, GC signature hit severe COVID-19 (overlap of first 50 genes in expression correlation profiles, obtained on severe COVID-19 samples, with genes present in exploratory GC signature 1 and 2); **11**, COR50 severe COVID-19 (first 50 genes in expression correlation profiles obtained on severe COVID-19 samples)

Sheet 9) GSE157103 severe COVID-19; severe COVID-19, frequent GC treatment, in ICU, not in ICU, no healthy controls, GSE157103 (Overmyer et al., 2021). 0.1 tpm unit was added to GSE157103 (table in tpm), before calculations. **columns 1**, IDENTIFIER (gene name); **2**, Log2FC ICU/not ICU (Log2 fold change in severe COVID-19 in ICU (n = 50), and severe COVID-19 not in ICU (n = 50); **3**, pval (corresponding p-values); **4**, Log10 pval (log10 of corresponding p-values); **5**, Log2 D10m/Q1m COVID-19 (Log2 of ratio of mean value above 9th decile, and mean value below first quartile in distribution for all (n = 100) severe COVID-19 samples); **6**, GC signature hit severe COVID-19 (overlap of first 50 genes in expression correlation profiles, obtained on all severe COVID-19 samples, with genes present in exploratory GC signature 1 and 2); **7**, COR50 severe COVID-19 (first 50 genes in expression correlation profiles obtained on all severe COVID-19 samples).

Sheet 10) GSE206264 severe COVID-19; severe COVID-19, documented GC usage, no healthy controls, GSE206264 (López-Martínez et al., 2023). 1 count was added to GSE206264 (table in counts), and values cpm normalized, before calculations. **columns 1**, IDENTIFIER (gene name); **2**, mean all (mean expression (cpm) in all samples); **3**, Log10 all (log10 of mean expression (cpm) in all samples); **4**, Log2FC +GC/-GC (Log2 fold change in GC-treated severe COVID-19 (n = 11), and GC-untreated severe COVID-19 (n = 16)); **5**, pval (corresponding p-values); **6**, Log10 pval (log10 of corresponding p-values); **7**, Q1m all (mean

medRxiv preprint doi: https://doi.org/10.1101/2023.05.10.23289779; this version posted November 4, 2024. The copyright holder for this preprint (which was not certified by peer review) is the author/funder, who has granted medRxiv a license to display the preprint in perpetuity. All rights reserved. No reuse allowed without permission.

of values below first quartile in distribution for all severe COVID-19 samples); **8**, D10m all (mean of values above 9th decile in distribution for all severe COVID-19 samples); **9** Log2 D10m/Q1m COVID-19 (Log2 of ratio of mean value above 9th decile, and mean value below first quartile in distribution for all (n = 27) severe COVID-19 samples); **10**, GC signature hit severe COVID-19 (overlap of first 50 genes in expression correlation profiles, obtained on all severe COVID-19 samples, with genes present in exploratory GC signature 1 and 2); **11**, COR50 severe COVID-19 (first 50 genes in expression correlation profiles obtained on all severe COVID-19 samples)

Sheet 11) GSE168400 severe COVID-19; severe COVID-19, no GC treatment, no healthy controls, GSE168400 (Amado-Rodríguez et al., 2022). 1 count was added to GSE168400 (table in counts), and values cpm normalized, before calculations. **columns 1**, IDENTIFIER (gene name); **2**, mean all (mean expression (cpm) in all samples (n= 42)); **3**, Log10 all (log10 of mean expression (cpm) in all samples); **4**, Q1m all (mean of values below first quartile in distribution for all severe COVID-19 samples); **5**, D10m all (mean of values above 9th decile in distribution for all severe COVID-19 samples); **6**, Log2 D10m/Q1m all (Log2 of ratio of mean value above 9th decile, and mean value below first quartile in distribution for all (n = 42) severe COVID-19 samples); **7**, GC signature hit severe COVID-19 (overlap of first 50 genes in expression correlation profiles, obtained on all severe COVID-19 samples, with genes present in exploratory GC signature 1 and 2); **8**, COR50 severe COVID-19 (first 50 genes in expression correlation profiles obtained on all severe COVID-19 samples).

Sheet 12) GSE197204 severe COVID-19; severe COVID-19, no GC treatment, no healthy controls, GSE197204 (López-Martínez et al., 2023). **columns 1**, IDENTIFIER (gene name); **2**, mean all (mean expression (cpm) in all samples (n= 56)); **3**, Log10 all (log10 of mean expression (cpm) in all samples); **4**, Q1m all (mean of values below first quartile in distribution for all severe COVID-19 samples); **5**, D10m all (mean of values above 9th decile in distribution for all severe COVID-19 samples); **6**, Log2 D10m/Q1m all (Log2 of ratio of mean value above 9th decile, and mean value below first quartile in distribution for all (n = 56) severe COVID-19 samples); **7**, GC signature hit severe COVID-19 (overlap of first 50 genes in expression correlation profiles, obtained on all severe COVID-19 samples, with genes present in exploratory GC signature 1 and 2); **8**, COR50 severe COVID-19 (first 50 genes in expression correlation profiles obtained on all severe COVID-19 samples).

medRxiv preprint doi: https://doi.org/10.1101/2023.05.10.23289779; this version posted November 4, 2024. The copyright holder for this preprint (which was not certified by peer review) is the author/funder, who has granted medRxiv a license to display the preprint in perpetuity. All rights reserved. No reuse allowed without permission.

REFERENCES

Abdelaziz, M. H., Abdelwahab, S. F., Wan, J., Cai, W., Huixuan, W., Jianjun, C.,…Xu, H. (2020). Alternatively activated macrophages; a double-edged sword in allergic asthma. *J Transl Med*, *18*(1), 58. https://doi.org/10.1186/s12967-020-02251-w

Ackermann, K., Revell, V. L., Lao, O., Rombouts, E. J., Skene, D. J., & Kayser, M. (2012). Diurnal rhythms in blood cell populations and the effect of acute sleep deprivation in healthy young men. *Sleep*, *35*(7), 933-940. https://doi.org/10.5665/sleep.1954

Alder, M. N., Opoka, A. M., & Wong, H. R. (2018). The glucocorticoid receptor and cortisol levels in pediatric septic shock. *Critical Care*, *22*(1). https://doi.org/10.1186/s13054-018-2177-8

Alexander, R. A. (1990). A note on averaging correlations. *Bulletin of the Psychonomic Society*, *28*(4). https://doi.org/10.3758/BF03334037

Altman, M. C., Gill, M. A., Whalen, E., Babineau, D. C., Shao, B., Liu, A. H.,…Jackson, D. J. (2019). Transcriptome networks identify mechanisms of viral and nonviral asthma exacerbations in children. *Nature Immunology*, *20*(5). https://doi.org/10.1038/s41590-019-0347-8

Altman, M. C., Rinchai, D., Baldwin, N., Toufiq, M., Whalen, E., Garand, M.,…Chaussabel, D. (2021). Development of a fixed module repertoire for the analysis and interpretation of blood transcriptome data. *Nature Communications*, *12*(1). https://doi.org/10.1038/s41467-021-24584-w

Amado-Rodríguez, L., Salgado Del Riego, E., Gomez de Ona, J., López Alonso, I., Gil-Pena, H., López-Martínez, C.,…Albaiceta, G. M. (2022). Effects of IFIH1 rs1990760 variants on systemic inflammation and outcome in critically ill COVID-19 patients in an observational translational study. *Elife*, *11*. https://doi.org/10.7554/eLife.73012

Annane, D., Bellissant, E., Bollaert, P. E., Briegel, J., Keh, D., Kupfer, Y.,…Rochwerg, B. (2019). Corticosteroids for treating sepsis in children and adults. *Cochrane Database Syst Rev*, *12*(12), Cd002243. https://doi.org/10.1002/14651858.CD002243.pub4

Annane, D., Pastores, S. M., Arlt, W., Balk, R. A., Beishuizen, A., Briegel, J.,…Van den Berghe, G. (2017). Critical illness-related corticosteroid insufficiency (CIRCI): a narrative review from a Multispecialty Task Force of the Society of Critical Care Medicine (SCCM) and the European Society of Intensive Care Medicine (ESICM). *Intensive Care Med*, *43*(12), 1781-1792. https://doi.org/10.1007/s00134-017-4914-x

Annane, D., Pastores, S. M., Rochwerg, B., Arlt, W., Balk, R. A., Beishuizen, A.,…Van Den Berghe, G. (2017). Guidelines for the diagnosis and management of Critical Illness-Related Corticosteroid Insufficiency (CIRCI) in critically ill patients (Part I): Society of Critical Care Medicine (SCCM) and European Society of Intensive Care Medicine (ESICM) 2017. *Critical Care Medicine*, *45*(12). https://doi.org/10.1097/CCM.0000000000002737

Annane, D., Renault, A., Brun-Buisson, C., Megarbane, B., Quenot, J. P., Siami, S.,…Bellissant, E. (2018). Hydrocortisone plus Fludrocortisone for Adults with Septic Shock. *N Engl J Med*, *378*(9), 809-818. https://doi.org/10.1056/NEJMoa1705716

Annane, D., Sébille, V., Troché, G., Raphaël, J. C., Gajdos, P., & Bellissant, E. (2000). A 3-level prognostic classification in septic shock based on cortisol levels and cortisol response to corticotropin. *Jama*, *283*(8), 1038-1045. https://doi.org/10.1001/jama.283.8.1038

Antcliffe, D. B., Burnham, K. L., Al-Beidh, F., Santhakumaran, S., Brett, S. J., Hinds, C. J.,…Gordon, A. C. (2019). Transcriptomic Signatures in Sepsis and a Differential Response to Steroids. From the VANISH Randomized Trial. *Am J Respir Crit Care Med*, *199*(8), 980-986. https://doi.org/10.1164/rccm.201807-1419OC

Archer, S. N., Laing, E. E., Möller-Levet, C. S., van der Veen, D. R., Bucca, G., Lazar, A. S.,…Dijk, D. J. (2014). Mistimed sleep disrupts circadian regulation of the human transcriptome. *Proc Natl Acad Sci U S A*, *111*(6), E682-691. https://doi.org/10.1073/pnas.1316335111

medRxiv preprint doi: https://doi.org/10.1101/2023.05.10.23289779; this version posted November 4, 2024. The copyright holder for this preprint (which was not certified by peer review) is the author/funder, who has granted medRxiv a license to display the preprint in perpetuity. All rights reserved. No reuse allowed without permission.

Arnardottir, E. S., Nikonova, E. V., Shockley, K. R., Podtelezhnikov, A. A., Anafi, R. C., Tanis, K. Q.,…Pack, A. I. (2014). Blood-gene expression reveals reduced circadian rhythmicity in individuals resistant to sleep deprivation. *Sleep*, *37*(10). https://doi.org/10.5665/sleep.4064

Aschenbrenner, A. C., Mouktaroudi, M., Krämer, B., Oestreich, M., Antonakos, N., Nuesch-Germano, M.,…Ulas, T. (2021). Disease severity-specific neutrophil signatures in blood transcriptomes stratify COVID-19 patients. *Genome medicine*, *13*(1). https://doi.org/10.1186/s13073-020-00823-5

Aso, K., & Satoh, M. (2021). ACTH-cortisol dissociation in patients with Kawasaki disease: a retrospective study. *Endocr J*, *68*(6), 683-689. https://doi.org/10.1507/endocrj.EJ20-0533

Athar, A., Füllgrabe, A., George, N., Iqbal, H., Huerta, L., Ali, A.,…Brazma, A. (2019). ArrayExpress update - From bulk to single-cell expression data. *Nucleic Acids Research*, *47*(D1). https://doi.org/10.1093/nar/gky964

Auguie, B., Antonov, A., Auguie, M. B., & Robinson, D. (2017). *Package 'gridExtra'* (Miscellaneous Functions for "Grid" Graphics, Issue.

Avancini, D., Testori, A., Fresolone, L., Andolfi, G., Vuono, M., Martinelli, V.,…Gregori, S. (2023). Aryl hydrocarbon receptor activity downstream of IL-10 signaling is required to promote regulatory functions in human dendritic cells. *Cell Rep*, *42*(3), 112193. https://doi.org/10.1016/j.celrep.2023.112193

Avendaño-Ortiz, J., Maroun-Eid, C., Martín-Quirós, A., Toledano, V., Cubillos-Zapata, C., Gómez-Campelo, P.,…López-Collazo, E. (2018). PD-L1 Overexpression During Endotoxin Tolerance Impairs the Adaptive Immune Response in Septic Patients via HIF1α. *J Infect Dis*, *217*(3), 393-404. https://doi.org/10.1093/infdis/jix279

Banchereau, R., Baldwin, N., Cepika, A. M., Athale, S., Xue, Y., Yu, C. I.,…Pascual, V. (2014). Transcriptional specialization of human dendritic cell subsets in response to microbial vaccines. *Nat Commun*, *5*, 5283. https://doi.org/10.1038/ncomms6283

Banchereau, R., Hong, S., Cantarel, B., Baldwin, N., Baisch, J., Edens, M.,…Pascual, V. (2016). Personalized Immunomonitoring Uncovers Molecular Networks that Stratify Lupus Patients. *Cell*, *165*(3), 551-565. https://doi.org/10.1016/j.cell.2016.03.008

Banchereau, R., Jordan-Villegas, A., Ardura, M., Mejias, A., Baldwin, N., Xu, H.,…Ramilo, O. (2012). Host immune transcriptional profiles reflect the variability in clinical disease manifestations in patients with Staphylococcus aureus infections. *PLoS One*, *7*(4), e34390. https://doi.org/10.1371/journal.pone.0034390

Barbie, D. A., Tamayo, P., Boehm, J. S., Kim, S. Y., Moody, S. E., Dunn, I. F.,…Hahn, W. C. (2009). Systematic RNA interference reveals that oncogenic KRAS-driven cancers require TBK1. *Nature*, *462*(7269), 108-112. https://doi.org/10.1038/nature08460

Barcella, M., Bollen Pinto, B., Braga, D., D'Avila, F., Tagliaferri, F., Cazalis, M. A.,…Barlassina, C. (2018). Identification of a transcriptome profile associated with improvement of organ function in septic shock patients after early supportive therapy. *Crit Care*, *22*(1), 312. https://doi.org/10.1186/s13054-018-2242-3

Barrett, T., Wilhite, S. E., Ledoux, P., Evangelista, C., Kim, I. F., Tomashevsky, M.,…Soboleva, A. (2013). NCBI GEO: Archive for functional genomics data sets - Update. *Nucleic Acids Research*, *41*(D1). https://doi.org/10.1093/nar/gks1193

Baty, F., Facompré, M., Wiegand, J., Schwager, J., & Brutsche, M. H. (2006). Analysis with respect to instrumental variables for the exploration of microarray data structures. *BMC Bioinformatics*, *7*. https://doi.org/10.1186/1471-2105-7-422

Bigler, J., Boedigheimer, M., Schofield, J. P. R., Skipp, P. J., Corfield, J., Rowe, A.,…Djukanović, R. (2017). A Severe Asthma Disease Signature from Gene Expression Profiling of Peripheral Blood from U-BIOPRED Cohorts. *Am J Respir Crit Care Med*, *195*(10), 1311-1320. https://doi.org/10.1164/rccm.201604-0866OC

Blankley, S., Graham, C. M., Turner, J., Berry, M. P. R., Bloom, C. I., Xu, Z.,…O'Garra, A. (2016). The transcriptional signature of active tuberculosis reflects symptom status in extra-pulmonary

medRxiv preprint doi: https://doi.org/10.1101/2023.05.10.23289779; this version posted November 4, 2024. The copyright holder for this preprint (which was not certified by peer review) is the author/funder, who has granted medRxiv a license to display the preprint in perpetuity. All rights reserved. No reuse allowed without permission.

and pulmonary tuberculosis. *PLoS ONE*, *11*(10). https://doi.org/10.1371/journal.pone.0162220

Bloom, C. I., Graham, C. M., Berry, M. P. R., Rozakeas, F., Redford, P. S., Wang, Y.,…O'Garra, A. (2013). Transcriptional Blood Signatures Distinguish Pulmonary Tuberculosis, Pulmonary Sarcoidosis, Pneumonias and Lung Cancers. *PLoS ONE*, *8*(8). https://doi.org/10.1371/journal.pone.0070630

Boonen, E., Vervenne, H., Meersseman, P., Andrew, R., Mortier, L., Declercq, P. E.,…Van den Berghe, G. (2013). Reduced cortisol metabolism during critical illness. *N Engl J Med*, *368*(16), 1477-1488. https://doi.org/10.1056/NEJMoa1214969

Bouwens, M., Bromhaar, M. G., Jansen, J., Müller, M., & Afman, L. A. (2010). Postprandial dietary lipid-specific effects on human peripheral blood mononuclear cell gene expression profiles. *American Journal of Clinical Nutrition*, *91*(1). https://doi.org/10.3945/ajcn.2009.28586

Brachat, A. H., Grom, A. A., Wulffraat, N., Brunner, H. I., Quartier, P., Brik, R.,…Morris, P. (2017). Early changes in gene expression and inflammatory proteins in systemic juvenile idiopathic arthritis patients on canakinumab therapy. *Arthritis Research and Therapy*, *19*(1). https://doi.org/10.1186/s13075-016-1212-x

Braun, D. A., Fribourg, M., & Sealfon, S. C. (2013). Cytokine response is determined by duration of receptor and signal transducers and activators of transcription 3 (STAT3) activation. *Journal of Biological Chemistry*, *288*(5). https://doi.org/10.1074/jbc.M112.386573

Braun, R., Kath, W. L., Iwanaszko, M., Kula-Eversole, E., Abbott, S. M., Reid, K. J.,…Allada, R. (2018). Universal method for robust detection of circadian state from gene expression. *Proceedings of the National Academy of Sciences of the United States of America*, *115*(39). https://doi.org/10.1073/pnas.1800314115

Briegel, J., Huge, V., & Möhnle, P. (2018). Hydrocortisone in septic shock: All the questions answered? In *Journal of Thoracic Disease* (Vol. 10).

Burnham, K. L., Davenport, E. E., Radhakrishnan, J., Humburg, P., Gordon, A. C., Hutton, P.,…Knight, J. C. (2017). Shared and distinct aspects of the sepsis transcriptomic response to fecal peritonitis and pneumonia. *American Journal of Respiratory and Critical Care Medicine*, *196*(3). https://doi.org/10.1164/rccm.201608-1685OC

Buttgereit, F. (2021). Glucocorticoids: surprising new findings on their mechanisms of actions. In *Annals of the Rheumatic Diseases* (Vol. 80).

Cajander, S., Bäckman, A., Tina, E., Strålin, K., Söderquist, B., & Källman, J. (2013). Preliminary results in quantitation of HLA-DRA by real-time PCR: a promising approach to identify immunosuppression in sepsis. *Crit Care*, *17*(5), R223. https://doi.org/10.1186/cc13046

Caldenhoven, E., Liden, J., Wissink, S., Van de Stolpe, A., Raaijmakers, J., Koenderman, L.,…Van der Saag, P. T. (1995). Negative cross-talk between RelA and the glucocorticoid receptor: a possible mechanism for the antiinflammatory action of glucocorticoids. *Mol Endocrinol*, *9*(4), 401-412. https://doi.org/10.1210/mend.9.4.7659084

Carlet, J., Payen, D., & Opal, S. M. (2020). Steroids for sepsis and ARDS: this eternal controversy remains with COVID-19. *Lancet*, *396*(10259), e61-e62. https://doi.org/10.1016/s0140-6736(20)32132-2

Carlet, M., Janjetovic, K., Rainer, J., Schmidt, S., Panzer-Grümayer, R., Mann, G.,…Kofler, R. (2010). Expression, regulation and function of phosphofructo-kinase/fructose-biphosphatases (PFKFBs) in glucocorticoid-induced apoptosis of acute lymphoblastic leukemia cells. *BMC Cancer*, *10*. https://doi.org/10.1186/1471-2407-10-638

Cazalis, M. A., Lepape, A., Venet, F., Frager, F., Mougin, B., Vallin, H.,…Monneret, G. (2014). Early and dynamic changes in gene expression in septic shock patients: a genome-wide approach. *Intensive Care Medicine Experimental*, *2*(1). https://doi.org/10.1186/s40635-014-0020-3

Chan, E. D., Chan, M. M., Chan, M. M., & Marik, P. E. (2020). Use of glucocorticoids in the critical care setting: Science and clinical evidence. In *Pharmacology and Therapeutics* (Vol. 206).

Chantzichristos, D., Svensson, P. A., Garner, T., Glad, C. A. M., Walker, B. R., Bergthorsdottir, R.,…Johannsson, G. (2021). Identification of human glucocorticoid response markers using

medRxiv preprint doi: https://doi.org/10.1101/2023.05.10.23289779; this version posted November 4, 2024. The copyright holder for this preprint (which was not certified by peer review) is the author/funder, who has granted medRxiv a license to display the preprint in perpetuity. All rights reserved. No reuse allowed without permission.

integrated multi-omic analysis from a randomized crossover trial. *eLife*, *10*. https://doi.org/10.7554/ELIFE.62236

Chaussabel, D., & Baldwin, N. (2014). Democratizing systems immunology with modular transcriptional repertoire analyses. In *Nat Rev Immunol* (Vol. 14, pp. 271-280). https://doi.org/10.1038/nri3642

Chaussabel, D., Quinn, C., Shen, J., Patel, P., Glaser, C., Baldwin, N.,…Pascual, V. (2008). A modular analysis framework for blood genomics studies: application to systemic lupus erythematosus. *Immunity*, *29*(1), 150-164. https://doi.org/10.1016/j.immuni.2008.05.012

Coulibaly, A., Velásquez, S. Y., Sticht, C., Figueiredo, A. S., Himmelhan, B. S., Schulte, J.,…Lindner, H. A. (2019). AKIRIN1: A potential new reference gene in human natural killer cells and granulocytes in sepsis. *International Journal of Molecular Sciences*, *20*(9). https://doi.org/10.3390/ijms20092290

Darcy, C. J., Minigo, G., Piera, K. A., Davis, J. S., McNeil, Y. R., Chen, Y.,…Woodberry, T. (2014). Neutrophils with myeloid derived suppressor function deplete arginine and constrain T cell function in septic shock patients. *Critical Care*, *18*(4). https://doi.org/10.1186/cc14003

Darden, D. B., Kelly, L. S., Fenner, B. P., Moldawer, L. L., Mohr, A. M., & Efron, P. A. (2021). Dysregulated Immunity and Immunotherapy after Sepsis. *J Clin Med*, *10*(8). https://doi.org/10.3390/jcm10081742

de Kleijn, S., Kox, M., Sama, I. E., Pillay, J., van Diepen, A., Huijnen, M. A.,…Pickkers, P. (2012). Transcriptome kinetics of circulating neutrophils during human experimental endotoxemia. *PLoS ONE*, *7*(6). https://doi.org/10.1371/journal.pone.0038255

DeBerg, H. A., Zaidi, M. B., Altman, M. C., Khaenam, P., Gersuk, V. H., Campos, F. D.,…Linsley, P. S. (2018). Shared and organism-specific host responses to childhood diarrheal diseases revealed by whole blood transcript profiling. *PLoS ONE*, *13*(1). https://doi.org/10.1371/journal.pone.0192082

Demaret, J., Venet, F., Friggeri, A., Cazalis, M.-A., Plassais, J., Jallades, L.,…Monneret, G. (2015). Marked alterations of neutrophil functions during sepsis-induced immunosuppression. *Journal of Leukocyte Biology*, *98*(6). https://doi.org/10.1189/jlb.4a0415-168rr

Desgeorges, T., Caratti, G., Mounier, R., Tuckermann, J., & Chazaud, B. (2019). Glucocorticoids shape macrophage phenotype for tissue repair. In *Frontiers in Immunology* (Vol. 10).

Devlin, J. C., Zwack, E. E., Tang, M. S., Li, Z., Fenyo, D., Torres, V. J.,…Loke, P. (2020). Distinct Features of Human Myeloid Cell Cytokine Response Profiles Identify Neutrophil Activation by Cytokines as a Prognostic Feature during Tuberculosis and Cancer. *J Immunol*, *204*(12), 3389-3399. https://doi.org/10.4049/jimmunol.1901133

Diamond, M. I., Miner, J. N., Yoshinaga, S. K., & Yamamoto, K. R. (1990). Transcription factor interactions: selectors of positive or negative regulation from a single DNA element. *Science*, *249*(4974), 1266-1272. https://doi.org/10.1126/science.2119054

Dolinay, T., Kim, Y. S., Howrylak, J., Hunninghake, G. M., An, C. H., Fredenburgh, L.,…Choi, A. M. K. (2012). Inflammasome-regulated cytokines are critical mediators of acute lung injury. *American Journal of Respiratory and Critical Care Medicine*, *185*(11). https://doi.org/10.1164/rccm.201201-0003OC

Dragulescu, A. A. (2012). Package 'xlsx'. *Cell*, *9*.

Dubois-Camacho, K., Ottum, P. A., Franco-Muñoz, D., De La Fuente, M., Torres-Riquelme, A., Díaz-Jiménez, D.,…Hermoso, M. A. (2017). Glucocorticosteroid therapy in inflammatory bowel diseases: From clinical practice to molecular biology. In *World Journal of Gastroenterology* (Vol. 23).

Dufort, M. J., Hanniffy, S., Conde-Álvarez, R., Arce-Gorvel, V., Altman, M. C., Khaenam, P.,…Gorvel, J.-P. (2016). Gene expression profiles predict treatment outcomes in Brucellosis. *the Journal of Immunology*, *196*. https://doi.org/https://doi.org/10.4049/jimmunol.196.Supp.66.21

Ehrchen, J., Steinmüller, L., Barczyk, K., Tenbrock, K., Nacken, W., Eisenacher, M.,…Roth, J. (2007). Glucocorticoids induce differentiation of a specifically activated, anti-inflammatory subtype of human monocytes. *Blood*, *109*(3). https://doi.org/10.1182/blood-2006-02-001115

medRxiv preprint doi: https://doi.org/10.1101/2023.05.10.23289779; this version posted November 4, 2024. The copyright holder for this preprint (which was not certified by peer review) is the author/funder, who has granted medRxiv a license to display the preprint in perpetuity. All rights reserved. No reuse allowed without permission.

Ehrchen, J. M., Roth, J., & Barczyk-Kahlert, K. (2019). More than suppression: Glucocorticoid action on monocytes and macrophages. In *Frontiers in Immunology* (Vol. 10).

ElTanbouly, M. A., Zhao, Y., Schaafsma, E., Burns, C. M., Mabaera, R., Cheng, C., & Noelle, R. J. (2021). VISTA: A Target to Manage the Innate Cytokine Storm. *Frontiers in Immunology*, *11*. https://doi.org/10.3389/fimmu.2020.595950

Enwonwu, C. O., Afolabi, B. M., Salako, L. A., Idigbe, E. O., Al-Hassan, H., & Rabiu, R. A. (1999). Hyperphenylalaninaemia in children with falciparum malaria. *QJM - Monthly Journal of the Association of Physicians*, *92*(9). https://doi.org/10.1093/qjmed/92.9.495

Escoter-Torres, L., Caratti, G., Mechtidou, A., Tuckermann, J., Uhlenhaut, N. H., & Vettorazzi, S. (2019). Fighting the fire: Mechanisms of inflammatory gene regulation by the glucocorticoid receptor. In *Frontiers in Immunology* (Vol. 10).

Escoter-Torres, L., Greulich, F., Quagliarini, F., Wierer, M., & Uhlenhaut, N. H. (2020). Anti-inflammatory functions of the glucocorticoid receptor require DNA binding. *Nucleic Acids Res*, *48*(15), 8393-8407. https://doi.org/10.1093/nar/gkaa565

Estupiñán-Moreno, E., Ortiz-Fernández, L., Li, T., Hernández-Rodríguez, J., Ciudad, L., Andrés-León, E.,…Martín, J. (2022). Methylome and transcriptome profiling of giant cell arteritis monocytes reveals novel pathways involved in disease pathogenesis and molecular response to glucocorticoids. *Ann Rheum Dis*, *81*(9), 1290-1300. https://doi.org/10.1136/annrheumdis-2022-222156

Evans, L., Rhodes, A., Alhazzani, W., Antonelli, M., Coopersmith, C. M., French, C.,…Levy, M. (2021). Surviving Sepsis Campaign: International Guidelines for Management of Sepsis and Septic Shock 2021. *Crit Care Med*, *49*(11), e1063-e1143. https://doi.org/10.1097/ccm.0000000000005337

Fadel, L., Dacic, M., Fonda, V., Sokolsky, B. A., Quagliarini, F., Rogatsky, I., & Uhlenhaut, N. H. (2023). Modulating glucocorticoid receptor actions in physiology and pathology: Insights from coregulators. *Pharmacol Ther*, *251*, 108531. https://doi.org/10.1016/j.pharmthera.2023.108531

Field, A. P. (2005). Is the meta-analysis of correlation coefficients accurate when population correlations vary? *Psychological Methods*, *10*(4). https://doi.org/10.1037/1082-989X.10.4.444

Fleuriet, J., Heming, N., Meziani, F., Reignier, J., Declerq, P. L., Mercier, E.,…Annane, D. (2023). Rapid rEcognition of COrticosteRoiD resistant or sensitive Sepsis (RECORDS): study protocol for a multicentre, placebo-controlled, biomarker-guided, adaptive Bayesian design basket trial. *BMJ Open*, *13*(3), e066496. https://doi.org/10.1136/bmjopen-2022-066496

Franco, L. M., Gadkari, M., Howe, K. N., Sun, J., Kardava, L., Kumar, P.,…Germain, R. N. (2019). Immune regulation by glucocorticoids can be linked to cell type–dependent transcriptional responses. *Journal of Experimental Medicine*, *216*(2). https://doi.org/10.1084/jem.20180595

Fu, X., Liu, Z., & Wang, Y. (2023). Advances in the Study of Immunosuppressive Mechanisms in Sepsis. *J Inflamm Res*, *16*, 3967-3981. https://doi.org/10.2147/jir.s426007

Gentile, L. F., Cuenca, A. G., Efron, P. A., Ang, D., Bihorac, A., McKinley, B. A.,…Moore, F. A. (2012). Persistent inflammation and immunosuppression: A common syndrome and new horizon for surgical intensive care. In *Journal of Trauma and Acute Care Surgery* (Vol. 72).

Gerber, A. N., Newton, R., & Sasse, S. K. (2021). Repression of transcription by the glucocorticoid receptor: A parsimonious model for the genomics. *Journal of Biological Chemistry*, *296*. https://doi.org/10.1016/j.jbc.2021.100687

Gharib, S. A., McMahan, R. S., Eddy, W. E., Long, M. E., Parks, W. C., Aitken, M. L., & Manicone, A. M. (2019). Transcriptional and functional diversity of human macrophage repolarization. *Journal of Allergy and Clinical Immunology*, *143*(4). https://doi.org/10.1016/j.jaci.2018.10.046

Ghosh, P., Katkar, G. D., Shimizu, C., Kim, J., Khandelwal, S., Tremoulet, A. H.,…Sahoo, D. (2022). An Artificial Intelligence-guided signature reveals the shared host immune response in MIS-C and Kawasaki disease. *Nat Commun*, *13*(1), 2687. https://doi.org/10.1038/s41467-022-30357-w

medRxiv preprint doi: https://doi.org/10.1101/2023.05.10.23289779; this version posted November 4, 2024. The copyright holder for this preprint (which was not certified by peer review) is the author/funder, who has granted medRxiv a license to display the preprint in perpetuity. All rights reserved. No reuse allowed without permission.

Gorby, C., Sotolongo Bellón, J., Wilmes, S., Warda, W., Pohler, E., Fyfe, P. K.,...Moraga, I. (2020). Engineered IL-10 variants elicit potent immunomodulatory effects at low ligand doses. *Sci Signal*, *13*(649). https://doi.org/10.1126/scisignal.abc0653

Green, D. S., Ning, F., Duemler, A., Myers, T. G., Trewhitt, K., Ekwede, I.,...Annunziata, C. M. (2023). Intraperitoneal Monocytes plus IFNs as a Novel Cellular Immunotherapy for Ovarian Cancer: Mechanistic Characterization and Results from a Phase I Clinical Trial. *Clin Cancer Res*, *29*(2), 349-363. https://doi.org/10.1158/1078-0432.ccr-22-1893

Groselj-Grenc, M., Ihan, A., & Derganc, M. (2008). Neutrophil and monocyte CD64 and CD163 expression in critically ill neonates and children with sepsis: Comparison of fluorescence intensities and calculated indexes. *Mediators of Inflammation*, *2008*. https://doi.org/10.1155/2008/202646

Grzywa, T. M., Sosnowska, A., Matryba, P., Rydzynska, Z., Jasinski, M., Nowis, D., & Golab, J. (2020). Myeloid Cell-Derived Arginase in Cancer Immune Response. In *Frontiers in Immunology* (Vol. 11).

Guignant, C., Venet, F., Planel, S., Demaret, J., Gouel-Chéron, A., Nougier, C.,...Monneret, G. (2013). Increased MerTK expression in circulating innate immune cells of patients with septic shock. *Intensive Care Medicine*, *39*(9). https://doi.org/10.1007/s00134-013-3006-9

Guo, X., Higgs, B. W., Bay-Jensen, A. C., Karsdal, M. A., Yao, Y., Roskos, L. K., & White, W. I. (2015). Suppression of T Cell Activation and Collagen Accumulation by an Anti-IFNAR1 mAb, Anifrolumab, in Adult Patients with Systemic Sclerosis. *Journal of Investigative Dermatology*, *135*(10). https://doi.org/10.1038/jid.2015.188

Gustafson, M. P., DiCostanzo, A. C., Wheatley, C. M., Kim, C. H., Bornschlegl, S., Gastineau, D. A.,...Dietz, A. B. (2017). A systems biology approach to investigating the influence of exercise and fitness on the composition of leukocytes in peripheral blood. *J Immunother Cancer*, *5*, 30. https://doi.org/10.1186/s40425-017-0231-8

Guthridge, J. M., Lu, R., Tran, L. T. H., Arriens, C., Aberle, T., Kamp, S.,...James, J. A. (2020). Adults with systemic lupus exhibit distinct molecular phenotypes in a cross-sectional study. *EClinicalMedicine*, *20*. https://doi.org/10.1016/j.eclinm.2020.100291

Harrison, P. W., Amode, M. R., Austine-Orimoloye, O., Azov, A. G., Barba, M., Barnes, I.,...Yates, A. D. (2024). Ensembl 2024. *Nucleic Acids Res*, *52*(D1), D891-d899. https://doi.org/10.1093/nar/gkad1049

He, Y. J., Xu, J. Q., Sun, M. M., Fang, X. Z., Peng, Z. K., Pan, S. W.,...Shang, Y. (2020). Glucocorticoid-Induced Leucine Zipper: A Promising Marker for Monitoring and Treating Sepsis. *Front Immunol*, *11*, 606649. https://doi.org/10.3389/fimmu.2020.606649

Heideveld, E., Hampton-O'Neil, L. A., Cross, S. J., van Alphen, F. P. J., van den Biggelaar, M., Toye, A. M., & van den Akker, E. (2018). Glucocorticoids induce differentiation of monocytes towards macrophages that share functional and phenotypical aspects with erythroblastic island macrophages. *Haematologica*, *103*(3), 395-405. https://doi.org/10.3324/haematol.2017.179341

Hellebrekers, P., Vrisekoop, N., & Koenderman, L. (2018). Neutrophil phenotypes in health and disease. In *European Journal of Clinical Investigation* (Vol. 48).

Herberg, J. A., Kaforou, M., Wright, V. J., Shailes, H., Eleftherohorinou, H., Hoggart, C. J.,...Levin, M. (2016). Diagnostic test accuracy of a 2-transcript host RNA signature for discriminating bacterial vs viral infection in febrile children. *JAMA - Journal of the American Medical Association*, *316*(8). https://doi.org/10.1001/jama.2016.11236

Herman, J. P., McKlveen, J. M., Ghosal, S., Kopp, B., Wulsin, A., Makinson, R.,...Myers, B. (2016). Regulation of the Hypothalamic-Pituitary-Adrenocortical Stress Response. *Compr Physiol*, *6*(2), 603-621. https://doi.org/10.1002/cphy.c150015

Herwanto, V., Tang, B., Wang, Y., Shojaei, M., Nalos, M., Shetty, A.,...Schughart, K. (2021). Blood transcriptome analysis of patients with uncomplicated bacterial infection and sepsis. *BMC Research Notes*, *14*(1). https://doi.org/10.1186/s13104-021-05488-w

medRxiv preprint doi: https://doi.org/10.1101/2023.05.10.23289779; this version posted November 4, 2024. The copyright holder for this preprint (which was not certified by peer review) is the author/funder, who has granted medRxiv a license to display the preprint in perpetuity. All rights reserved. No reuse allowed without permission.

Hesselink, L., Hoepelman, R. J., Spijkerman, R., de Groot, M. C. H., van Wessem, K. J. P., Koenderman, L.,…Hietbrink, F. (2020). Persistent Inflammation, Immunosuppression and Catabolism Syndrome (PICS) after Polytrauma: A Rare Syndrome with Major Consequences. *J Clin Med*, *9*(1). https://doi.org/10.3390/jcm9010191

Hesselink, L., Spijkerman, R., Van Wessem, K. J. P., Koenderman, L., Leenen, L. P. H., Huber-Lang, M., & Hietbrink, F. (2019). Neutrophil heterogeneity and its role in infectious complications after severe trauma. In *World Journal of Emergency Surgery* (Vol. 14).

Hibbert, J. E., Currie, A., & Strunk, T. (2018). Sepsis-Induced Immunosuppression in Neonates. *Front Pediatr*, *6*, 357. https://doi.org/10.3389/fped.2018.00357

Hotchkiss, R. S., Moldawer, L. L., Opal, S. M., Reinhart, K., Turnbull, I. R., & Vincent, J. L. (2016). Sepsis and septic shock. In *Nature Reviews Disease Primers* (Vol. 2).

Hu, Y., Carman, J. A., Holloway, D., Kansal, S., Fan, L., Goldstine, C.,…Nadler, S. G. (2018). Development of a Molecular Signature to Monitor Pharmacodynamic Responses Mediated by In Vivo Administration of Glucocorticoids. *Arthritis and Rheumatology*, *70*(8). https://doi.org/10.1002/art.40476

Huber, W., Carey, V. J., Gentleman, R., Anders, S., Carlson, M., Carvalho, B. S.,…Morgan, M. (2015). Orchestrating high-throughput genomic analysis with Bioconductor. *Nature Methods*, *12*(2). https://doi.org/10.1038/nmeth.3252

Huber-Lang, M., Lambris, J. D., & Ward, P. A. (2018). Innate immune responses to trauma review-article. In *Nature Immunology* (Vol. 19).

Hughey, J. J. (2017). Machine learning identifies a compact gene set for monitoring the circadian clock in human blood. *Genome Medicine*, *9*(1). https://doi.org/10.1186/s13073-017-0406-4

Hung, T., Pratt, G. A., Sundararaman, B., Townsend, M. J., Chaivorapol, C., Bhangale, T.,…Behrens, T. W. (2015). The Ro60 autoantigen binds endogenous retroelements and regulates inflammatory gene expression. *Science*, *350*(6259), 455-459. https://doi.org/10.1126/science.aac7442

Hung, T., Pratt, G. A., Sundararaman, B., Towsend, M. J., Chaivorapol, C., Bhangale, T.,…Behrens, T. W. (2015). The Ro60 autoantigen binds endogenous retroelements and regulates inflammatory gene expression. *Science*, *350*(6259). https://doi.org/10.1126/science.aac7442

Idaghdour, Y., Quinlan, J., Goulet, J. P., Berghout, J., Gbeha, E., Bruat, V.,…Awadalla, P. (2012). Evidence for additive and interaction effects of host genotype and infection in malaria. *Proceedings of the National Academy of Sciences of the United States of America*, *109*(42). https://doi.org/10.1073/pnas.1204945109

Ince, L. M., Weber, J., & Scheiermann, C. (2019). Control of leukocyte trafficking by stress-associated hormones. In *Frontiers in Immunology* (Vol. 10).

Inouye, M., Silander, K., Hamalainen, E., Salomaa, V., Harald, K., Jousilahti, P.,…Peltonen, L. (2010). An immune response network associated with blood lipid levels. *PLoS Genetics*, *6*(9). https://doi.org/10.1371/journal.pgen.1001113

Italiani, P., Mazza, E. M., Lucchesi, D., Cifola, I., Gemelli, C., Grande, A.,…Boraschi, D. (2014). Transcriptomic profiling of the development of the inflammatory response in human monocytes in vitro. *PLoS One*, *9*(2), e87680. https://doi.org/10.1371/journal.pone.0087680

Jarczak, D., Kluge, S., & Nierhaus, A. (2021). Sepsis—Pathophysiology and Therapeutic Concepts. In *Frontiers in Medicine* (Vol. 8).

Jiang, Y., Rosborough, B. R., Chen, J., Das, S., Kitsios, G. D., McVerry, B. J.,…Ray, P. (2020). Single cell RNA sequencing identifies an early monocyte gene signature in acute respiratory distress syndrome. *JCI Insight*, *5*(13). https://doi.org/10.1172/jci.insight.135678

Johannsson, G., Falorni, A., Skrtic, S., Lennernäs, H., Quinkler, M., Monson, J. P., & Stewart, P. M. (2015). Adrenal insufficiency: Review of clinical outcomes with current glucocorticoid replacement therapy. In *Clinical Endocrinology* (Vol. 82).

Johnson, T. A., Paakinaho, V., Kim, S., Hager, G. L., & Presman, D. M. (2021). Genome-wide binding potential and regulatory activity of the glucocorticoid receptor's monomeric and dimeric forms. *Nature Communications*, *12*(1). https://doi.org/10.1038/s41467-021-22234-9

medRxiv preprint doi: https://doi.org/10.1101/2023.05.10.23289779; this version posted November 4, 2024. The copyright holder for this preprint (which was not certified by peer review) is the author/funder, who has granted medRxiv a license to display the preprint in perpetuity. All rights reserved. No reuse allowed without permission.

Jubb, A. W., Young, R. S., Hume, D. A., & Bickmore, W. A. (2016). Enhancer Turnover Is Associated with a Divergent Transcriptional Response to Glucocorticoid in Mouse and Human Macrophages. *The Journal of Immunology*, *196*(2). https://doi.org/10.4049/jimmunol.1502009

Juss, J. K., House, D., Amour, A., Begg, M., Herre, J., Storisteanu, D. M. L.,…Chilvers, E. R. (2016). Acute respiratory distress syndrome neutrophils have a distinct phenotype and are resistant to phosphoinositide 3-kinase inhibition. *American Journal of Respiratory and Critical Care Medicine*, *194*(8). https://doi.org/10.1164/rccm.201509-1818OC

Karakike, E., Scicluna, B. P., Roumpoutsou, M., Mitrou, I., Karampela, N., Karageorgos, A.,…Giamarellos-Bourboulis, E. J. (2022). Effect of intravenous clarithromycin in patients with sepsis, respiratory and multiple organ dysfunction syndrome: a randomized clinical trial. *Crit Care*, *26*(1), 183. https://doi.org/10.1186/s13054-022-04055-4

Khaenam, P., Rinchai, D., Altman, M. C., Chiche, L., Buddhisa, S., Kewcharoenwong, C.,…Chaussabel, D. (2014). A transcriptomic reporter assay employing neutrophils to measure immunogenic activity of septic patients' plasma. *J Transl Med*, *12*, 65. https://doi.org/10.1186/1479-5876-12-65

Kim, O. Y., Monsel, A., Bertrand, M., Coriat, P., Cavaillon, J. M., & Adib-Conquy, M. (2010). Differential down-regulation of HLA-DR on monocyte subpopulations during systemic inflammation. *Critical Care*, *14*(2). https://doi.org/10.1186/cc8959

Knoll, R., Helbig, E. T., Dahm, K., Bolaji, O., Hamm, F., Dietrich, O.,…Kurth, F. (2024). The life-saving benefit of dexamethasone in severe COVID-19 is linked to a reversal of monocyte dysregulation. *Cell*, *187*(16), 4318-4335.e4320. https://doi.org/10.1016/j.cell.2024.06.014

Kolde, R. (2019). Package 'pheatmap': Pretty heatmaps. *Version 1.0.12*.

Kolte, A. (2020). Improving the outcome of the critically ill with cortico- and sex-steroids employing clinico-transcriptomics approaches. In. Jena: Digitale Bibliothek Thueringen.

Komorowski, M., Green, A., Tatham, K. C., Seymour, C., & Antcliffe, D. (2022). Sepsis biomarkers and diagnostic tools with a focus on machine learning. *EBioMedicine*, *86*, 104394. https://doi.org/10.1016/j.ebiom.2022.104394

Kossenkov, A. V., Qureshi, R., Dawany, N. B., Wickramasinghe, J., Liu, Q., Majumdar, R. S.,…Showe, L. C. (2019). A Gene Expression Classifier from Whole Blood Distinguishes Benign from Malignant Lung Nodules Detected by Low-Dose CT. *Cancer Res*, *79*(1), 263-273. https://doi.org/10.1158/0008-5472.can-18-2032

Koth, L. L., Solberg, O. D., Peng, J. C., Bhakta, N. R., Nguyen, C. P., & Woodruff, P. G. (2011). Sarcoidosis blood transcriptome reflects lung inflammation and overlaps with tuberculosis. *American Journal of Respiratory and Critical Care Medicine*, *184*(10). https://doi.org/10.1164/rccm.201106-1143OC

Kovtun, A., Messerer, D. A. C., Scharffetter-Kochanek, K., Huber-Lang, M., & Ignatius, A. (2018). Neutrophils in tissue trauma of the skin, bone, and lung: Two sides of the same coin. In *Journal of Immunology Research* (Vol. 2018).

Kuan, P. F., Waszczuk, M. A., Kotov, R., Clouston, S., Yang, X., Singh, P. K.,…Luft, B. J. (2017). Gene expression associated with PTSD in World Trade Center responders: An RNA sequencing study. *Translational Psychiatry*, *7*(12). https://doi.org/10.1038/s41398-017-0050-1

Kwok, A. J., Allcock, A., Ferreira, R. C., Cano-Gamez, E., Smee, M., Burnham, K. L.,…Knight, J. C. (2023). Neutrophils and emergency granulopoiesis drive immune suppression and an extreme response endotype during sepsis. *Nat Immunol*, *24*(5), 767-779. https://doi.org/10.1038/s41590-023-01490-5

Kwok, I., Becht, E., Xia, Y., Ng, M., Teh, Y. C., Tan, L.,…Ng, L. G. (2020). Combinatorial Single-Cell Analyses of Granulocyte-Monocyte Progenitor Heterogeneity Reveals an Early Uni-potent Neutrophil Progenitor. *Journal of Cleaner Production*. https://doi.org/10.1016/j.immuni.2020.06.005

medRxiv preprint doi: https://doi.org/10.1101/2023.05.10.23289779; this version posted November 4, 2024. The copyright holder for this preprint (which was not certified by peer review) is the author/funder, who has granted medRxiv a license to display the preprint in perpetuity. All rights reserved. No reuse allowed without permission.

König, R., Kolte, A., Ahlers, O., Oswald, M., Krauss, V., Roell, D.,…Bauer, M. (2021). Use of IFNγ/IL10 Ratio for Stratification of Hydrocortisone Therapy in Patients With Septic Shock. *Frontiers in Immunology*, *12*. https://doi.org/10.3389/fimmu.2021.607217

Laing, E. E., Möller-Levet, C. S., Poh, N., Santhi, N., Archer, S. N., & Dijk, D. J. (2017). Blood transcriptome based biomarkers for human circadian phase. *eLife*, *6*. https://doi.org/10.7554/eLife.20214

Lange, T., Luebber, F., Grasshoff, H., & Besedovsky, L. (2022). The contribution of sleep to the neuroendocrine regulation of rhythms in human leukocyte traffic. *Semin Immunopathol*, *44*(2), 239-254. https://doi.org/10.1007/s00281-021-00904-6

Langfelder, P., & Horvath, S. (2008). WGCNA: an R package for weighted correlation network analysis. *BMC Bioinformatics*, *9*, 559. https://doi.org/10.1186/1471-2105-9-559

Langouche, L., Téblick, A., Gunst, J., & Van den Berghe, G. (2023). The Hypothalamus-pituitary-adrenocortical Response to Critical Illness: A Concept in Need of Revision. *Endocr Rev*, *44*(6), 1096-1106. https://doi.org/10.1210/endrev/bnad021

Leite, G. G. F., de Brabander, J., Michels, E. H. A., Butler, J. M., Cremer, O. L., Scicluna, B. P.,…van der Poll, T. (2024). Monocyte state 1 (MS1) cells in critically ill patients with sepsis or non-infectious conditions: association with disease course and host response. *Crit Care*, *28*(1), 88. https://doi.org/10.1186/s13054-024-04868-5

Leliefeld, P. H. C., Wessels, C. M., Leenen, L. P. H., Koenderman, L., & Pillay, J. (2016). The role of neutrophils in immune dysfunction during severe inflammation. In *Critical Care* (Vol. 20).

Leligdowicz, A., & Matthay, M. A. (2019). Heterogeneity in sepsis: New biological evidence with clinical applications. In *Critical Care* (Vol. 23).

Liepelt, A., Hohlstein, P., Gussen, H., Xue, J., Aschenbrenner, A. C., Ulas, T.,…Tacke, F. (2020). Differential Gene Expression in Circulating CD14(+) Monocytes Indicates the Prognosis of Critically Ill Patients with Sepsis. *J Clin Med*, *9*(1). https://doi.org/10.3390/jcm9010127

Linsley, P. S., Speake, C., Whalen, E., & Chaussabel, D. (2014). Copy number loss of the interferon gene cluster in melanomas is linked to reduced T cell infiltrate and poor patient prognosis. *PLoS ONE*, *9*(10). https://doi.org/10.1371/journal.pone.0109760

Liu, C., Martins, A. J., Lau, W. W., Rachmaninoff, N., Chen, J., Imberti, L.,…Tsang, J. S. (2021). Time-resolved systems immunology reveals a late juncture linked to fatal COVID-19. *Cell*, *184*(7). https://doi.org/10.1016/j.cell.2021.02.018

Liu, D., Huang, S. Y., Sun, J. H., Zhang, H. C., Cai, Q. L., Gao, C.,…Zeng, L. (2022). Sepsis-induced immunosuppression: mechanisms, diagnosis and current treatment options. *Mil Med Res*, *9*(1), 56. https://doi.org/10.1186/s40779-022-00422-y

Liu, N., Jiang, C., Cai, P., Shen, Z., Sun, W., Xu, H.,…Qu, K. (2021). Single-cell analysis of COVID-19, sepsis, and HIV infection reveals hyperinflammatory and immunosuppressive signatures in monocytes. *Cell Reports*, *37*(1). https://doi.org/10.1016/j.celrep.2021.109793

Liu, T. Y., Burke, T., Park, L. P., Woods, C. W., Zaas, A. K., Ginsburg, G. S., & Hero, A. O. (2016). An individualized predictor of health and disease using paired reference and target samples. *BMC Bioinformatics*, *17*(1). https://doi.org/10.1186/s12859-016-0889-9

Lord, J. M., Midwinter, M. J., Chen, Y. F., Belli, A., Brohi, K., Kovacs, E. J.,…Lilford, R. J. (2014). The systemic immune response to trauma: an overview of pathophysiology and treatment. *Lancet*, *384*(9952), 1455-1465. https://doi.org/10.1016/s0140-6736(14)60687-5

Lurier, E. B., Dalton, D., Dampier, W., Raman, P., Nassiri, S., Ferraro, N. M.,…Spiller, K. L. (2017). Transcriptome analysis of IL-10-stimulated (M2c) macrophages by next-generation sequencing. *Immunobiology*, *222*(7). https://doi.org/10.1016/j.imbio.2017.02.006

Lévy, Y., Wiedemann, A., Hejblum, B. P., Durand, M., Lefebvre, C., Surénaud, M.,…Thiébaut, R. (2021). CD177, a specific marker of neutrophil activation, is associated with coronavirus disease 2019 severity and death. *iScience*, *24*(7). https://doi.org/10.1016/j.isci.2021.102711

López-Martínez, C., Martín-Vicente, P., Gómez de Oña, J., López-Alonso, I., Gil-Peña, H., Cuesta-Llavona, E.,…Amado-Rodríguez, L. (2023). Transcriptomic clustering of critically ill COVID-19 patients. *Eur Respir J*, *61*(1). https://doi.org/10.1183/13993003.00592-2022

medRxiv preprint doi: https://doi.org/10.1101/2023.05.10.23289779; this version posted November 4, 2024. The copyright holder for this preprint (which was not certified by peer review) is the author/funder, who has granted medRxiv a license to display the preprint in perpetuity. All rights reserved. No reuse allowed without permission.

Maranville, J. C., Baxter, S. S., Torres, J. M., & Di Rienzo, A. (2013). Inter-ethnic differences in lymphocyte sensitivity to glucocorticoids reflect variation in transcriptional response. *Pharmacogenomics J*, *13*(2), 121-129. https://doi.org/10.1038/tpj.2011.55

Marik, P. E., Pastores, S. M., Annane, D., Meduri, G. U., Sprung, C. L., Arlt, W.,…Vogeser, M. (2008). Recommendations for the diagnosis and management of corticosteroid insufficiency in critically ill adult patients: consensus statements from an international task force by the American College of Critical Care Medicine. *Crit Care Med*, *36*(6), 1937-1949. https://doi.org/10.1097/CCM.0b013e31817603ba

Mayerle, J., Den Hoed, C. M., Schurmann, C., Stolk, L., Homuth, G., Peters, M. J.,…Kuipers, E. (2013). Identification of genetic loci associated with Helicobacter pylori serologic status. *JAMA*, *309*(18). https://doi.org/10.1001/jama.2013.4350

McClain, M. T., Constantine, F. J., Henao, R., Liu, Y., Tsalik, E. L., Burke, T. W.,…Woods, C. W. (2021). Dysregulated transcriptional responses to SARS-CoV-2 in the periphery. *Nat Commun*, *12*(1), 1079. https://doi.org/10.1038/s41467-021-21289-y

Melo, R. C. N., & Weller, P. F. (2016). Lipid droplets in leukocytes: Organelles linked to inflammatory responses. In *Experimental Cell Research* (Vol. 340).

Mengos, A. E., Gastineau, D. A., & Gustafson, M. P. (2019). The CD14+HLA-DrlO/NEG monocyte: An immunosuppressive phenotype that restrains responses to cancer immunotherapy. In *Frontiers in Immunology* (Vol. 10).

Mo, A., Marigorta, U. M., Arafat, D., Chan, L. H. K., Ponder, L., Jang, S. R.,…Gibson, G. (2018). Disease-specific regulation of gene expression in a comparative analysis of juvenile idiopathic arthritis and inflammatory bowel disease. *Genome Medicine*, *10*(1). https://doi.org/10.1186/s13073-018-0558-x

Mo, S., Shi, C., Cai, Y., Xu, M., Xu, H., Xu, Y.,…Liu, E. (2024). Single-cell transcriptome reveals highly complement activated microglia cells in association with pediatric tuberculous meningitis. *Front Immunol*, *15*, 1387808. https://doi.org/10.3389/fimmu.2024.1387808

Monneret, G., & Venet, F. (2014). Monocyte HLA-DR in sepsis: shall we stop following the flow? *Crit Care*, *18*(1), 102. https://doi.org/10.1186/cc13179

Montoya, D., Inkeles, M. S., Liu, P. T., Realegeno, S., Teles, R. M., Vaidya, P.,…Modlin, R. L. (2014). IL-32 is a molecular marker of a host defense network in human tuberculosis. *Sci Transl Med*, *6*(250), 250ra114. https://doi.org/10.1126/scitranslmed.3009546

Mortaz, E., Alipoor, S. D., Adcock, I. M., Mumby, S., & Koenderman, L. (2018). Update on neutrophil function in severe inflammation. In *Frontiers in Immunology* (Vol. 9).

Murrell, P. (2002). The \pkg{grid} Graphics Package. *\proglang{R} News*, *2*(2).

Möller-Levet, C. S., Archer, S. N., Bucca, G., Laing, E. E., Slak, A., Kabiljo, R.,…Dijk, D. J. (2013). Effects of insufficient sleep on circadian rhythmicity and expression amplitude of the human blood transcriptome. *Proc Natl Acad Sci U S A*, *110*(12), E1132-1141. https://doi.org/10.1073/pnas.1217154110

Nallandhighal, S., Park, G. S., Ho, Y. Y., Opoka, R. O., John, C. C., & Tran, T. M. (2019). Whole-blood transcriptional signatures composed of erythropoietic and NRF2-Regulated genes differ between cerebral malaria and severe malarial anemia. *Journal of Infectious Diseases*, *219*(1). https://doi.org/10.1093/infdis/jiy468

Northcott, M., Gearing, L. J., Nim, H. T., Nataraja, C., Hertzog, P., Jones, S. A., & Morand, E. F. (2021). Glucocorticoid gene signatures in systemic lupus erythematosus and the effects of type I interferon: a cross-sectional and in-vitro study. *The Lancet Rheumatology*, *3*(5). https://doi.org/10.1016/S2665-9913(21)00006-0

Oh, K. S., Patel, H., Gottschalk, R. A., Lee, W. S., Baek, S., Fraser, I. D. C.,…Sung, M. H. (2017). Anti-Inflammatory Chromatinscape Suggests Alternative Mechanisms of Glucocorticoid Receptor Action. *Immunity*, *47*(2), 298-309.e295. https://doi.org/10.1016/j.immuni.2017.07.012

Okun, J. G., Conway, S., Schmidt, K. V., Schumacher, J., Wang, X., de Guia, R.,…Rose, A. J. (2015). Molecular regulation of urea cycle function by the liver glucocorticoid receptor. *Molecular Metabolism*, *4*(10). https://doi.org/10.1016/j.molmet.2015.07.006

medRxiv preprint doi: https://doi.org/10.1101/2023.05.10.23289779; this version posted November 4, 2024. The copyright holder for this preprint (which was not certified by peer review) is the author/funder, who has granted medRxiv a license to display the preprint in perpetuity. All rights reserved. No reuse allowed without permission.

Olnes, M. J., Kotliarov, Y., Biancotto, A., Cheung, F., Chen, J., Shi, R.,…Nussenblatt, R. (2016). Effects of Systemically Administered Hydrocortisone on the Human Immunome. *Sci Rep*, *6*, 23002. https://doi.org/10.1038/srep23002

Ono, S., Tsujimoto, H., Hiraki, S., & Aosasa, S. (2018). Mechanisms of sepsis-induced immunosuppression and immunological modification therapies for sepsis. *Ann Gastroenterol Surg*, *2*(5), 351-358. https://doi.org/10.1002/ags3.12194

Oster, H., Challet, E., Ott, V., Arvat, E., de Kloet, E. R., Dijk, D. J.,…Van Cauter, E. (2017). The Functional and Clinical Significance of the 24-Hour Rhythm of Circulating Glucocorticoids. *Endocr Rev*, *38*(1), 3-45. https://doi.org/10.1210/er.2015-1080

Overmyer, K. A., Shishkova, E., Miller, I. J., Balnis, J., Bernstein, M. N., Peters-Clarke, T. M.,…Jaitovich, A. (2021). Large-Scale Multi-omic Analysis of COVID-19 Severity. *Cell Systems*, *12*(1). https://doi.org/10.1016/j.cels.2020.10.003

Padovani, C. M., & Yin, K. (2024). Immunosuppression in Sepsis: Biomarkers and Specialized Pro-Resolving Mediators. *Biomedicines*, *12*(1). https://doi.org/10.3390/biomedicines12010175

Palmer, N. P., Silvester, J. A., Lee, J. J., Beam, A. L., Fried, I., Valtchinov, V. I.,…Kohane, I. S. (2019). Concordance between gene expression in peripheral whole blood and colonic tissue in children with inflammatory bowel disease. *PLoS ONE*, *14*(10). https://doi.org/10.1371/journal.pone.0222952

Pelaia, T. M., Shojaei, M., & McLean, A. S. (2023). The Role of Transcriptomics in Redefining Critical Illness. *Crit Care*, *27*(1), 89. https://doi.org/10.1186/s13054-023-04364-2

Pelekanou, V., Kampa, M., Kiagiadaki, F., Deli, A., Theodoropoulos, P., Agrogiannis, G.,…Notas, G. (2016). Estrogen anti-inflammatory activity on human monocytes is mediated through cross-talk between estrogen receptor ERα36 and GPR30/GPER1. *J Leukoc Biol*, *99*(2), 333-347. https://doi.org/10.1189/jlb.3A0914-430RR

Petri, M., Fu, W., Ranger, A., Allaire, N., Cullen, P., Magder, L. S., & Zhang, Y. (2019). Association between changes in gene signatures expression and disease activity among patients with systemic lupus erythematosus. *BMC Med Genomics*, *12*(1), 4. https://doi.org/10.1186/s12920-018-0468-1

Petri, M., Singh, S., Tesfasyone, H., Dedrick, R., Fry, K., Lal, P.,…Baechler, E. (2009). Longitudinal expression of type I interferon responsive genes in systemic lupus erythematosus. *Lupus*, *18*(11), 980-989. https://doi.org/10.1177/0961203309105529

Petta, I., Dejager, L., Ballegeer, M., Lievens, S., Tavernier, J., De Bosscher, K., & Libert, C. (2016). The Interactome of the Glucocorticoid Receptor and Its Influence on the Actions of Glucocorticoids in Combatting Inflammatory and Infectious Diseases. *Microbiology and Molecular Biology Reviews*, *80*(2). https://doi.org/10.1128/mmbr.00064-15

Pillay, J., Kamp, V. M., Van Hoffen, E., Visser, T., Tak, T., Lammers, J. W.,…Koenderman, L. (2012). A subset of neutrophils in human systemic inflammation inhibits T cell responses through Mac-1. *Journal of Clinical Investigation*, *122*(1). https://doi.org/10.1172/JCI57990

Plassais, J., Venet, F., Cazalis, M. A., Le Quang, D., Pachot, A., Monneret, G.,…Textoris, J. (2017). Transcriptome modulation by hydrocortisone in severe burn shock: Ancillary analysis of a prospective randomized trial. *Critical Care*, *21*(1). https://doi.org/10.1186/s13054-017-1743-9

Pottecher, J., Meyer, A., Wenceslau, C. F., Timmermans, K., Hauser, C. J., & Land, W. G. (2019). Editorial: Trauma-induced, DAMP-mediated remote organ injury, and immunosuppression in the acutely Ill patient. In *Frontiers in Immunology* (Vol. 10).

Quatrini, L., & Ugolini, S. (2021). New insights into the cell- and tissue-specificity of glucocorticoid actions. In *Cellular and Molecular Immunology* (Vol. 18).

Radom-Aizik, S., Zaldivar, F., Leu, S. Y., & Cooper, D. M. (2009a). A brief bout of exercise alters gene expression and distinct gene pathways in peripheral blood mononuclear cells of early- and late-pubertal females. *Journal of Applied Physiology*, *107*(1). https://doi.org/10.1152/japplphysiol.00121.2009

medRxiv preprint doi: https://doi.org/10.1101/2023.05.10.23289779; this version posted November 4, 2024. The copyright holder for this preprint (which was not certified by peer review) is the author/funder, who has granted medRxiv a license to display the preprint in perpetuity. All rights reserved. No reuse allowed without permission.

Radom-Aizik, S., Zaldivar, F., Leu, S. Y., & Cooper, D. M. (2009b). Brief bout of exercise alters gene expression in peripheral blood mononuclear cells of early- and late-pubertal males. *Pediatric Research*, *65*(4). https://doi.org/10.1203/PDR.0b013e3181993473

Ranjan, A., Iyer, S. V., & Iwakuma, T. (2017). Suppressive roles of A3AR and TMIGD3 i1 in osteosarcoma malignancy. In *Cell Cycle* (Vol. 16, pp. 903-904). https://doi.org/10.1080/15384101.2017.1308153

Ray, A., & Prefontaine, K. E. (1994). Physical association and functional antagonism between the p65 subunit of transcription factor NF-kappa B and the glucocorticoid receptor. *Proc Natl Acad Sci U S A*, *91*(2), 752-756. https://doi.org/10.1073/pnas.91.2.752

Raymond, S. L., Holden, D. C., Mira, J. C., Stortz, J. A., Loftus, T. J., Mohr, A. M.,…Efron, P. A. (2017). Microbial recognition and danger signals in sepsis and trauma. *Biochim Biophys Acta Mol Basis Dis*, *1863*(10 Pt B), 2564-2573. https://doi.org/10.1016/j.bbadis.2017.01.013

Reichardt, S. D., Amouret, A., Muzzi, C., Vettorazzi, S., Tuckermann, J. P., Lühder, F., & Reichardt, H. M. (2021). The Role of Glucocorticoids in Inflammatory Diseases. *Cells*, *10*(11). https://doi.org/10.3390/cells10112921

Relja, B., & Land, W. G. (2020). Damage-associated molecular patterns in trauma. *Eur J Trauma Emerg Surg*, *46*(4), 751-775. https://doi.org/10.1007/s00068-019-01235-w

Reusch, N., De Domenico, E., Bonaguro, L., Schulte-Schrepping, J., Baßler, K., Schultze, J. L., & Aschenbrenner, A. C. (2021). Neutrophils in COVID-19. In *Frontiers in Immunology* (Vol. 12).

Reyes, M., Filbin, M. R., Bhattacharyya, R. P., Billman, K., Eisenhaure, T., Hung, D. T.,…Hacohen, N. (2020). An immune-cell signature of bacterial sepsis. In *Nature Medicine* (Vol. 26).

Reyes, M., Filbin, M. R., Bhattacharyya, R. P., Sonny, A., Mehta, A., Billman, K.,…Hacohen, N. (2021). Plasma from patients with bacterial sepsis or severe COVID-19 induces suppressive myeloid cell production from hematopoietic progenitors in vitro. *Science Translational Medicine*, *13*(598). https://doi.org/10.1126/scitranslmed.abe9599

Rezai, M., Fullwood, C., Hird, B., Chawla, M., Tetlow, L., Banerjee, I., & Patel, L. (2022). Cortisol Levels During Acute Illnesses in Children and Adolescents: A Systematic Review. *JAMA Netw Open*, *5*(6), e2217812. https://doi.org/10.1001/jamanetworkopen.2022.17812

Rinchai, D., Altman, M. C., Konza, O., Hässler, S., Martina, F., Toufiq, M.,…Chaussabel, D. (2020). Definition of erythroid cell-positive blood transcriptome phenotypes associated with severe respiratory syncytial virus infection. *Clin Transl Med*, *10*(8), e244. https://doi.org/10.1002/ctm2.244

Ronchetti, S., Ricci, E., Migliorati, G., Gentili, M., & Riccardi, C. (2018). How glucocorticoids affect the neutrophil life. In *International Journal of Molecular Sciences* (Vol. 19).

Roszer, T. (2015). Understanding the mysterious M2 macrophage through activation markers and effector mechanisms. In *Mediators of Inflammation* (Vol. 2015).

Russell, J. A. (2018). When and how to use predictive biomarkers for corticosteroid treatment of septic shock. In *Critical Care* (Vol. 22).

Sano, S., Nakagawa, Y., Iwashima, S., Ishikawa, T., Satake, E., Matsushita, R.,…Ohzeki, T. (2010). Dynamics of endogenous glucocorticoid secretion and its metabolism in Kawasaki disease. *Steroids*, *75*(12). https://doi.org/10.1016/j.steroids.2010.06.006

Sautron, V., Terenina, E., Gress, L., Lippi, Y., Billon, Y., Larzul, C.,…Mormède, P. (2015). Time course of the response to ACTH in pig: Biological and transcriptomic study. *BMC Genomics*, *16*(1). https://doi.org/10.1186/s12864-015-2118-8

Scheinman, R. I., Gualberto, A., Jewell, C. M., Cidlowski, J. A., & Baldwin, A. S., Jr. (1995). Characterization of mechanisms involved in transrepression of NF-kappa B by activated glucocorticoid receptors. *Mol Cell Biol*, *15*(2), 943-953. https://doi.org/10.1128/mcb.15.2.943

Schramm, K., Marzi, C., Schurmann, C., Carstensen, M., Reinmaa, E., Biffar, R.,…Prokisch, H. (2014). Mapping the genetic architecture of gene regulation in whole blood. *PLoS ONE*, *9*(4). https://doi.org/10.1371/journal.pone.0093844

Schrijver, I. T., Théroude, C., & Roger, T. (2019). Myeloid derived suppressor cells sepsis. In *Frontiers in Immunology* (Vol. 10).

medRxiv preprint doi: https://doi.org/10.1101/2023.05.10.23289779; this version posted November 4, 2024. The copyright holder for this preprint (which was not certified by peer review) is the author/funder, who has granted medRxiv a license to display the preprint in perpetuity. All rights reserved. No reuse allowed without permission.

Schulte-Schrepping, J., Reusch, N., Paclik, D., Baßler, K., Schlickeiser, S., Zhang, B.,…Ziebuhr, J. (2020). Severe COVID-19 Is Marked by a Dysregulated Myeloid Cell Compartment. *Cell*, *182*(6). https://doi.org/10.1016/j.cell.2020.08.001

Seah, C., Breen, M. S., Rusielewicz, T., Bader, H. N., Xu, C., Hunter, C. J.,…Yehuda, R. (2022). Modeling gene × environment interactions in PTSD using human neurons reveals diagnosis-specific glucocorticoid-induced gene expression. *Nat Neurosci*, *25*(11), 1434-1445. https://doi.org/10.1038/s41593-022-01161-y

Seal, R. L., Braschi, B., Gray, K., Jones, T. E. M., Tweedie, S., Haim-Vilmovsky, L., & Bruford, E. A. (2023). Genenames.org: the HGNC resources in 2023. *Nucleic Acids Res*, *51*(D1), D1003-d1009. https://doi.org/10.1093/nar/gkac888

Sean, D., & Meltzer, P. S. (2007). GEOquery: A bridge between the Gene Expression Omnibus (GEO) and BioConductor. *Bioinformatics*, *23*(14). https://doi.org/10.1093/bioinformatics/btm254

Shalova, I. N., Lim, J. Y., Chittezhath, M., Zinkernagel, A. S., Beasley, F., Hernández-Jiménez, E.,…Biswas, S. K. (2015). Human monocytes undergo functional re-programming during sepsis mediated by hypoxia-inducible factor-1α. *Immunity*, *42*(3). https://doi.org/10.1016/j.immuni.2015.02.001

Shen, X. F., Cao, K., Jiang, J. P., Guan, W. X., & Du, J. F. (2017). Neutrophil dysregulation during sepsis: an overview and update. In *Journal of Cellular and Molecular Medicine* (Vol. 21).

Shimba, A., & Ikuta, K. (2020). Glucocorticoids Regulate Circadian Rhythm of Innate and Adaptive Immunity. In *Frontiers in Immunology* (Vol. 11).

Silvestre-Roig, C., Fridlender, Z. G., Glogauer, M., & Scapini, P. (2019). Neutrophil Diversity in Health and Disease. *Trends Immunol*, *40*(7), 565-583. https://doi.org/10.1016/j.it.2019.04.012

Singer, M., Deutschman, C. S., Seymour, C., Shankar-Hari, M., Annane, D., Bauer, M.,…Angus, D. C. (2016). The third international consensus definitions for sepsis and septic shock (sepsis-3). In *JAMA - Journal of the American Medical Association* (Vol. 315).

Singhania, A., Verma, R., Graham, C. M., Lee, J., Tran, T., Richardson, M.,…O'Garra, A. (2018). A modular transcriptional signature identifies phenotypic heterogeneity of human tuberculosis infection. *Nature Communications*, *9*(1). https://doi.org/10.1038/s41467-018-04579-w

Sinha, S., Rosin, N. L., Arora, R., Labit, E., Jaffer, A., Cao, L.,…Biernaskie, J. (2022). Dexamethasone modulates immature neutrophils and interferon programming in severe COVID-19. *Nat Med*, *28*(1), 201-211. https://doi.org/10.1038/s41591-021-01576-3

Stanski, N. L., & Wong, H. R. (2020). Prognostic and predictive enrichment in sepsis. *Nat Rev Nephrol*, *16*(1), 20-31. https://doi.org/10.1038/s41581-019-0199-3

Steinbrink, J. M., Myers, R. A., Hua, K., Johnson, M. D., Seidelman, J. L., Tsalik, E. L.,…McClain, M. T. (2021). The host transcriptional response to Candidemia is dominated by neutrophil activation and heme biosynthesis and supports novel diagnostic approaches. *Genome Medicine*, *13*(1). https://doi.org/10.1186/s13073-021-00924-9

Stelzer, G., Rosen, N., Plaschkes, I., Zimmerman, S., Twik, M., Fishilevich, S.,…Lancet, D. (2016). The GeneCards Suite: From Gene Data Mining to Disease Genome Sequence Analyses. *Curr Protoc Bioinformatics*, *54*, 1.30.31-31.30.33. https://doi.org/10.1002/cpbi.5

Strehl, C., Ehlers, L., Gaber, T., & Buttgereit, F. (2019). Glucocorticoids-All-Rounders Tackling the Versatile Players of the Immune System. In *Frontiers in immunology* (Vol. 10).

Strickland, B. A., Ansari, S. A., Dantoft, W., & Uhlenhaut, N. H. (2022). How to tame your genes: mechanisms of inflammatory gene repression by glucocorticoids. *FEBS Lett*, *596*(20), 2596-2616. https://doi.org/10.1002/1873-3468.14409

Sweeney, T. E., Shidham, A., Wong, H. R., & Khatri, P. (2015). A comprehensive time-course-based multicohort analysis of sepsis and sterile inflammation reveals a robust diagnostic gene set. *Science Translational Medicine*, *7*(287). https://doi.org/10.1126/scitranslmed.aaa5993

Sævik, Å. B., Wolff, A. B., Björnsdottir, S., Simunkova, K., Hynne, M. S., Dolan, D. W. P.,…Øksnes, M. (2021). Potential Transcriptional Biomarkers to Guide Glucocorticoid Replacement in Autoimmune Addison's Disease. *Journal of the Endocrine Society*, *5*(3). https://doi.org/10.1210/jendso/bvaa202

medRxiv preprint doi: https://doi.org/10.1101/2023.05.10.23289779; this version posted November 4, 2024. The copyright holder for this preprint (which was not certified by peer review) is the author/funder, who has granted medRxiv a license to display the preprint in perpetuity. All rights reserved. No reuse allowed without permission.

Tan, T., Khoo, B., Mills, E. G., Phylactou, M., Patel, B., Eng, P. C.,…Dhillo, W. S. (2020). Association between high serum total cortisol concentrations and mortality from COVID-19. In *The Lancet Diabetes and Endocrinology* (Vol. 8).

Tang, B. M. P., McLean, A. S., Dawes, I. W., Huang, S. J., & Lin, R. C. Y. (2009). Gene-expression profiling of peripheral blood mononuclear cells in sepsis. *Critical Care Medicine*, *37*(3). https://doi.org/10.1097/CCM.0b013e31819b52fd

Tasaki, S., Suzuki, K., Kassai, Y., Takeshita, M., Murota, A., Kondo, Y.,…Takeuchi, T. (2018). Multi-omics monitoring of drug response in rheumatoid arthritis in pursuit of molecular remission. *Nature Communications*, *9*(1). https://doi.org/10.1038/s41467-018-05044-4

Teles, R. M., Graeber, T. G., Krutzik, S. R., Montoya, D., Schenk, M., Lee, D. J.,…Modlin, R. L. (2013). Type I interferon suppresses type II interferon-triggered human anti-mycobacterial responses. *Science*, *339*(6126), 1448-1453. https://doi.org/10.1126/science.1233665

Thair, S. A., He, Y. D., Hasin-Brumshtein, Y., Sakaram, S., Pandya, R., Toh, J.,…Sweeney, T. E. (2021). Transcriptomic similarities and differences in host response between SARS-CoV-2 and other viral infections. *iScience*, *24*(1), 101947. https://doi.org/10.1016/j.isci.2020.101947

Timmermans, S., Souffriau, J., & Libert, C. (2019). A general introduction to glucocorticoid biology. In *Frontiers in Immunology* (Vol. 10).

Torres, L. K., Pickkers, P., & van der Poll, T. (2022). Sepsis-Induced Immunosuppression. *Annu Rev Physiol*, *84*, 157-181. https://doi.org/10.1146/annurev-physiol-061121-040214

Tran, T. M., Jones, M. B., Ongoiba, A., Bijker, E. M., Schats, R., Venepally, P.,…Crompton, P. D. (2016). Transcriptomic evidence for modulation of host inflammatory responses during febrile Plasmodium falciparum malaria. *Scientific Reports*, *6*. https://doi.org/10.1038/srep31291

Tsakiroglou, M., Evans, A., & Pirmohamed, M. (2023). Leveraging transcriptomics for precision diagnosis: Lessons learned from cancer and sepsis. *Frontiers in Genetics*, *14*. https://doi.org/https://doi.org/10.3389/fgene.2023.1100352

Tsalik, E. L., Willig, L. K., Rice, B. J., Van Velkinburgh, J. C., Mohney, R. P., McDunn, J. E.,…Langley, R. J. (2015). Renal systems biology of patients with systemic inflammatory response syndrome. *Kidney International*, *88*(4). https://doi.org/10.1038/ki.2015.150

Tulzo, Y. L., Pangault, C., Amiot, L., Guilloux, V., Tribut, O., Arvieux, C.,…Drénou, B. (2004). Monocyte human leukocyte antigen-DR transcriptional downregulation by cortisol during septic shock. *American Journal of Respiratory and Critical Care Medicine*, *169*(10). https://doi.org/10.1164/rccm.200309-1329oc

Téblick, A., Gunst, J., & Van den Berghe, G. (2022). Critical Illness-induced Corticosteroid Insufficiency: What It Is Not and What It Could Be. *J Clin Endocrinol Metab*, *107*(7), 2057-2064. https://doi.org/10.1210/clinem/dgac201

Uhel, F., Azzaoui, I., Grégoire, M., Pangault, C., Dulong, J., Tadié, J. M.,…Tarte, K. (2017). Early expansion of circulating granulocytic myeloid-derived suppressor cells predicts development of nosocomial infections in patients with sepsis. *American Journal of Respiratory and Critical Care Medicine*, *196*(3). https://doi.org/10.1164/rccm.201606-1143OC

Van den Berghe, G., Téblick, A., Langouche, L., & Gunst, J. (2022). The hypothalamus-pituitary-adrenal axis in sepsis- and hyperinflammation-induced critical illness: Gaps in current knowledge and future translational research directions. *EBioMedicine*, *84*, 104284. https://doi.org/10.1016/j.ebiom.2022.104284

van der Poll, T., Shankar-Hari, M., & Wiersinga, W. J. (2021). The immunology of sepsis. In *Immunity* (Vol. 54).

Van Der Poll, T., Van De Veerdonk, F. L., Scicluna, B. P., & Netea, M. G. (2017). The immunopathology of sepsis and potential therapeutic targets. In *Nature Reviews Immunology* (Vol. 17).

Vandermosten, L., Prenen, F., Fogang, B., Dagneau de Richecour, P., Knoops, S., Donkeu, C. J.,…Van den Steen, P. E. (2023). Glucocorticoid dysfunction in children with severe malaria. *Front Immunol*, *14*, 1187196. https://doi.org/10.3389/fimmu.2023.1187196

Vandewalle, J., & Libert, C. (2020). Glucocorticoids in Sepsis: To Be or Not to Be. *Front Immunol*, *11*, 1318. https://doi.org/10.3389/fimmu.2020.01318

medRxiv preprint doi: https://doi.org/10.1101/2023.05.10.23289779; this version posted November 4, 2024. The copyright holder for this preprint (which was not certified by peer review) is the author/funder, who has granted medRxiv a license to display the preprint in perpetuity. All rights reserved. No reuse allowed without permission.

Vangeti, S., Falck-Jones, S., Yu, M., Österberg, B., Liu, S., Asghar, M.,…Smed-Sörensen, A. (2023). Human influenza virus infection elicits distinct patterns of monocyte and dendritic cell mobilization in blood and the nasopharynx. *Elife*, *12*. https://doi.org/10.7554/eLife.77345

Venet, F., Demaret, J., Gossez, M., & Monneret, G. (2021). Myeloid cells in sepsis-acquired immunodeficiency. *Ann N Y Acad Sci*, *1499*(1), 3-17. https://doi.org/10.1111/nyas.14333

Venet, F., & Monneret, G. (2018). Advances in the understanding and treatment of sepsis-induced immunosuppression. *Nat Rev Nephrol*, *14*(2), 121-137. https://doi.org/10.1038/nrneph.2017.165

Venet, F., Plassais, J., Textoris, J., Cazalis, M. A., Pachot, A., Bertin-Maghit, M.,…Tissot, S. (2015). Low-dose hydrocortisone reduces norepinephrine duration in severe burn patients: A randomized clinical trial. *Critical Care*, *19*(1). https://doi.org/10.1186/s13054-015-0740-0

Venkatesh, B., Finfer, S., Cohen, J., Rajbhandari, D., Arabi, Y., Bellomo, R.,…Myburgh, J. (2018). Adjunctive Glucocorticoid Therapy in Patients with Septic Shock. *N Engl J Med*, *378*(9), 797-808. https://doi.org/10.1056/NEJMoa1705835

Vettorazzi, S., Nalbantoglu, D., Gebhardt, J. C. M., & Tuckermann, J. (2021). A guide to changing paradigms of glucocorticoid receptor function—a model system for genome regulation and physiology. *FEBS Journal*. https://doi.org/10.1111/febs.16100

Vieira Da Silva Pellegrina, D., Severino, P., Barbeiro, H. V., Andreghetto, F. M., Velasco, I. T., Possolo De Souza, H.,…Pinheiro Da Silva, F. (2015). Septic shock in advanced age: Transcriptome analysis reveals altered molecular signatures in neutrophil granulocytes. *PLoS ONE*, *10*(6). https://doi.org/10.1371/journal.pone.0128341

Wang, C., Nanni, L., Novakovic, B., Megchelenbrink, W., Kuznetsova, T., Stunnenberg, H. G.,…Logie, C. (2019). Extensive epigenomic integration of the glucocorticoid response in primary human monocytes and in vitro derived macrophages. *Scientific Reports*, *9*(1). https://doi.org/10.1038/s41598-019-39395-9

Wang, T., Zhang, X., Liu, Z., Yao, T., Zheng, D., Gan, J.,…Sun, J. (2021). Single-cell RNA sequencing reveals the sustained immune cell dysfunction in the pathogenesis of sepsis secondary to bacterial pneumonia. *Genomics*, *113*(3). https://doi.org/10.1016/j.ygeno.2021.01.026

Wang, Y., Schughart, K., Pelaia, T. M., Chew, T., Kim, K., Karvunidis, T.,…Shojaei, M. (2022). Blood transcriptome responses in patients correlate with severity of COVID-19 disease. *Front Immunol*, *13*, 1043219. https://doi.org/10.3389/fimmu.2022.1043219

Washburn, M. L., Wang, Z., Walton, A. H., Goedegebuure, S. P., Figueroa, D. J., Van Horn, S.,…Hotchkiss, R. S. (2019). T Cell– and Monocyte-Specific RNA-Sequencing Analysis in Septic and Nonseptic Critically Ill Patients and in Patients with Cancer. *The Journal of Immunology*, *203*(7). https://doi.org/10.4049/jimmunol.1900560

Weller, P. F. (2016). LEUKOCYTE LIPID BODIES - STRUCTURE AND FUNCTION AS "EICOSASOMES". *Transactions of the American Clinical and Climatological Association*, *127*.

Wen, M., Cai, G., Ye, J., Liu, X., Ding, H., & Zeng, H. (2020). Single-cell transcriptomics reveals the alteration of peripheral blood mononuclear cells driven by sepsis. *Annals of Translational Medicine*, *8*(4). https://doi.org/10.21037/atm.2020.02.35

Westra, H. J., Peters, M. J., Esko, T., Yaghootkar, H., Schurmann, C., Kettunen, J.,…Franke, L. (2013). Systematic identification of trans eQTLs as putative drivers of known disease associations. *Nature Genetics*, *45*(10). https://doi.org/10.1038/ng.2756

Wickham, H. (2016). *ggplot2: Elegant Graphics for Data Analysis. Springer-Verlag New York* (Vol. 35).

Wickham, H., Bryan, J., Rstudio, Kalicinski, M., Valery, K., Leitienne, C.,…Miller, E. (2019). readxl: Read Excel files. R package version 1.3.1. In *https://CRAN.R-project.org/package=readxl*.

Wiersinga, W. J., & van der Poll, T. (2022). Immunopathophysiology of human sepsis. *EBioMedicine*, *86*, 104363. https://doi.org/10.1016/j.ebiom.2022.104363

Wittenbrink, N., Ananthasubramaniam, B., Münch, M., Koller, B., Maier, B., Weschke, C.,…Kramer, A. (2018). High-accuracy determination of internal circadian time from a single blood sample. *Journal of Clinical Investigation*, *128*(9). https://doi.org/10.1172/JCI120874

medRxiv preprint doi: https://doi.org/10.1101/2023.05.10.23289779; this version posted November 4, 2024. The copyright holder for this preprint (which was not certified by peer review) is the author/funder, who has granted medRxiv a license to display the preprint in perpetuity. All rights reserved. No reuse allowed without permission.

Wong, H. R., Cvijanovich, N. Z., Allen, G. L., Thomas, N. J., Freishtat, R. J., Anas, N.,…Zimmerman, J. J. (2014). Corticosteroids are associated with repression of adaptive immunity gene programs in pediatric septic shock. *American Journal of Respiratory and Critical Care Medicine*, *189*(8). https://doi.org/10.1164/rccm.201401-0171OC

Wong, H. R., Cvijanovich, N. Z., Anas, N., Allen, G. L., Thomas, N. J., Bigham, M. T.,…Lindsell, C. J. (2015). Developing a clinically feasible personalized medicine approach to pediatric septic shock. *Am J Respir Crit Care Med*, *191*(3), 309-315. https://doi.org/10.1164/rccm.201410-1864OC

Wong, H. R., Hart, K. W., Lindsell, C. J., & Sweeney, T. E. (2021). External Corroboration That Corticosteroids May Be Harmful to Septic Shock Endotype A Patients. *Crit Care Med*, *49*(1), e98-e101. https://doi.org/10.1097/ccm.0000000000004709

Wright, V. J., Herberg, J. A., Kaforou, M., Shimizu, C., Eleftherohorinou, H., Shailes, H.,…Levin, M. (2018). Diagnosis of Kawasaki Disease Using a Minimal Whole-Blood Gene Expression Signature. *JAMA Pediatrics*, *172*(10). https://doi.org/10.1001/jamapediatrics.2018.2293

Xiao, W., Mindrinos, M. N., Seok, J., Cuschieri, J., Cuenca, A. G., Gao, H.,…Wong, W. H. (2011). A genomic storm in critically injured humans. *Journal of Experimental Medicine*, *208*(13). https://doi.org/10.1084/jem.20111354

Yang-Yen, H. F., Chambard, J. C., Sun, Y. L., Smeal, T., Schmidt, T. J., Drouin, J., & Karin, M. (1990). Transcriptional interference between c-Jun and the glucocorticoid receptor: mutual inhibition of DNA binding due to direct protein-protein interaction. *Cell*, *62*(6), 1205-1215. https://doi.org/10.1016/0092-8674(90)90396-v

Zhai, Y., Franco, L. M., Atmar, R. L., Quarles, J. M., Arden, N., Bucasas, K. L.,…Couch, R. B. (2015). Host Transcriptional Response to Influenza and Other Acute Respiratory Viral Infections – A Prospective Cohort Study. *PLoS Pathogens*, *11*(6). https://doi.org/10.1371/journal.ppat.1004869

A

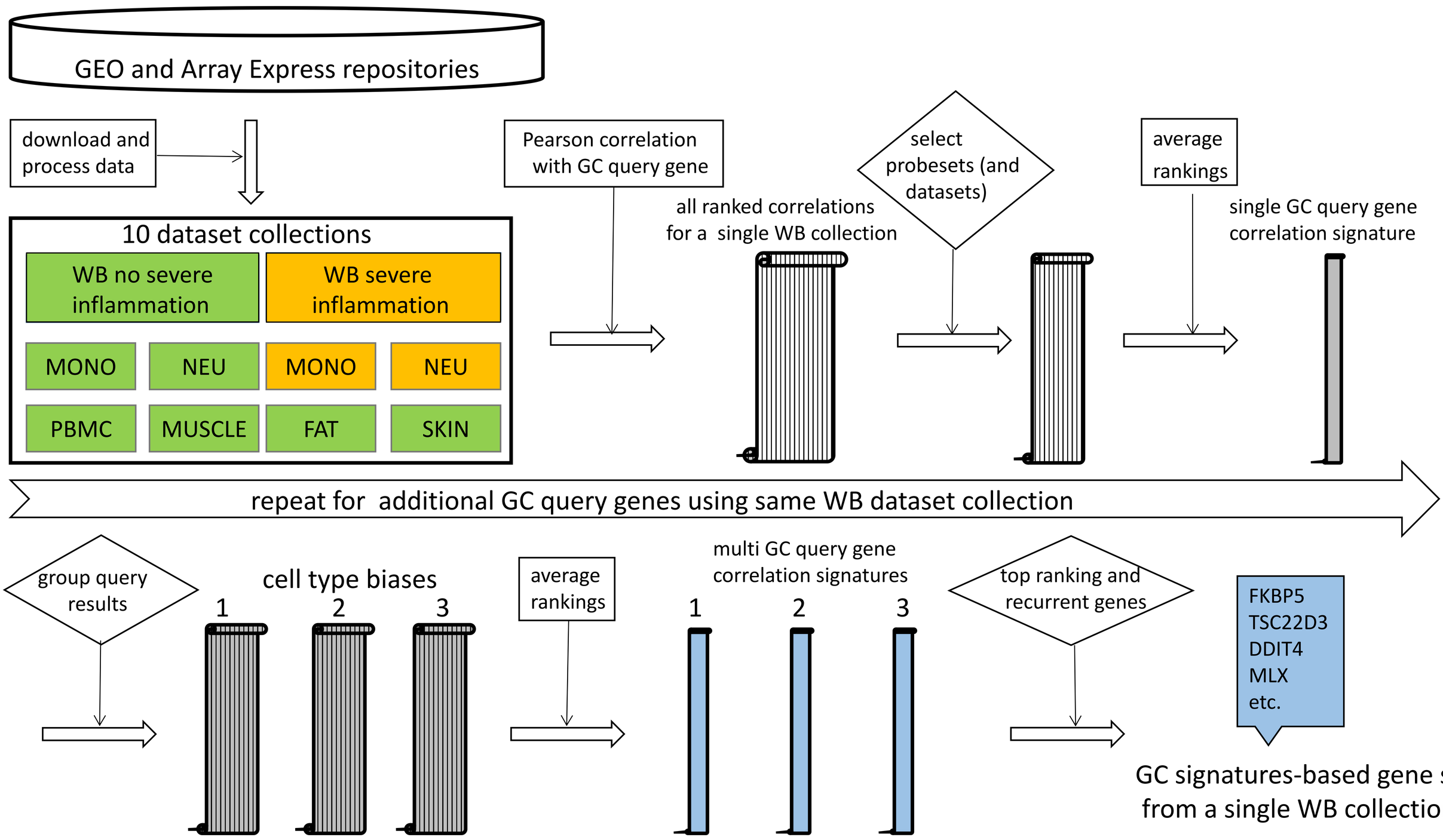

B

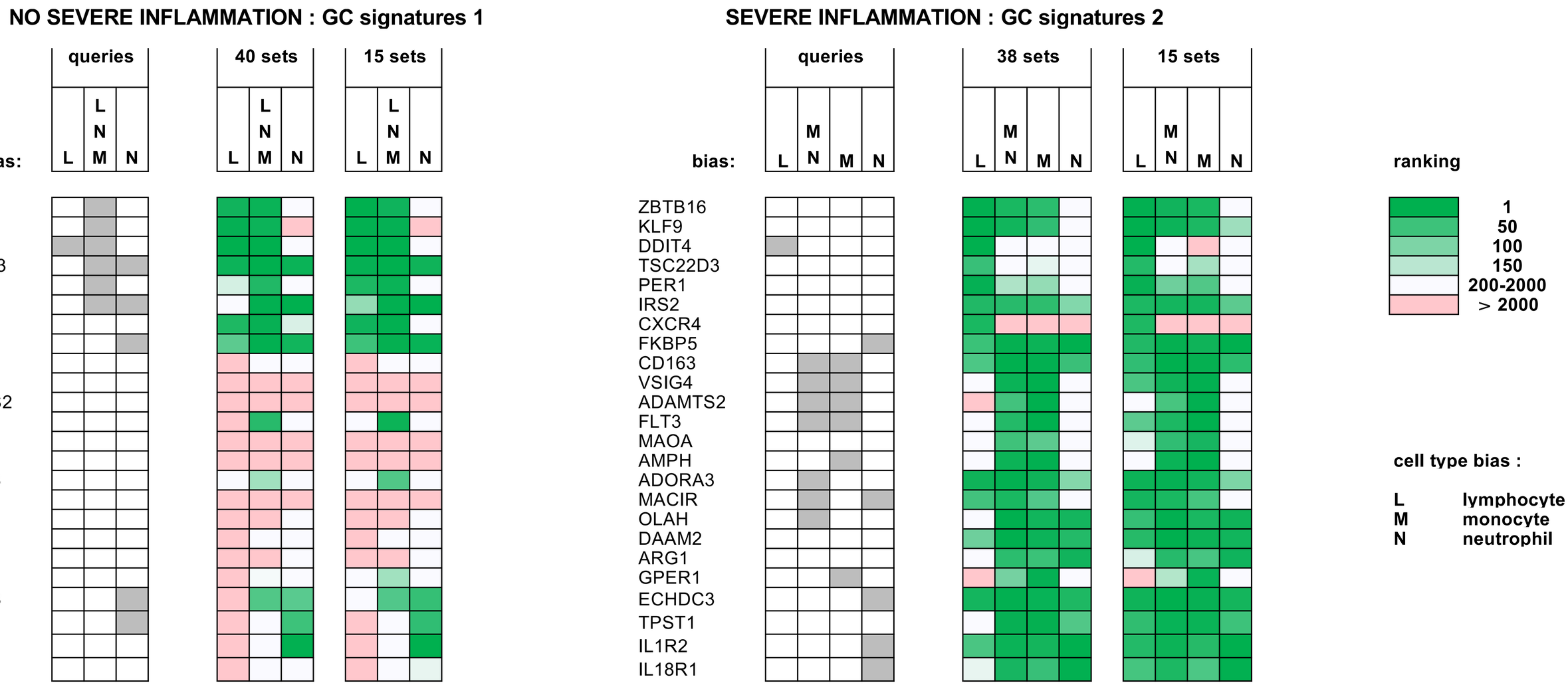

C

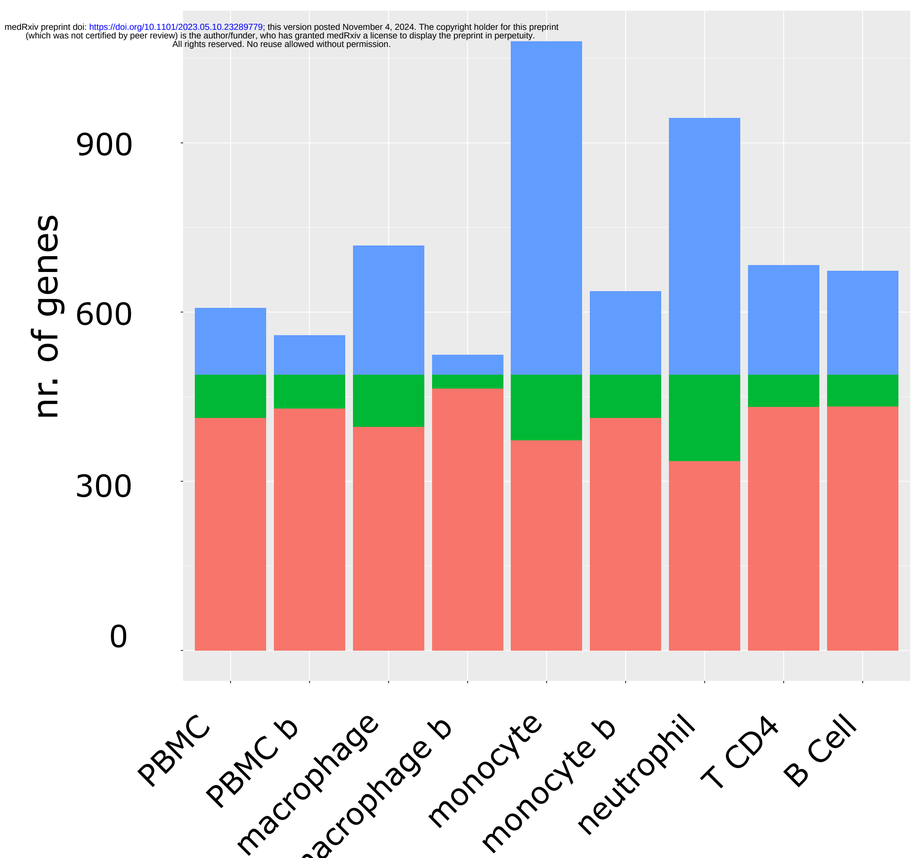

D

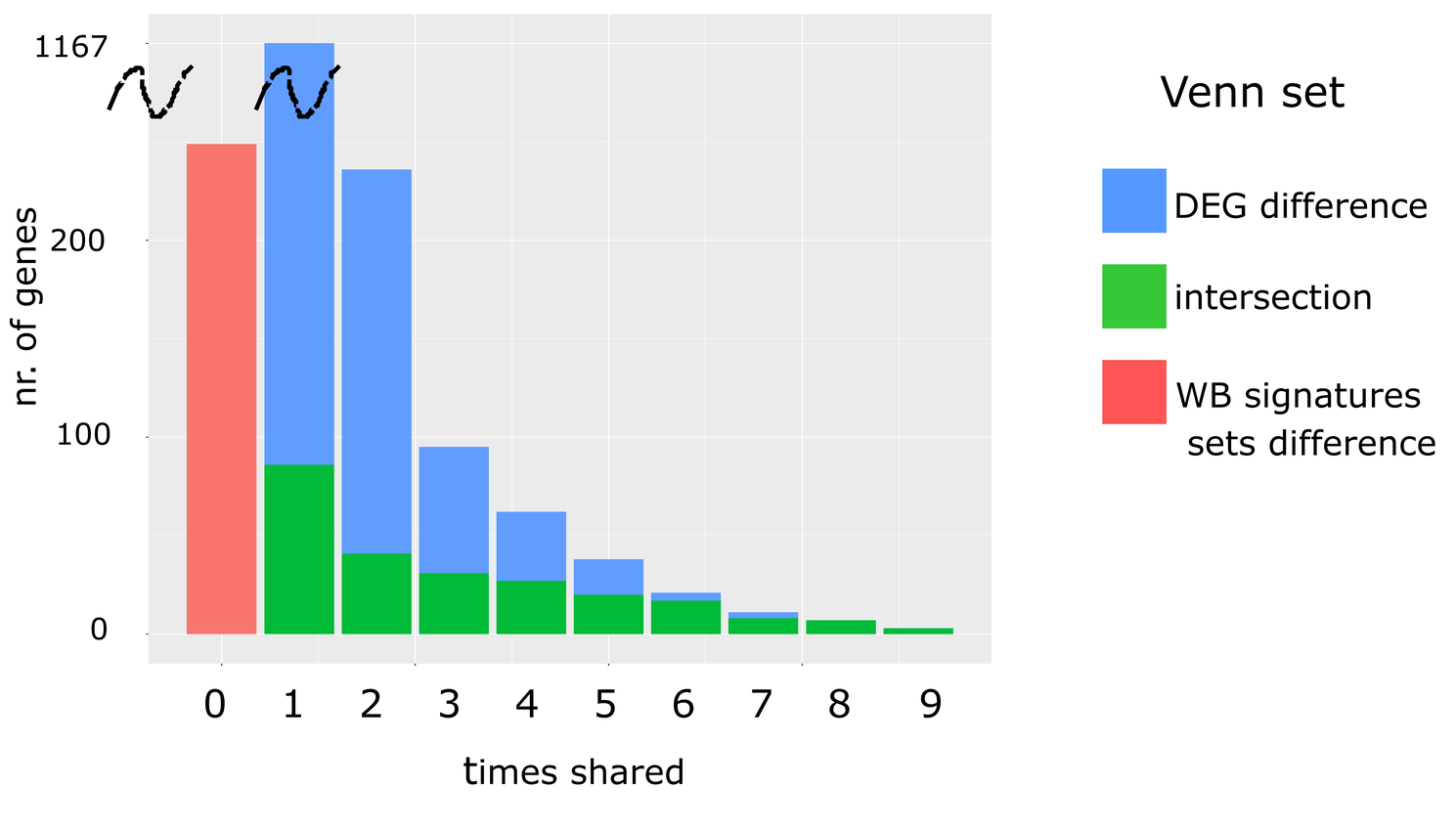

medRxiv preprint doi: https://doi.org/10.1101/2023.05.10.23289779; this version posted November 4, 2024. The copyright holder for this preprint (which was not certified by peer review) is the author/funder, who has granted medRxiv a license to display the preprint in perpetuity.
All rights reserved. No reuse allowed without permission.

A

query	high in GC sign.	biomarker gene set	gene / alias	protein / function	functional category
1	1 and 2	GC-1	ZBTB16 (PLZF)	transcription factor	regulation of gene expression
1	1 and 2	GC-1	KLF9	transcription factor	regulation of gene expression
1 and 2	1 and 2	GC-1	DDIT4 (REDD1)	inhibitory in mTOR signaling	intracellular signaling
1	1 and 2	GC-1	TSC22D3 (GILZ)	inhibitory in NF-kB and MAPK signaling	regulation of gene expression
1	1 and 2	GC-1	PER1	repression of transcription by CLOCK/BMAL1	regulation of gene expression
1	1 and 2	GC-1	IRS2	signaling adaptor	intracellular signaling
	1 and 2	GC-1	CXCR4	CXCL12 GPCR	chemotaxis
2	1 and 2		FKBP5 (FKBP51)	GC receptor complex component	regulation of gene expression
2	2		CD163	scavenger receptor	endocytosis
2	2	GC-2	VSIG4 (CRig)	C3b receptor	phagocytosis of apoptotic cells
2	2	GC-2	ADAMTS2	procollagen proteinase	extracellular matrix
2	1 and 2	GC-2	FLT3	receptor tyrosine kinase	
	2	GC-2	MAOA	monoamine oxidase A	
2	2	GC-2	AMPH	amphiphysin	phagocytosis and cell motility
2	1 and 2	GC-2	ADORA3	adenosine GPCR, Gi coupled	
2	2	GC-2	MACIR (C5orf30)	macrophage immunometabolism regulator	
2	2	GC-2	OLAH (THEDC1)	thioesterase 2	
2	2	GC-2	DAAM2	actin nucleation	phagocytosis and cell motility
	2		ARG1	arginase 1	

B

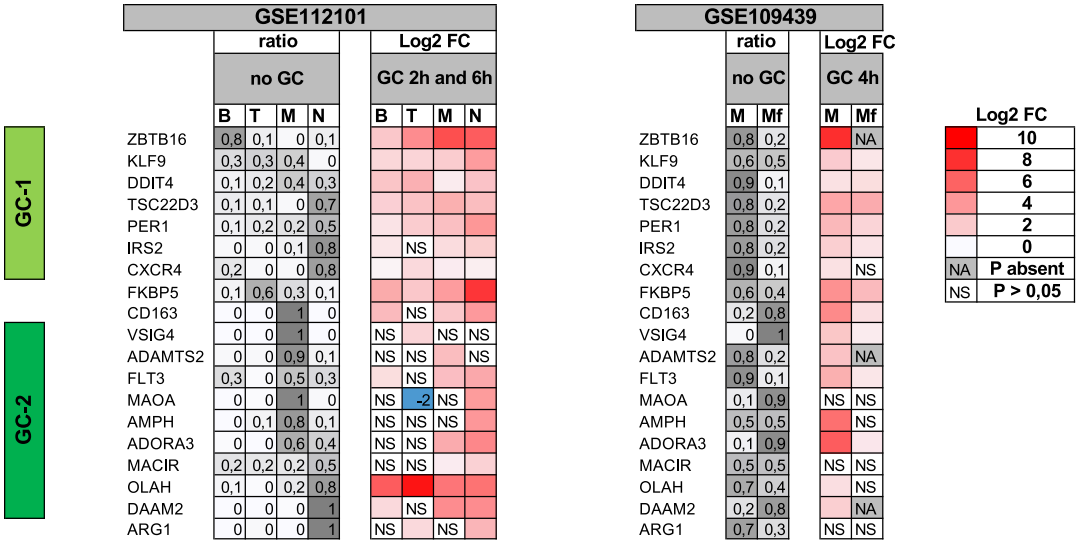

C

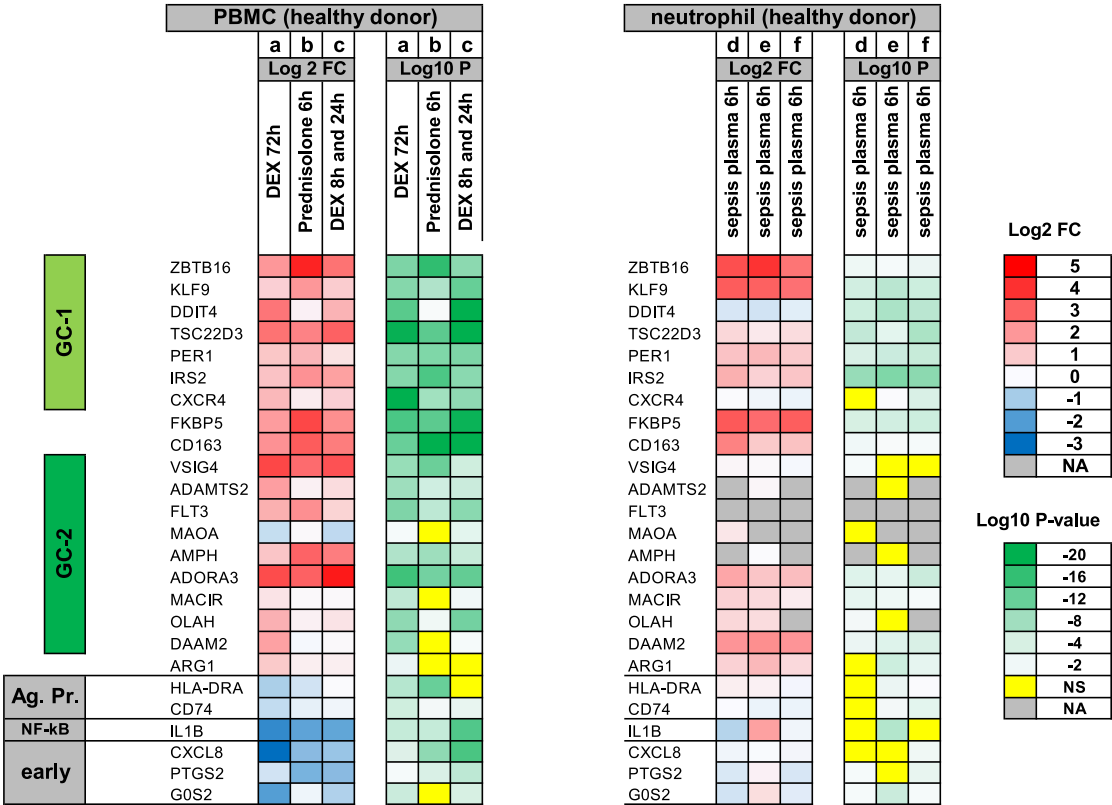

medRxiv preprint doi: https://doi.org/10.1101/2023.05.10.23289779; this version posted November 4, 2024. The copyright holder for this preprint (which was not certified by peer review) is the author/funder, who has granted medRxiv a license to display the preprint in perpetuity.
All rights reserved. No reuse allowed without permission.

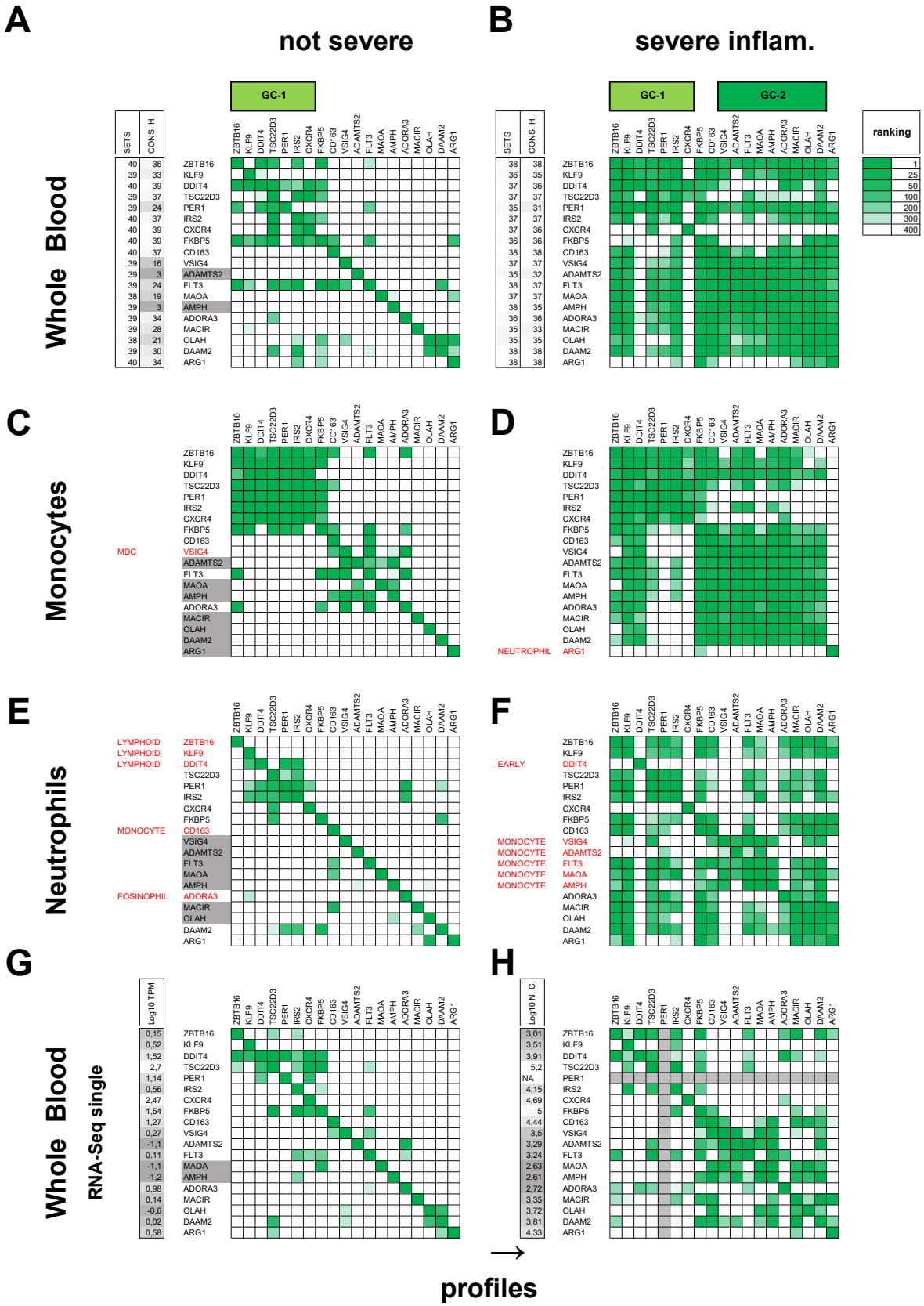

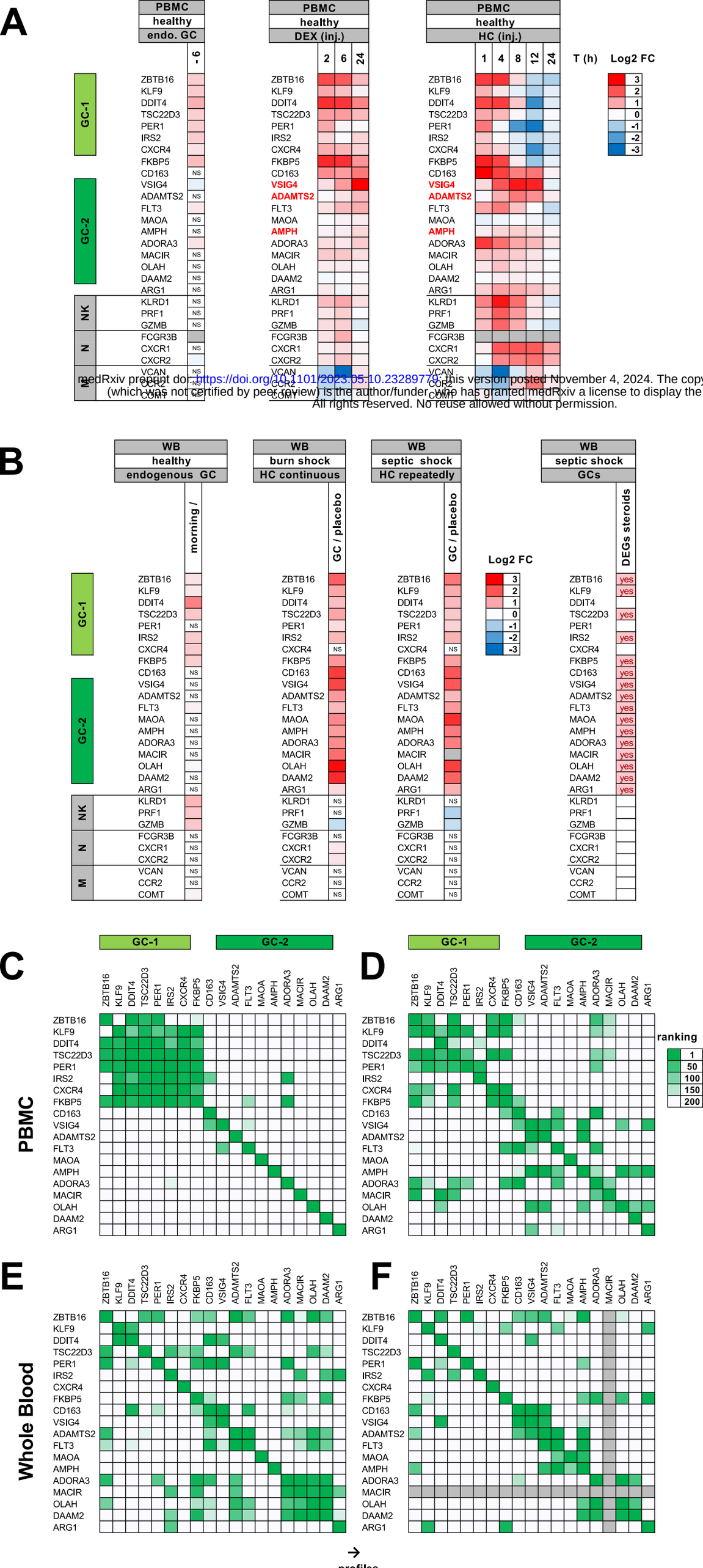

medRxiv preprint doi: https://doi.org/10.1101/2023.05.10.23289778; this version posted November 4, 2024. The copyright holder for this preprint (which was not certified by peer review) is the author/funder, who has granted medRxiv a license to display the preprint in perpetuity.
All rights reserved. No reuse allowed without permission.

neutrophil

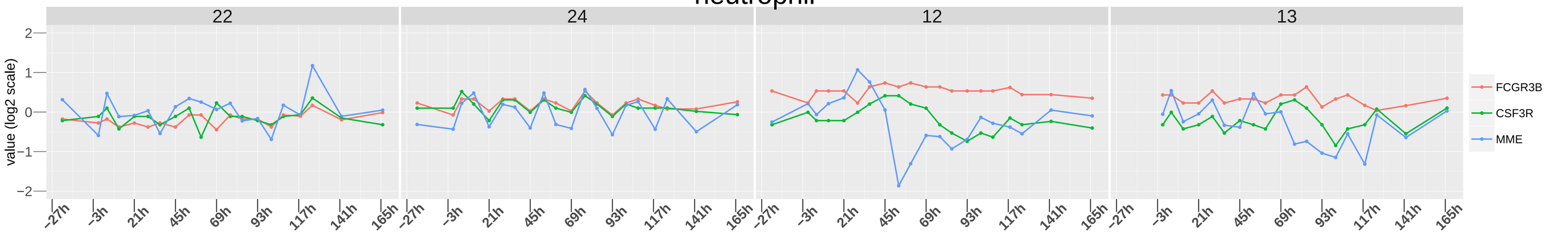

classical monocyte

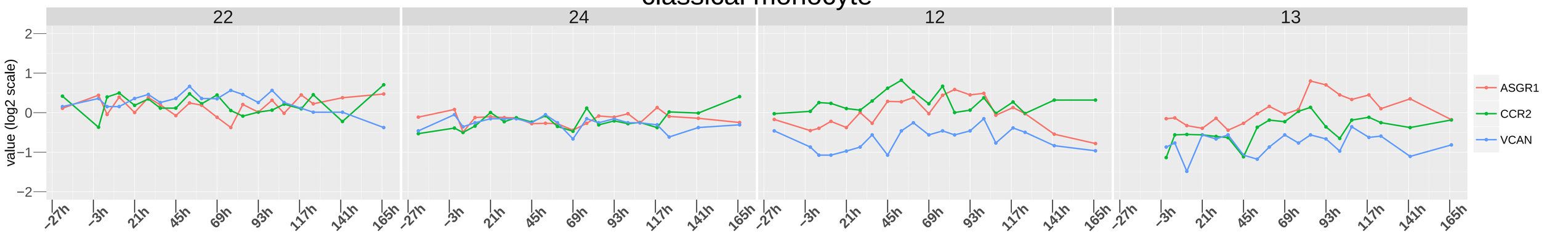

non−classical / intermediate monocyte (mainly)

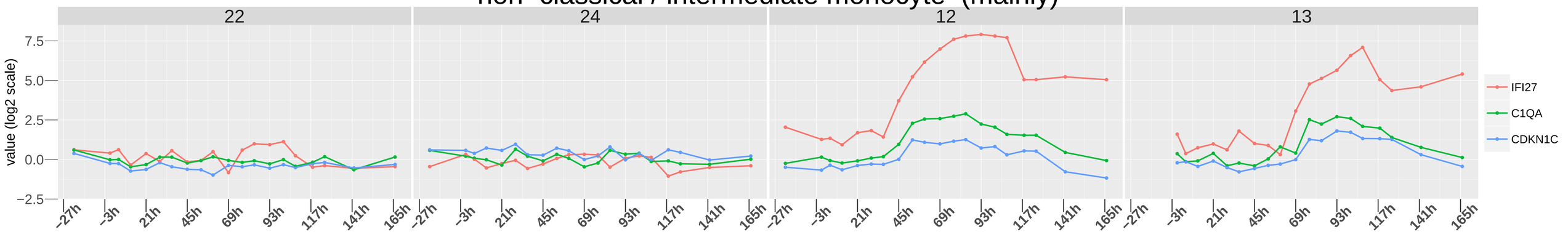

induced by IFN, and NF−kB dependent (IL1B)

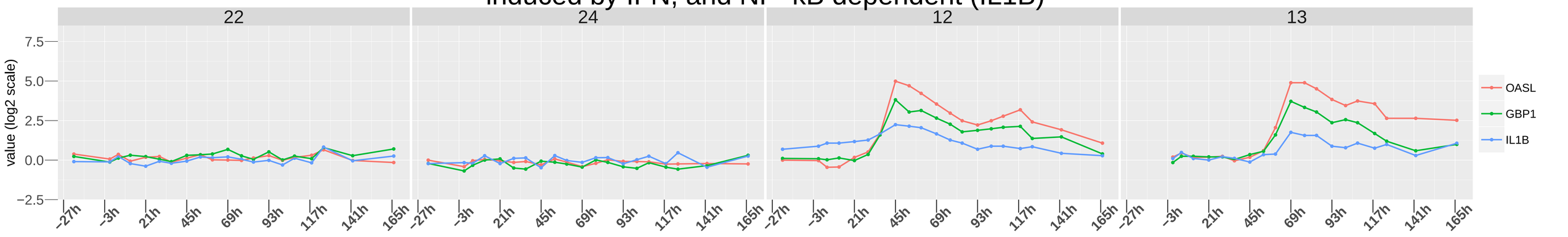

induced by GC

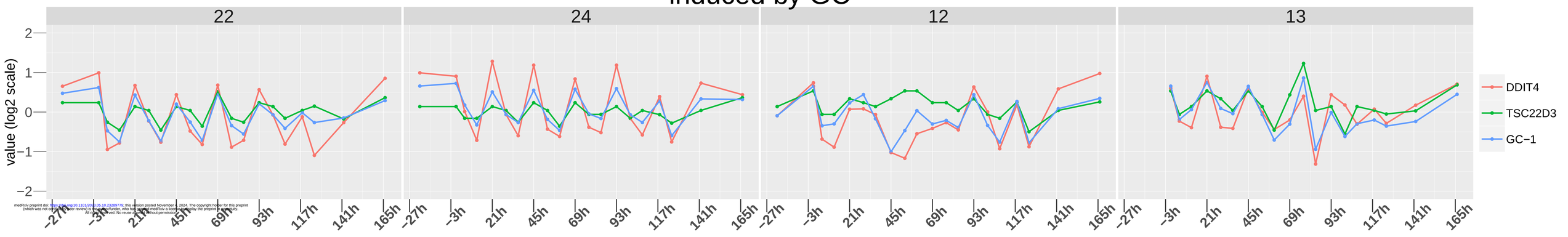

medRxiv preprint doi: https://doi.org/10.1101/2024.05.10.23289770; this version posted November 4, 2024. The copyright holder for this preprint (which was not certified by peer review) is the author/funder, who has granted medRxiv a license to display the preprint in perpetuity.
All rights reserved. No reuse allowed without permission.

GC (circadian) and inflammation

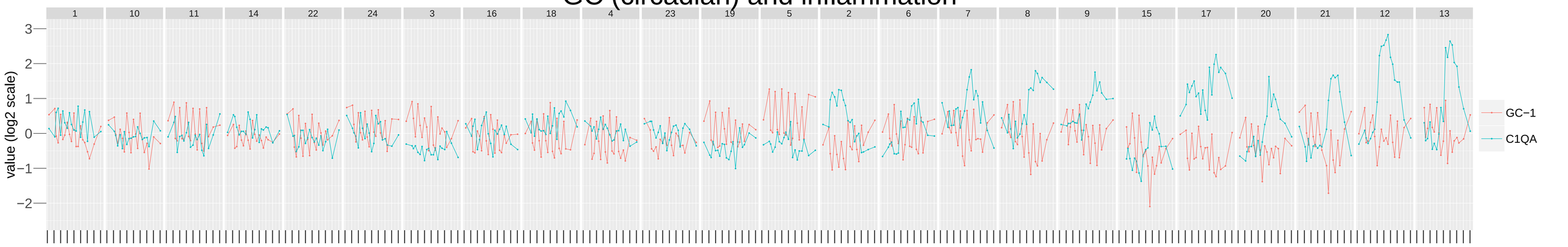

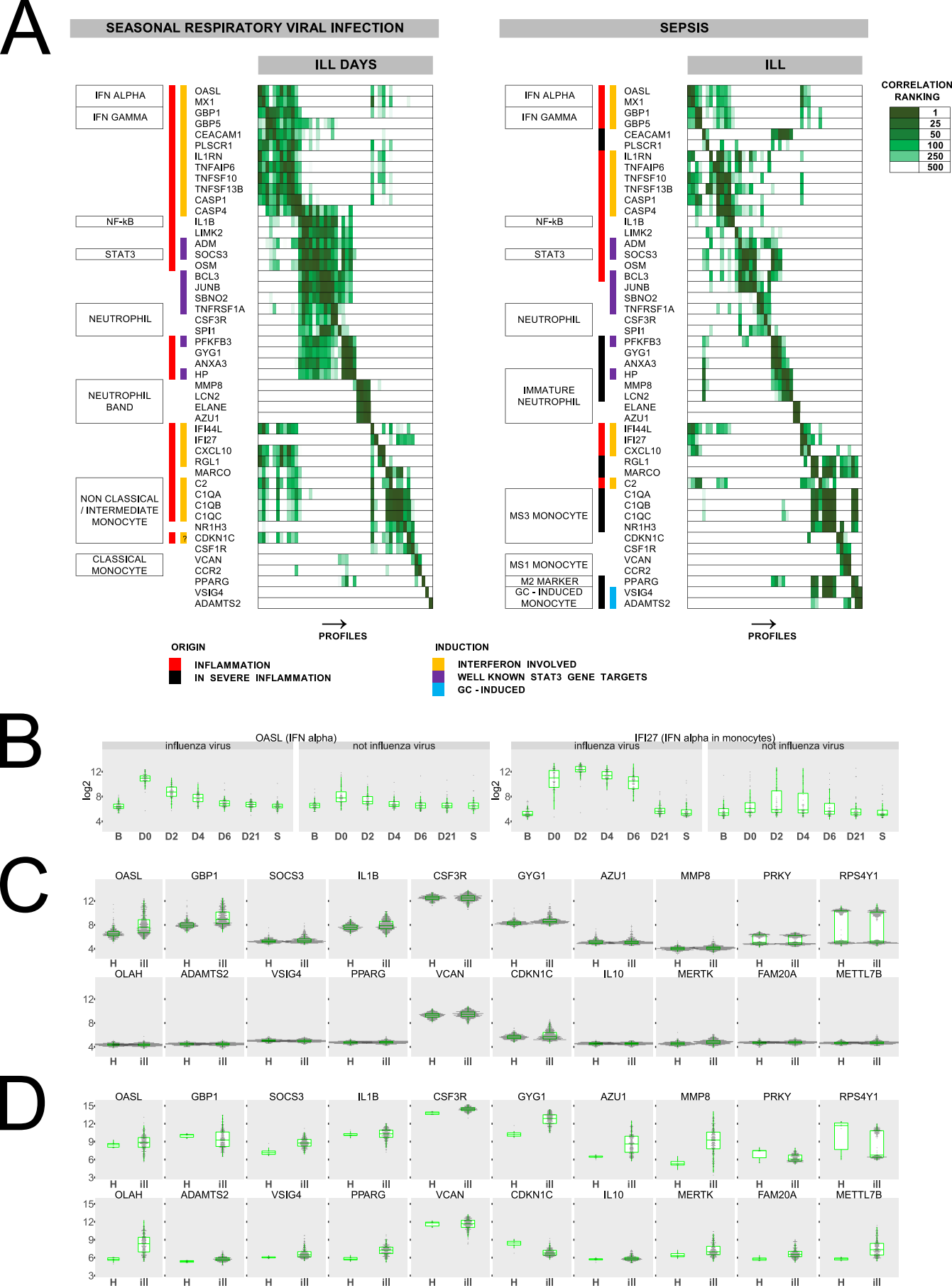
A
SEASONAL RESPIRATORY VIRAL INFECTION
SEPSIS
ILL DAYS
ILL
CORRELATION RANKING
1
25
50
100
250
500
IFN ALPHA
IFN GAMMA
NF-kB
STAT3
NEUTROPHIL
NEUTROPHIL BAND
NON CLASSICAL / INTERMEDIATE MONOCYTE
CLASSICAL MONOCYTE
IMMATURE NEUTROPHIL
MS3 MONOCYTE
MS1 MONOCYTE
M2 MARKER
GC - INDUCED MONOCYTE
OASL
MX1
GBP1
GBP5
CEACAM1
PLSCR1
IL1RN
TNFAIP6
TNFSF10
TNFSF13B
CASP1
CASP4
IL1B
LIMK2
ADM
SOCS3
OSM
BCL3
JUNB
SBNO2
TNFRSF1A
CSF3R
SPI1
PFKFB3
GYG1
ANXA3
HP
MMP8
LCN2
ELANE
AZU1
IFI44L
IFI27
CXCL10
RGL1
MARCO
C2
C1QA
C1QB
C1QC
NR1H3
CDKN1C
CSF1R
VCAN
CCR2
PPARG
VSIG4
ADAMTS2
PROFILES
ORIGIN
INFLAMMATION
IN SEVERE INFLAMMATION
INDUCTION
INTERFERON INVOLVED
WELL KNOWN STAT3 GENE TARGETS
GC - INDUCED
B
OASL (IFN alpha)
IFI27 (IFN alpha in monocytes)
influenza virus
not influenza virus
log2
B D0 D2 D4 D6 D21 S
C
OASL GBP1 SOCS3 IL1B CSF3R GYG1 AZU1 MMP8 PRKY RPS4Y1
OLAH ADAMTS2 VSIG4 PPARG VCAN CDKN1C IL10 MERTK FAM20A METTL7B
H ill
D
OASL GBP1 SOCS3 IL1B CSF3R GYG1 AZU1 MMP8 PRKY RPS4Y1
OLAH ADAMTS2 VSIG4 PPARG VCAN CDKN1C IL10 MERTK FAM20A METTL7B
H ill

medRxiv preprint doi: https://doi.org/10.1101/2023.05.10.23289779; this version posted November 4, 2024. The copyright holder for this preprint (which was not certified by peer review) is the author/funder, who has granted medRxiv a license to display the preprint in perpetuity.
All rights reserved. No reuse allowed without permission.

HOMEOSTASIS

ZBTB16
KLF9
TSC22D3
PER1
IRS2

DDIT4
CXCR4
GPER1
ECHDC3 ?
IL1R2
FKBP5
FLT3

GC

TSC22D3
PER1
IRS2
DDIT4 ?
CXCR4 ?
VSIR

ECHDC3
IL1R2
FKBP5
IRAK3
DAAM2

GC

developmental cytokines and induction by GC

ILs,
IFNs,
CSFs,
TNF

INFLAMMATION

OASL etc.
GBP2 etc.
IL1B ? (E)
CASP1 etc.
FCGR1A/B/C

IFI27
CXCL9/10/11
PLAC8
BLVRA
C1QA/B/C (I/NC)
C2 (I/NC)
TCN2 (I/NC))
RGL1

NAMPT
SOD2
ADM
GK
SOCS3 ? (E)
OSM ? (E)
SLC2A3
PFKFB3

OASL etc.
GBP2 etc.
IL1B
CASP1 etc.
FCGR1A/B/C

CEACAM1

NAMPT
SOD2
ADM
GK
SOCS3 *
OSM *
SLC2A3
PFKFB3

HK3
GYG1
IRAK3
HP

inflammatory cytokines (eg IFN and known STAT3 - dependent induction)

SYSTEMIC DAMP / MAMP

SYSTEMIC DAMP / MAMP

SEVERE INFLAMMATION

OASL etc.
GBP2 etc.
IL1B ? (E)
CASP1 etc.
IFI27
CXCL9/10/11
BLVRA
C2 (I/NC)

NAMPT
HIF1A
SOD2
GK
SOCS3
OSM ? (E)
SLC2A3
PFKFB3

OASL etc.
GBP2 etc.
IL1B
CASP1 etc.
FCGR1A/B/C

NAMPT
HIF1A ?
SOD2
ADM
GK

A

B

GYG1
PGD
LDHA
IDH1
PPARG
MERTK

HP
RETN (MS1)
ADM
FCGR1/A/B/C
PLAC8
EDNRB

LYVE1 (MFL)
OLFML2B (MFL)
C1QA/B/C (MFL)
TCN2 (MFL))
RGL1 (MFL)

FAM20A
METTL7B
ITGA7
CYP19A1

ZBTB16
KLF9
TSC22D3
PER1
IRS2
DDIT4
CXCR4
GPER1

ECHDC3
FKBP5
CD163
ADORA3
MACIR
OLAH
DAAM2
MAOA

VSIG4 (MFL)
MFGE8
ADAMTS2
FLT3
AMPH
IL1R2 (MS1)
IL18R1 ?
IRAK3

X

GC

SOCS3
OSM *
SLC2A3
PFKFB3
HK3
GYG1
PGD
LDHA
MERTK

IL1R2
Il18R1
IRAK3
PFKFB2
ARG1

AZU1 (IM)
ELANE (IM)

MMP8 (IM)
HP (IM)
RETN (IM)
CEACAM1
PLAC8

FAM20A
METTL7B
ITGA7
CYP19A1
GPR137B
VWA5A

ZBTB16
KLF9
TSC22D3
PER1
IRS2
CXCR4 ?
VSIR

ECHDC3
FKBP5
CD163
ADORA3
MACIR
OLAH
DAAM2

IL1R2
IL18R1
IRAK3
PFKFB2
ARG1

inflammatory cytokines (eg IFN and known STAT3 - dependent induction), and induction by GC

band / myelocyte

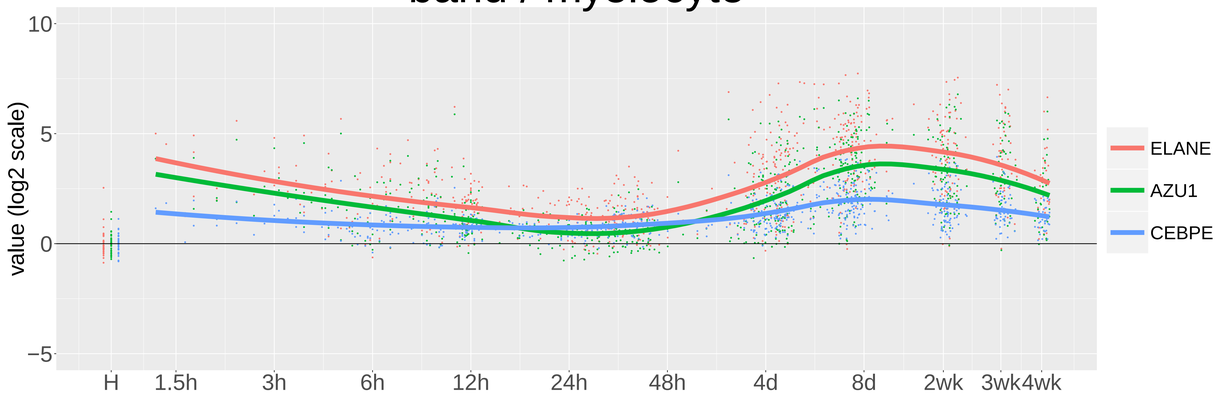

band / metamyelocyte (and induced)

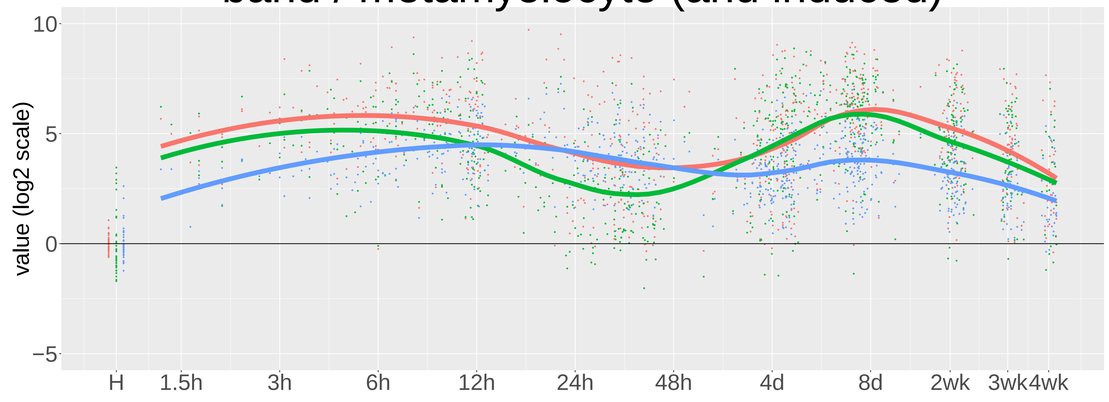

neutrophil

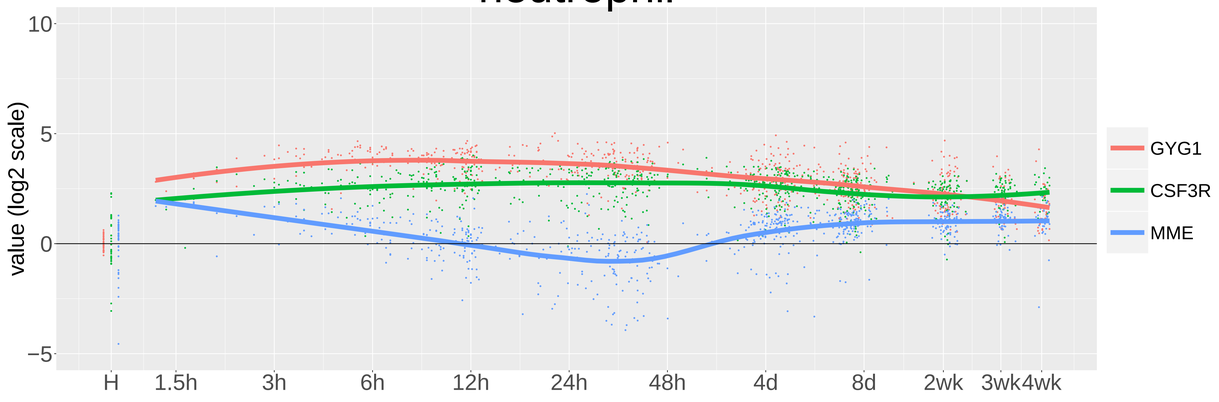

monocyte

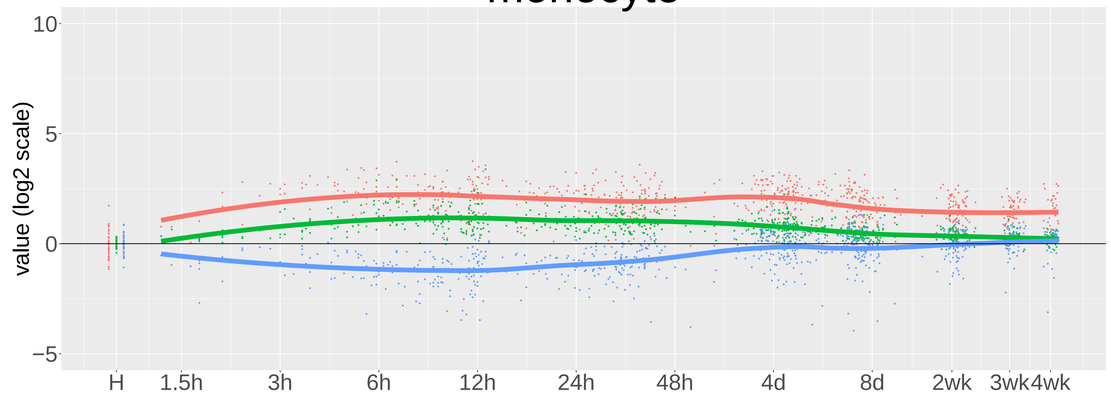

neutrophil (genes induced by GC)

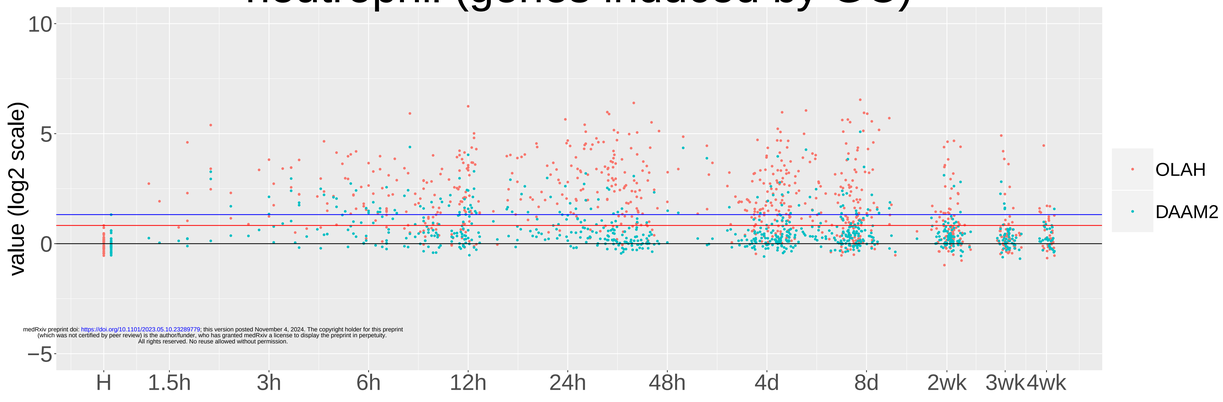

medRxiv preprint doi: https://doi.org/10.1101/2023.05.10.23289779; this version posted November 4, 2024. The copyright holder for this preprint (which was not certified by peer review) is the author/funder, who has granted medRxiv a license to display the preprint in perpetuity.
All rights reserved. No reuse allowed without permission.

monocyte (genes induced by GC)

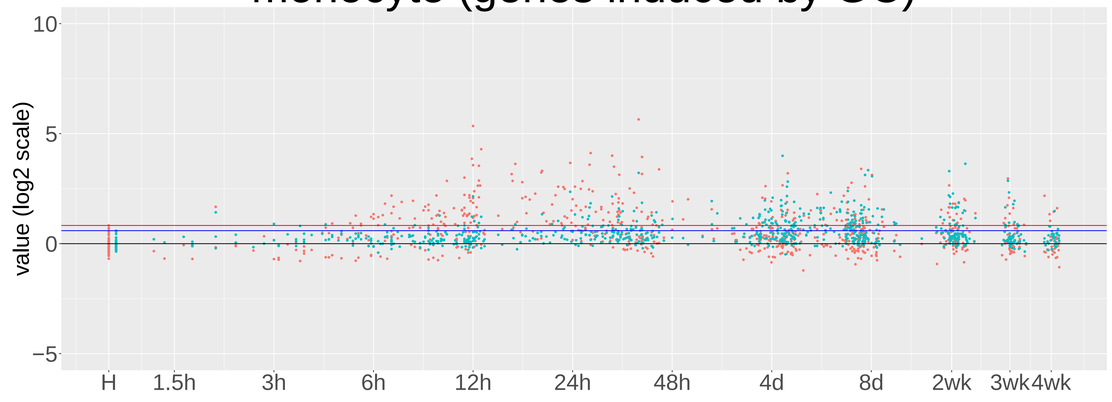

modules / set

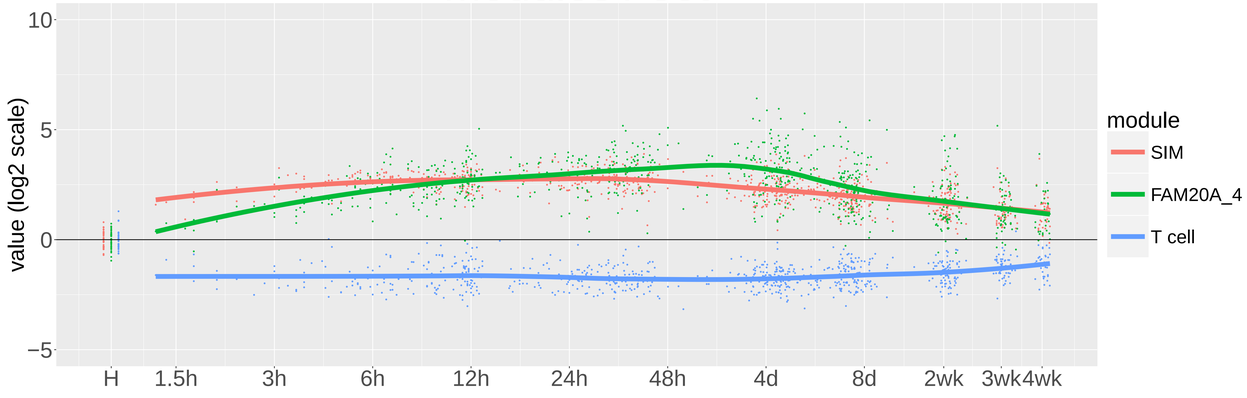

modules / set

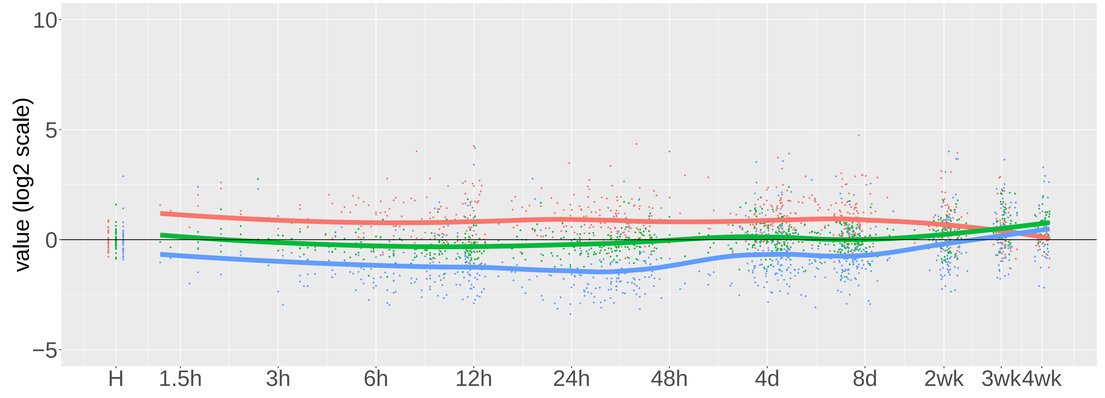

A

BURN Shock

T cell

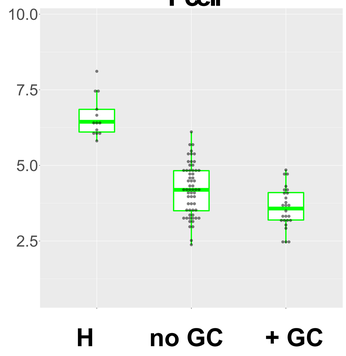

SIM

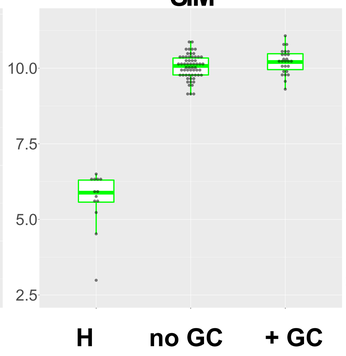

FAM20A (4)

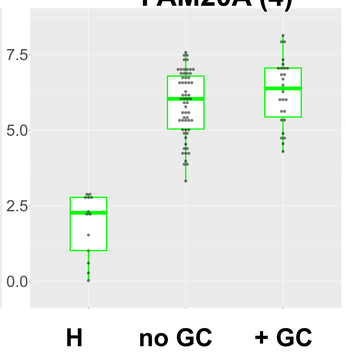

GC - 2

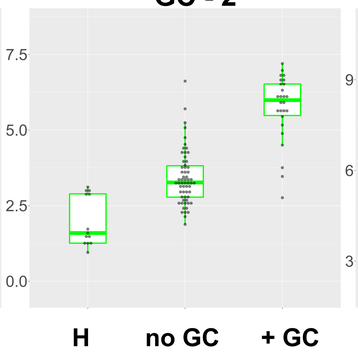

GC - 1

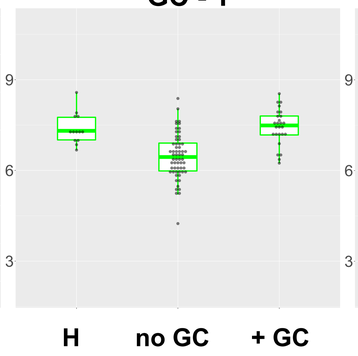

IFN gamma

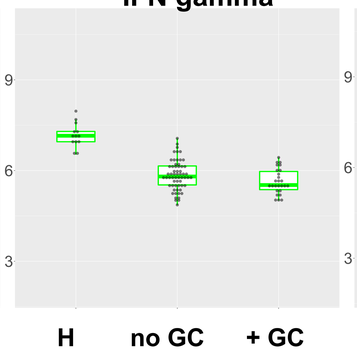

IFN alpha

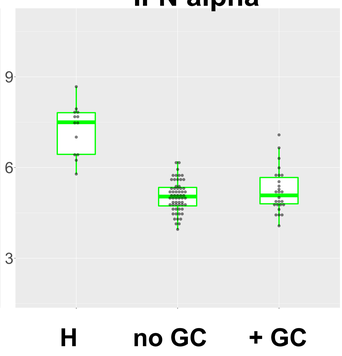

B

SEPTIC Shock

T cell

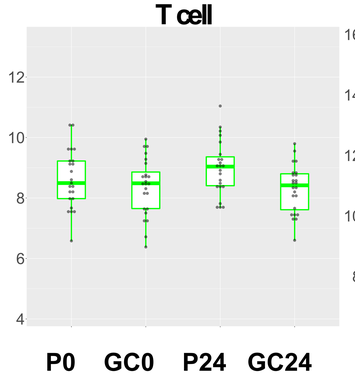

SIM

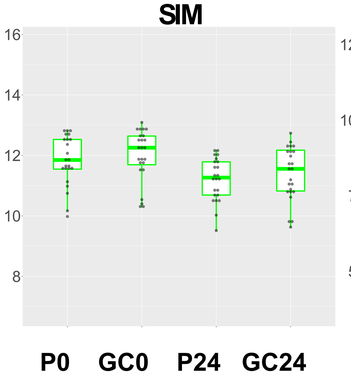

FAM20A (4)

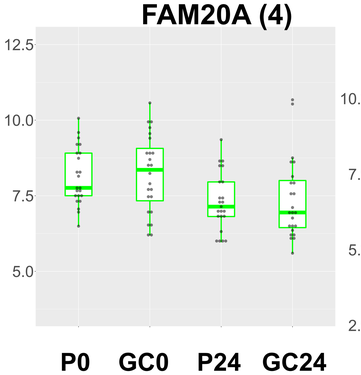

GC - 2

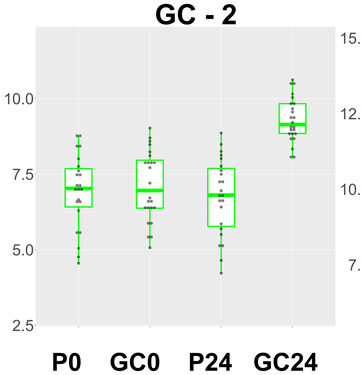

GC - 1

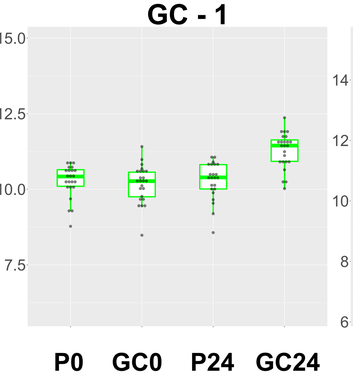

IFN gamma

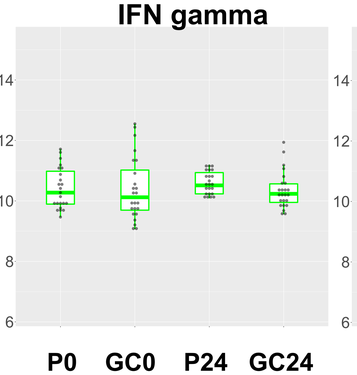

IFN alpha

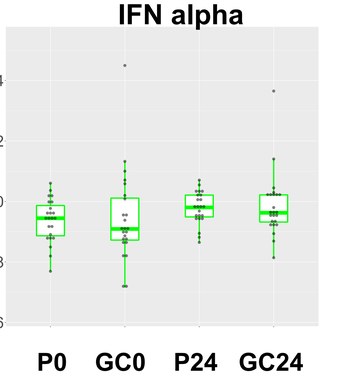

C

SLE

T cell

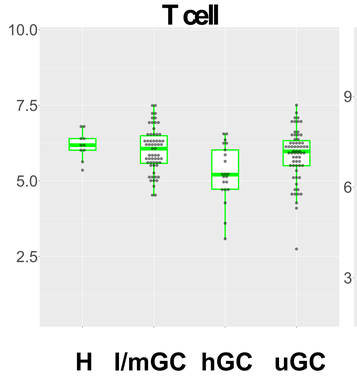

SIM

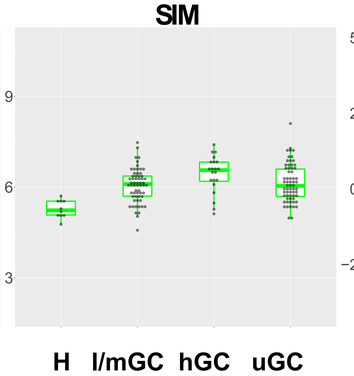

FAM20A (4)

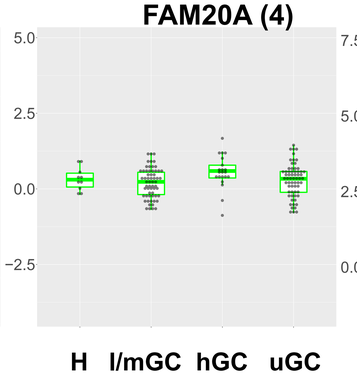

GC - 2

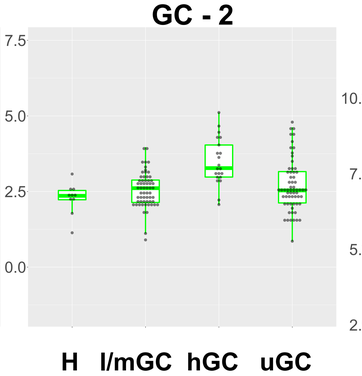

GC - 1

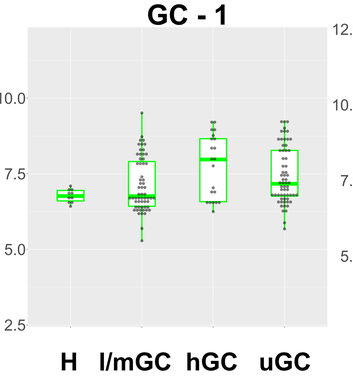

IFN gamma

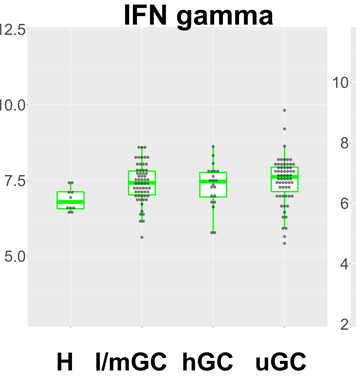

IFN alpha

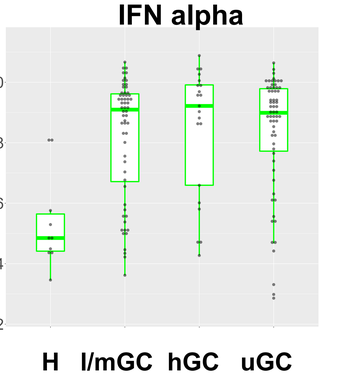

D

RA

T cell

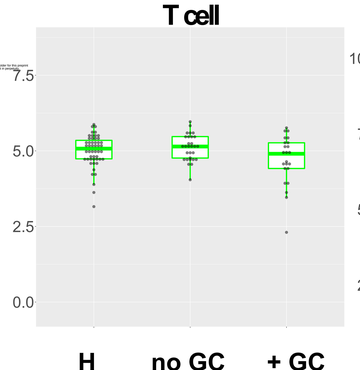

SIM

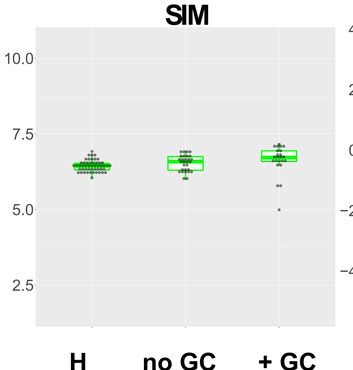

FAM20A (4)

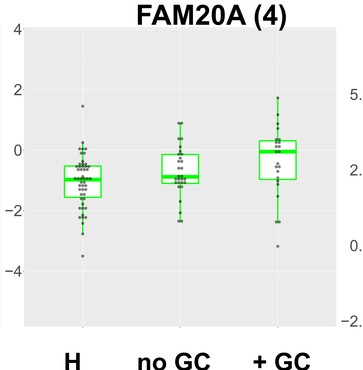

GC - 2

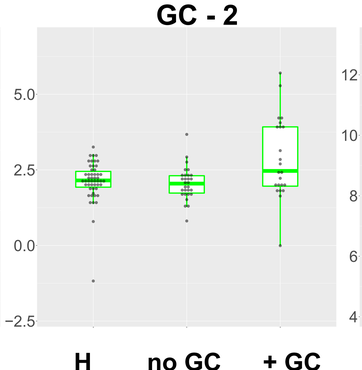

GC - 1

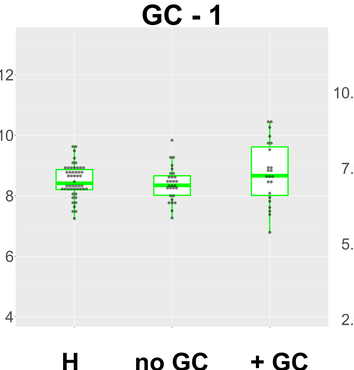

IFN gamma

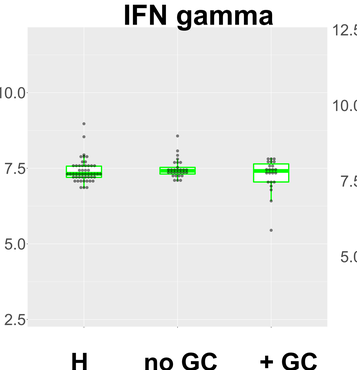

IFN alpha

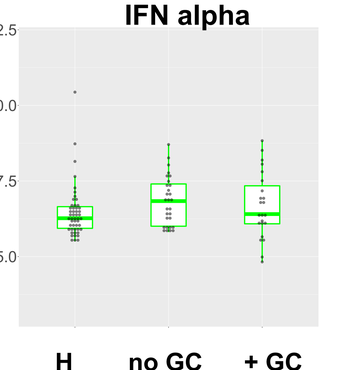

medRxiv preprint doi: https://doi.org/10.1101/2023.05.10.23289779; this version posted November 4, 2024. The copyright holder for this preprint (which was not certified by peer review) is the author/funder, who has granted medRxiv a license to display the preprint in perpetuity. All rights reserved. No reuse allowed without permission.

disease	SIM	FAM20A (A)	GC-2	IFN-G	IFN-A	dataset	platform	supporting
moderate asthma	·	·	·	·	·	GSE69683	GPL570-like	Fig S14H
severe asthma	·	·	↑	·	·	GSE69683	GPL570-like	Fig S14H
RA	↑	·	↑	↑	↑	GSE93272	GPL570	Fig S14G
SJIA plus canakinumab	↑	↑	↑	↑	↑	GSE80060	GPL570	Fig S14D
SJIA no canakinumab	↑	↑	↑	↑	↑	GSE80060	GPL570	Fig S14D
sarcoidosis	↑	↑	↑	↑	↑	GSE19314	GPL570	Fig S14E
trauma < 99h	↑	↑	↑	↓↑	↓↑	GSE36809	GPL570	Fig S14B
trauma > 99h	↑	↑	↑	·	↓↑	GSE36809	GPL570	Fig S14B
burn shock **no** GC	↑	↑	↑	↓	↓	GSE77791	GPL570	Fig S14C / Fig 9A
burn shock **+** GC	↑	↑	↑	↓	↓	GSE77791	GPL570	Fig S14C / Fig 9A
SIRS	↑	↑	↑	↓↑	↓↑	GSE66099	GPL570	Fig S14A
sepsis	↑	↑	↑	↓↑	↓↑	GSE66099	GPL570	Fig S14A
septic shock	↑	↑	↑	↓↑	↓↑	GSE66099	GPL570	Fig S14A

mild resp. vir. influenza	↑	·	·	↑	↑	GSE68310	GPL10558	Fig S15L
mild resp. vir. not influenza	↑	·	·	↑	↑	GSE68310	GPL10558	Fig S15M
SLE low SLEDAI	·	·	↑	↑	↑	GSE138458	GPL10558	Fig S15H
SLE high SLEDAI	·	·	↑	↑	↑	GSE138458	GPL10558	Fig S15H
sarcoidosis	↑	·	·	↑	↑	GSE83456	GPL10558	Fig S15I
tuberculosis (active)	↑	↑	↑	↑	↑	GSE83456	GPL10558	Fig S15I
sarcoidosis (non active)	·	·	·	↑	↑	GSE42834	GPL10558	Fig S15J
sarcoidosis (active)	↑	↑	?	↑	↑	GSE42834	GPL10558	Fig S15J
tuberculosis (active)	↑	↑	↑	↑	↑	GSE42834	GPL10558	Fig S15J
lung cancer	↑	?	↑	?	?	GSE42834	GPL10558	Fig S15J
malaria (children)	↑	↑	↑	↑	↓↑	GSE34404	GPL10558	Fig S15F
malaria (cerebral)	↑	↑	↑	?	↓↑	GSE117613	GPL10558	Fig S15G
malaria (anemia)	↑	↑	↑	?	↓↑	GSE117613	GPL10558	Fig S15G
kawasaki acute **no** GC	↑	↑	↑	↑	↓↑	GSE73463	GPL10558	Fig S15E
sepsis SRS1	↑	↑	↑	↓↑	↓↑	E-MTAB-5273	GPL10558	Fig S15B
sepsis SRS2	↑	↑	↑	↓↑	↓↑	E-MTAB-5273	GPL10558	Fig S15B
sepsis pneumonitis	↑	↑	↑	↓↑	↓↑	E-MTAB-5273	GPL10558	Fig S15A
sepsis peritonitis	↑	↑	↑	↓↑	↓↑	E-MTAB-5273	GPL10558	Fig S15A

PTSD	·	·	·	·	·	GSE97356	RNA-seq	Fig S16K
moderate asthma	·	·	·	·	·	GSE207751	RNA seq	Fig S17I
severe asthma	·	·	↑	·	·	GSE207751	RNAseq	Fig S17I
SLE	↑	↑	↑	↑	↑	GSE72509	RNA-seq	Fig S16H
RA no GC	·	·	·	·	↑	GSE117769	RNA-seq	Fig S17D / Fig 9D
RA + GC	·	↑	↑	·	↑	GSE117769	RNA-seq	Fig S17D / Fig 9D
JIA	·	·	↑	·	↑	GSE112057	RNA-seq	Fig S16G
SJIA	↑	↑	↑	?	?	GSE112057	RNA-seq	Fig S16G
IBD-Crohn	↑	↑	↑	↑	?	GSE112057	RNA-seq	Fig S16G
IBD-UC	↑	↑	↑	?	·	GSE112057	RNA-seq	Fig S16G
tuberculosis (latent)	·	·	·	↑	·	GSE107793	RNA-seq	Fig S16J
tuberculosis (latent)	·	·	·	·	·	GSE107794	RNA-seq	Fig S16I
tuberculosis (active)	↑	↑	↑	↑	↑	GSE107794	RNA-seq	Fig S16I
malaria (adults)	↑	↑	·	↑	↑	GSE52166	RNA-seq	Fig S16F
leishmaniasis	↑	↑	?	↑	↑	GSE69597	RNA-seq	Fig S16E
brucellosis	·	↑	·	↑	↑	GSE69597	RNA-seq	Fig S16E
diarrhea rota viral	↑	↑	↑	↑	↑	GSE69529	RNA-seq	Fig S16D
diarrhea bacterial	↑	↑	↑	↑	↑	GSE69529	RNA-seq	Fig S16D
COVID-19 (severe)	↑	↑	↑	↑	↑	GSE171110	RNA-seq	Fig S17C
COVID-19 (severe)	↑	↑	↑	↑	↑	GSE152641	RNA-seq	Fig S16C
mild resp. vir. not influenza	↑	·	·	↑	↑	GSE161731	RNA-seq	Fig S17J
bacterial pneumonia	↑	↑	↑	↓↑	↓?	GSE161731	RNA-seq	Fig S17J
bacterial (pneumonia/bacteremia)	↑	↑	↑	↓↑	↓↑	GSE176260	RNA-seq	Fig S17A
SIRS	↑	↑	↑	↓↑	↓↑	GSE176260	RNA-seq	Fig S17A
resp. viral infection (acute)	↑	↑	↑	↑	↑	GSE176260	RNA-seq	Fig S17A
candidemia	↑	↑	↑	↓↑	↓↑	GSE176260	RNA-seq	Fig S17A
kawasaki acute **no** GC	↑	↑	↑	↓↑	↓↑	GSE178491	RNA-seq	Fig S17L
sepsis	↑	↑	↑	↓↑	↓↑	GSE154918	RNA-seq	Fig S17G
sepsis, no recent high GC	↑	↑	↑	↓↑	↓↑	GSE196117	RNA-seq	Fig S17K

medRxiv preprint doi: https://doi.org/10.1101/2023.05.10.23289779; this version posted November 4, 2024. The copyright holder for this preprint (which was not certified by peer review) is the author/funder, who has granted medRxiv a license to display the preprint in perpetuity.
All rights reserved. No reuse allowed without permission.

		SUITABLE GC BIOMARKER GENES						TIME TELLING GENES (existing)			GC BIOMARKER GENES (existing)		
		CIRCADIAN	ASTHMA	RA	SLE	COVID - 19	SEPSIS	T T - 1	T T - 2	T T - 3	ADDISON	SLE - 1	SLE - 2
GC - 1	ZBTB16	✓	✓	✓	✓	✓	✓		4			yes	
	KLF9	✓	✗	✗	✗	✗	✗		2				
	DDIT4	✓	✓	✗	✓	✗	✗	4	4	4	yes		
	PER1	✓	✓	✓	✓	✓	✓	1	4	4			
	IRS2	✓	✓	✓	✓	✗	✗					yes	
	CXCR4	✓	✗	✗	✗	✗	✗						
	TSC22D3	✓	✓	✓	✓	✗	✗				yes		
	DUSP1	✓	✓	✗	✓	✗	✗		3			yes	
	FKBP5	✓	✓	✓	✓	✓	✓	2	4		yes	yes	
	ALOX15B	✗	✓	✓	✓	✓	✓						yes
	CD163	✗	✓	✓	✓	✓	✓						yes
GC - 2	ADAMTS2	✗	✓	✓	✓	✓	✓						
	FLT3	✓	✓	✓	✓	✓	✓	1	2				
	VSIG4	✗	✓	✓	✓	✓	✓						yes
	MAOA *	✗	✗	✓	✓	✓	✓						
	AMPH	✗	✓	✓	✓	✓	✓						yes
	ADORA3 *	✗	✗	✗	✗	✗	✗						
	TMIGD3	✓	✓	✓	✓	✓	✓						
	MACIR	✗	✗	✓	✓	✓	✓						
	OLAH	✗	✓	✓	✓	✓	✓						
	DAAM2	✓	✓	✓	✓	✓	✓	1	3				
	IL1R2	✗	✓	✓	✓	✓	✗					yes	yes
	IRAK3	✗	✓	✓	✓	✓	✗					yes	
	ECHDC3	✓	✓	✓	✓	✓	✓					yes	
	ARG1	✗	✓	✓	✓	✗	✗						
	ACSL1	✗	✗	✗	✗	✗	✗					yes	